

Ministry of Higher Education and Scientific Research

وزارة التعليم العالي والبحث العلمي

Badji Mokhtar Annaba University
Université Badji Mokhtar – Annaba
Faculty of Technology



جامعة باجي مختار – عنابة

كلية التكنولوجيا

Department of Electronics

قسم الإلكترونيك

Thesis

Submitted to obtain the diploma of

Doctorate Third Cycle

Field: Telecommunications

Specialty: Multimedia and Digital Communications

By:

ZIDANI Nesrine

Title:

Compression d'images fixes et en stéréovision à faible complexité sur WSN

Thesis defended on 27/06/2024 in front of the jury composed of:

N°	Name and Surname	Grade	Establishement	Role
01	LAFIFI Saddek	Pr.	University of Badji Mokhtar Annaba	President
02	DOGHMANE Nouredine	Pr.	University of Badji Mokhtar Annaba	Supervisor
03	KOUADRIA Nasreddine	Pr.	University of Badji Mokhtar Annaba	Co-supervisor
04	BENMOUSSA Samir	Pr.	University of Badji Mokhtar Annaba	Examiner
05	BOUDEN Toufik	Pr.	University of Jijel	Examiner
06	BEKHOUCHE Amara	Pr.	University of Souk-Ahras	Examiner
07	HARIZE Saliha	Pr.	University of Badji Mokhtar Annaba	Invited

Dedication

I humbly dedicate my efforts with a special feeling of gratitude to my loving parents, Mourad and Farida. Their affection, love, and words of encouragement for my tenacity continue to ring in my ears. Without their love, support, and prayers, this thesis would not have achieved such success and honor. To my sister Marwa and brothers Ishak & Yakoub. I am sincerely grateful to have you in my life.

I would like to dedicate this work to my beloved daughters Sarah & Eline, whos have fought with me from the first letter of this thesis was written. God bless them. I also dedicated to my husband, who offered me unconditional support and patience throughout the process. I will always appreciate all that he has done.

This work is also dedicated to my lovely aunt, Nadjet, and my cousin, Ryma, for their support and advice in accomplishing this work.

Acknowledge

All praise to Allah, the Almighty, the Most Gracious, and the Most Merciful, for granting me the strength, knowledge, ability, opportunity, and guidance to achieve my goal and complete this thesis.

First and foremost, I would like to express my sincerest appreciation to my supervisor, Professor. Doghmane Nourddine, for his invaluable advice, unwavering support, guidance, and remarkable patience throughout my PhD studies. I have been exceptionally fortunate to have a supervisor who cares so deeply about my work and promptly addresses my questions and inquiries.. He has been a constant source of reassurance, especially during the ups and downs of the research process. His immense knowledge and extensive experience have enriched my academic journey in countless ways.

I want to express my gratitude to my co-supervisor, Kouadria Nasreddine, for his assistance during my Ph.D. His expertise shaped my research, enhanced its quality, and his feedback and suggestions guided me in refining my work and broadening my understanding of the subject matter. Additionally, I would like to express my heartfelt gratitude and appreciation to Mrs. S. Hariz for her unwavering support and invaluable assistance in completing this work. Furthermore, I extend a special thanks to Mrs. K. Mechouek for her kind help and unwavering support during my PhD studies.

I am immensely grateful to my thesis committee members of the jury : LAFIFI Saddek, BENMOUSSA Samir, BOUDEN Toufik and BEKHOUCHE Amara. Their willingness to evaluate and assess this research work is greatly appreciated. We sincerely thank our jury members for their time, dedication, and thoughtful judgment. Your contributions and hard work are deeply appreciated. Thank you for your invaluable service.

The last but not the least, I would like to express my heartfelt gratitude to my parents, and my wonderful children. Their unwavering support, understanding, and love have been integral to my achievements. Additionally, I am immensely grateful for all my friends who have consistently provided me with encouragement and valuable advice throughout the entirety of my doctorate program. Their support has been instrumental in my journey.

"ضغط الصور الثابتة والستريو بتعقيد منخفض على شبكة الاستشعار اللاسلكية"

الملخص

يعد إطالة عمر شبكات الاستشعار اللاسلكية القضية الأكثر تحدياً في شبكات المستشعرات المتعددة الوسائط اللاسلكية (WMSN)، تحتوي عقدة الاستشعار على موارد طاقة محدودة ولزيادة عمر الشبكة ، فإنه من الضروري تصميم خوارزمية سريعة فعالة تهدف إلى تقليل الطاقة المستهلكة. في هذه الأطروحة، اقترحنا تقريب فعالاً لتحويل جيب التمام المنفصل (DCT) الموفر للطاقة والذي يتطلب 12 إضافة فقط مقترناً بسلسلة ضغط JPEG. يضمن هذا التقريب حل وسط جيد جداً لتشيوية المعدل ، ولكن قبل كل شيء ، هو تعقيد حسابي منخفض جداً ومتوافق بشكل كبير مع DCT الدقيق. تم تطبيق هذا التحويل على الصور الثابتة وكذلك صورة الستيريو. تظهر نتائج المحاكاة بوضوح أن الخوارزمية السريعة للتحويل المقترح تحقق توازناً أفضل بين جودة الصورة وتعقيد الحساب واستهلاك الطاقة مقارنةً بأي تقريبات DCT التقليدية الموجودة. علاوة على ذلك ، فهي مناسبة للغاية لشبكات الاستشعار البصرية اللاسلكية ذات الموارد المحدودة (WVSN) التي تتطلب معدلات بت منخفضة.

كلمات مفتاحية: تقريب DCT, شبكات الاستشعار اللاسلكية, ضغط الصورة, نهج التقييم, حفظ الطاقة, التعقيد الخوارزمي المنخفض. صورة الستيريو.

« Compression d'images fixes et en stéréovision à faible complexité sur WSN »

Résumé

Prolonger la durée de vie des réseaux de capteurs sans fil (WSN) est le plus grand défi à relever. Dans les réseaux de capteurs multimédias sans fil (WMSN), les nœuds de capteurs disposent d'une ressource énergétique limitée et pour augmenter la durée de vie du réseau, il est nécessaire de concevoir un algorithme rapide efficace visant à réduire la consommation d'énergie. Dans cette thèse, nous avons proposé une approximation économe en énergie de la transformée en cosinus discrète (DCT) ne nécessitant que 12 additions. Associée à une chaîne de compression JPEG, cette approximation garantit un très bon compromis taux-distorsion, mais surtout une complexité de calcul très faible et une compatibilité significative avec la DCT exacte. Cette transformation est appliquée aux images fixes ainsi qu'aux images stéréo. Les résultats de simulation montrent clairement que la transformation rapide proposée permet d'obtenir un meilleur compromis entre la qualité d'image, la complexité de calcul et la consommation d'énergie par rapport à toutes les approximations de la DCT existantes. De plus, elle est très appropriée pour les réseaux de capteurs visuels sans fil (WVSN) limités en ressources et nécessitant des débits binaires faibles.

Mots clés : DCT approximative, réseaux de capteurs sans fil, compression d'images, approche zonale, conservation d'énergie, faible complexité algorithmique, image stéréo.

« Fixed and stereovision images compression at low-complexity in WSNs»

Abstract

Prolonging the lifetime of wireless sensor networks (WSN) is the biggest challenging issue. In wireless multimedia Sensor Networks (WMSNs), sensor nodes have limited energy resource and to increase the lifetime of the network, it is necessary to design an effective fast algorithm that aims at reducing the consumed power. In this thesis we proposed an energy-efficient discrete cosine transform (DCT) approximation requiring only 12 additions. Associated with a JPEG compression chain, this DCT approximation ensures a very good rate-distortion compromise, but above all, a very low computational complexity and significant compatibility with the exact DCT. This transformation is applied to still image as well as stereo images. Simulation results clearly show that the proposed fast transform algorithm achieves a better trade-off between image quality, computational complexity and energy consumption compared to any existing pruned DCT approximations. Furthermore, it is very suitable for the resource constrained wireless visual sensor networks (WVSNs) requiring low bitrates.

Key words: DCT approximation; wireless sensor networks; image compression; pruning approach; energy conservation; low algorithmic complexity, Stereo image.

List of Abbreviations

1-D	one-dimensional
2-D	two-dimensional
3-D	Three-dimensional
AC	Alternative Components
ADC	Analog to Digital Converter
BAS	Bouguezel Ahmad Swamy
BDCT	Binary Discrete Cosine Transform
Bps	Bit per pixel
CMOS	Complementary Metal Oxide Semiconductor
DA	Distributed Arithmetic
DC	Direct Component
DCT 1D	Discrete Cosine Transform one dimensional
DCT 2D	Discrete Cosine Transform two dimensional
DFT	Discrete Fourier Transform
DPCM	Differential pulse code Modulation
DWT	Discrete Wavelet Transform
EBCOT	Embedded Block Coding with Optimised Truncation
EZW	Embedded Zerotree Wavelet
FDCT	Forward Discrete Cosine Transform
FOV	Field Of View
GPS	Global Positioning system
HH	High High
HL	High Low
HVS	Human Visual System

HPF	High Pass Filter
IWT	integer wavelet transform
JPEG	Joint Photographic Experts Group
JPEG2000	Joint Photographic Experts Group 2000
KLT	Karhunen-Loeve Transform
LH	Low High
LL	Low Low
LPF	low Pass Filter
MAC	Media Access Control
MCU	Micro-Controller Unit
MEMS	MicroElectro Mechanical Systems
MRA	Multi-Resolution Analyze
MSE	Mean Square Error
MRDCT	Modified Rounded Discrete Cosine Transform
mW	Milli Watt
P-BDCT	Pruned Binary Discrete Cosine Transform
P-DCT	Pruned Discrete Cosine Transform
P-MRDCT	Pruned Modified Rounded Discrete Cosine Transform
P-RDCT	Pruned Rounded Discrete Cosine Transform
PSNR	Peak Signal to Noise Ratio
QF	Quantization Factor
QoS	Quality of Service
RDCT	Rounded Discrete Cosine Transform
RF	Radio Frequency
RLC	Run Length Encoding
SAD	Sum of Absolute Difference

SC	Statistical Coding
SDCT	Signed Discrete Cosine Transform
SFG	Signal Flow Graph
SPIHT	Set Partitioning In Hierarchical Trees
SQ	Scalar Quantization
SRAM	Static Random Access Memory
SSIM	Structural Similarity Index Metric
UWB	The Ultra Wide Band
VLC	Variable-Length Code
VQ	Vector Quantization (VQ)
WCH	Wireless Cluster Head
WHT	Walsh Hadamard Transform
WiFi	Wireless Internet Frequent Interface
WMN	Wireless Multimedia Node
WMSN	Wireless Multimedia Sensor Network
WNN	Wireless Network Node
WSN	Wireless Sensor Network
WVSN	Wireless visual Sensor Network

List of Figure

Figure.1.1. <i>Hardware architecture of a sensor node</i>	8
Figure.1.2. <i>General architecture of a wireless sensor network (WSN)</i>	10
Figure.1.3. <i>WSN fat architecture</i>	12
Figure.1.4. <i>WSN hierarchical architecture</i>	13
Figure.1.5. <i>Architecture of a Wireless Multimedia Sensor Network</i>	21
Figure.2.1. <i>Classification of image compression technique</i>	26
Figure.2.2. <i>The basic Image compression/ decompression model</i>	29
Figure.2.3. <i>Baseline JPEG Compression scheme</i>	31
Figure.2.4. <i>Zigzag scanning</i>	34
Figure.2.5. <i>Block diagram of DWT</i>	37
Figure.2.6. <i>Example of two level DWT decomposition</i>	38
Figure.2.7. <i>The JPEG2000 encoder/decoder</i>	39
Figure.3.1. <i>(a) Baboon and its DCT. (b) Child and its DCT. (c) Saturn and its DCT</i>	44
Figure.3.2. <i>Pruned method adopted in several approximations</i>	54
Figure.4.1. <i>The signal flow graph (SFG) of the Pruned RDCT</i>	61
Figure.4.2. <i>The proposed pruned 2-DCT approximation for L=4</i>	63
Figure.4.3. <i>The flow graph of the proposed algorithm</i>	65
Figure.4.4. <i>PSNR acquired by different transforms for lena image</i>	71
Figure.4.5. <i>Reconstructed images at 0.35 bpp using different approximations</i>	72
Figure.4.6. <i>MSE of several pruned DCT approximations</i>	73
Figure 4.7. <i>Testbed used to real measurement of execution time and the current consumed during</i>	77
Figure.4.8. <i>Testbed photograph</i>	77

Figure.4.9. <i>Measured currents for the different DCT approximations</i>	79
Figure.4.10. <i>Visualized currents for the different DCT approximations</i>	80
Figure.5.1. <i>Demonstration of how a pair of stereo images creates an illusion of 3D scene/objects.</i>	84
Figure.5.2. <i>A stereo vision system using a couple of cameras</i>	85
Figure.5.3. <i>The proposed Stereo coder</i>	87
Figure.5.4. <i>Typical standard test stereo images used in the simulation</i>	87
Figure.5.5. <i>Reconstructed stereo image: ‘fruit’ and ‘pentagon’ using DCT Loeffler at 0.45 bpp....</i>	88
Figure.5.6. <i>Reconstructed stereo image: ‘fruit’ and ‘pentagon’ using proposed transform at 0.45 bpp.</i>	89

List of tables

Table.3.1.*Pruned DCT approximations* 56

Tbale.4.1.*Computational complexity comparison of different 1D pruned approximation*..... 70

Table.4.2.*Energy consumption obtained by several transforms* 74

Table.4.3.*Execution time of the four pruned DCT*..... 80

Tbale.5.1.*Computational complexity comparison of 1D/2D by exact DCT and the proposed transform for stereo image* 90

Table.5.2.*Energy consumption obtained by exact DCT and the proposed transform*..... 91

List of publications

- **Journal publications:**

Zidani, N., Doghmane, N., Kaddeche, M., Kouadria, N., & Harize, S., (2021) "An Efficient Low Complexity Pruned DCT Approximation for Image Compression in Wireless Multimedia Sensor Networks". Journal of Circuits, Systems and Computers (World scientific), 30 (11), 2150199. *IF=1.333*.

- **Conference publications:**

Zidani, N., Kouadria, N., Doghmane, N., & Harize, S., " Low Complexity Pruned DCT Approximation for Image Compression in Wireless Multimedia Sensor Networks". 2019 5th International Conference on Frontiers of Signal Processing (ICFSP). Marseille, France

Contents

<i>List of Abbreviations</i>	VII
<i>List of Figures</i>	X
<i>List of Tables</i>	XI
<i>List of Publications</i>	XIII

General introduction.....2

Chapter 1: An Introduction to Wireless Multimedia sensor Networks

1.1 Introduction.....	7
1.2. Sensor Network architecture.....	8
1.2.1 Hardware Architecture of a Sensor Node.....	8
1.2.2 Sensor Network communication architecture.....	9
1.2.3 Types of Network architecture.....	11
1.3 Factors influencing WSN design.....	13
1.4 Energy consumption in wireless sensor Network.....	15
1.4.1 Power dissipation in a wireless sensor node.....	15
1.4.2 Major reasons of energy waste in WSN.....	16
1.4.3 Energy conserving techniques.....	17
1.5 Wireless Multimedia Sensor Network.....	18
1.5.1 WMSN and applications.....	18
1.5.2 Components of a Wireless Multimedia Sensor Network.....	18
1.5.3 Network Architecture of WMSN.....	20
1.5.4 Characteristics of wireless multimedia sensor nodes.....	22
1.6 Conclusion.....	22

Chapter 2: Image compression in wireless multimedia sensor network

2.1 Introduction.....	25
2.2 Image compression in wireless Multimedia sensor network.....	26
2.2.1 Lossless image compression techniques.....	27
2.2.2 Lossy image compression techniques.....	27
2.3 Principle of image compression algorithm.....	28
2.4 Transform-Based DCT Methods.....	30
2.4.1 The Discrete cosine transform (DCT).....	31
2.4.2 Quantization.....	33
2.4.3 Zigzag Scanning.....	34
2.4.4 Entropy encoder.....	34
2.4 JPEG - Based Schemes for WMSN.....	35
2.5 Transform-Based DWT Methods.....	36
2.5.1 Joint photograph expert group 2000(JPEG2000).....	39
2.5.1.1 JPEG 2000 -Based Schemes for WMSN.....	40
2.5.2 Set partitioning in hierarchical tree (SPIHT).....	40
2.5.2.1 SPIHT-Based Schemes for WMSN.....	41
2.6 Conclusion.....	41

Chapter 3: Energy efficient image compression techniques in WMSNs

3.1 Introduction.....	42
3.2 The properties of DCT.....	43
3.2.1 Decorrelation.....	43
3.2.2 Energy compaction.....	43
3.2.3 Separability.....	45
3.2.4 Orthogonality.....	46
3.3 Review of approximate DCT methods.....	46
3.4 The Mathematical background.....	47
3.4.1 8-point DCT approximations.....	47
3.4.2 Pruned approximate DCT.....	53
3.5 Conclusion.....	57

Chapter 4: Proposed low complexity pruned DCT approximation for image compression

4.1 Introduction.....	58
4.2 Proposed transform.....	60
4.2.1 Pruned RDCT approximation.....	60
4.2.2 New pruned DCT approximation.....	61
4.3 Performance evaluation.....	65
4.4.1 Evaluation in terms of complexity assessment.....	65
4.4.2 Evaluation in terms of image quality.....	66
4.4.3 Evaluation in terms of energy consumption.....	69
4.4 Results and discussion.....	70
4.4.1 Results in term of Arithmetic complexity.....	70
4.4.2 Results in terms of image quality.....	70
4.4.3 Results in terms of mean square error.....	73
4.4.4 Results in terms of energy consumption.....	74
4.5 Testbed for real measurement.....	75
4.5.1 Experiment.....	76
4.5.2 Real execution time for different DCTs on 8×8 image block.....	78
4.5.3 Real energy consumption for the four Pruned DCTs on 8×8 image block.....	78
4.6 Conclusion.....	81

Chapter 5: Stereo Image compression using proposed pruned transform

5.1 Introduction.....	83
5.2 Principles of stereoscopic vision.....	83
5.2.1 Principles of function in the Human Visual System.....	83
5.2.2 Stereoscopic imaging systems.....	84
5.3 Experimental results and discussion.....	85
5.3.1 Stereo image compression.....	87
5.3.2 Computational complexity.....	89
5.3.3 Energy consumption.....	90
5.4 Conclusion.....	91

Conclusion and perspectives	93
References	98

General introduction

1. Introduction

In the last decade, wireless sensor networks (WSNs) have become an increasingly prominent technology, drawing global research attention, especially with the proliferation of the recent technological advances in Micro Electro Mechanical Systems (MEMS) technology and wireless communications [1-5], which have facilitated the evolution of smart sensor nodes. WSNs find application in diverse areas [7,8], including real-time object tracking, environmental condition monitoring, health infrastructure surveillance, and the establishment of a pervasive computing environment..etc

A Wireless Sensor Network (WSN) is ad hoc networks consist of tiny miniature electronic devices known as sensor nodes [9-12]. These sensors are distributed in space in an unknown fashion in an unattended and hostile milieu [7] to sense, measure, and gather information from the surrounding environment and then convert these measurements, such as temperature, humidity, or light, into an electric signal. The sensor sends the gathered data to the user. usually via radio transmitter to the sink (also known as the base station), either directly or via multiple wireless hops[8-12]. Generally, sensor nodes are powered by small batteries with limited energy capacities[15,16]. These nodes are deployed in rugged regions, making it often difficult to recharge or replace their batteries[10]. Therefore, the most challenging issue in WSN design lies in conserving node energy while maintaining the network's functionality [17-19].

Recently, the emergence of low-cost multimedia devices such as CMOS cameras and microphones has led to the development of Wireless Multimedia Sensor Networks (WMSNs) [20-23], which handle a significant amount of multimedia data, including images and videos, in addition to scalar sensor data. However, compared to traditional Wireless Sensor Networks (WSNs), WMSNs face additional challenges due to the nature and volume of the multimedia data they transmit. One of the major challenges faced by WMSNs is energy consumption because transmitting multimedia data requires more resources and power than transmitting scalar sensor data. This can lead to shorter network lifetimes and increased maintenance costs. To address this challenge, researchers have suggested different methods, such as data compression, data aggregation, and energy-efficient routing protocols. These techniques aim to decrease the volume of transmitted data, minimize the number of transmissions, and balance energy consumption among nodes [24-29].

In general, transmitting multimedia information such as images over WMSNs requires a much higher bandwidth because it contains a huge amount of information. Therefore, image compression is the most effective solution to reduce the size of the image by exploiting data correlation and redundancy [30]. However, traditional compression algorithms such as JPEG, JPEG 2000, and SPIHT are often not energy-efficient and require high computational costs and memory access, making them unsuitable for resource-constrained sensor nodes. To overcome this issue, researchers are investigating new approaches for developing energy-efficient image compression algorithms that take into account the specific requirements and constraints of WMSNs, such as limited bandwidth, processing power, and battery life. These algorithms must strike a balance between compression efficiency, computational complexity, memory usage, and energy consumption while still ensuring acceptable image quality [31, 32].

This thesis aims to develop new energy-efficient image compression methods that can extend the lifetime of both sensor nodes and the entire network. Our objective is to decrease the computational algorithmic of the DCT transform by introducing a new pruned DCT approximation. This approach significantly decreases the computational complexity of the DCT and consequently, the energy consumption of the sensor node. We believe that our proposed method will be the best choice for image compression in wireless multimedia sensor networks. However, transmitting or storing a stereo image over a wireless multimedia sensor network requires twice the bandwidth and energy compared to a single image. This can cause severe problems for the entire network. Therefore, compressing stereo images using the proposed transform can greatly preserve the functionality of the network.

2. Thesis outlines

The structure of this thesis is outlined as follows:

In Chapter 1, we will present an overview of the state-of-the-art wireless sensor network. This will include a description of the hardware architecture of the sensor node, the types of network architecture, the protocol architecture, as well as the main factors that impact its design. We will then focus our attention on the energy problem in wireless sensor networks by explaining the power dissipation in sensor nodes and discussing the major reasons for energy waste in WSNs. We will also briefly discuss the most important energy conservation techniques. Additionally, this chapter will present a specific case study of image sensor networks, which are a type of wireless multimedia

sensor network. We will discuss its main components and network architecture, and conclude with a discussion of the major factors that influence their design.

In Chapter 2, we will provide an overview of image compression and its basic principles. We will discuss the types of image compression methods, including both lossy and lossless methods. Additionally, we will provide a brief review of several established standards, such as JPEG, JPEG 2000, and SPIHT, which are commonly used for wireless multimedia sensor networks (WMSN), highlighting their strengths and limitations. Finally, we will also discuss various techniques proposed in the literature to enhance the speed of each compression method.

In Chapter 3, our focus will be on the presentation of the Discrete Cosine Transform (DCT). Our objective is twofold: firstly, to present the most important and useful properties of this transformation, and secondly, to discuss the various techniques that have been proposed in the literature to reduce its computational complexity. Specifically, we will concentrate on the techniques that require only addition/shift operations, which are commonly referred to as fast DCT algorithms. These algorithms are important in real-time applications as they significantly reduce the computational time and resources required to perform the DCT.

In Chapter 4, we will present our contribution. Firstly, we will introduce a low-complexity pruned DCT approximation proposed for wireless multimedia sensor networks. We will assess this approximation by examining its arithmetic complexity, image quality, and energy consumption and will compare it against state-of-the-art methods. Furthermore, we will implement a testbed based on an Arduino Due module to evaluate the efficiency of the proposed method in terms of execution time and consumed current, comparing it to well-known pruned approximations.

Chapter 5 is dedicated to testing the effectiveness of the proposed fast approximation method, specifically on stereo images. The primary objective of this chapter is to demonstrate that the proposed fast approximation is the superior choice for encoding stereo images in resource-constrained Wireless Multimedia Sensor Networks (WMSNs), when compared to the exact Discrete Cosine Transform (DCT) method. The performance evaluation will be conducted in terms of image quality, computational complexity, and energy consumption.

Chapter 1

An introduction to Wireless sensor Network

1.1. Introduction

In the last years, Wireless Sensor Networks (WSNs) have gained significant attention in research and have emerged as one of the most highly promising technologies for a diverse range of potential applications in our daily lives including healthcare, military, and security. WSNs offer several advantages over traditional networking techniques, such as low-cost, low-power consumption, scalability, and flexibility, making them suitable for deployment in different environments. In a military context, sensor nodes are utilized to detect, locate, or track enemy movements at all times. In situations involving natural disasters, these sensor nodes play a crucial role in sensing and detecting environmental changes, enabling the prediction of disasters in advance. In security, sensors can provide vigilant surveillance to increase the awareness of potential terrorist attacks. In healthcare, doctors can remotely monitor a patient's physiological data, which not only provides convenience for the patient but also helps the doctor better understand the patient's condition [1,2].

A Wireless Sensor Network (WSN) is typically an ad hoc network comprising thousands of small nodes, known as sensor nodes, deployed within a specific geographical area. Each node detects or measures a physical attribute, such as temperature, pressure, or humidity, in a controlled environment. Subsequently, the node converts this data into signals for monitoring and transmission. These sensor nodes are compact, autonomous systems equipped with advanced sensing capabilities, serving as the fundamental components of WSNs [3].

One of the most crucial limitations for sensor nodes is the necessity for low power consumption. Typically, these nodes are powered by small batteries that are not easily replaceable or rechargeable. As a result, their functionality is limited by the amount of energy available. The lifetime of a wireless sensor node is closely related to its battery current usage profile. Several research works have been carried out to address the energy problem, resulting in various schemes and protocols. These techniques have been employed to minimize energy consumption and extend the network lifetime [4, 5].

1.2. Sensor Network architecture

1.2.1. Hardware Architecture of a Sensor Node

In general, a sensor node comprises four primary components: a sensing unit, a processing unit, a transceiver unit, and a power supply unit. Additionally, depending on the specific application requirements [1, 5-6], sensor nodes may include additional components such as a location-finding system, a power generator, and a mobilizer. Figure.1.1. illustrates the hardware architecture of a sensor node.

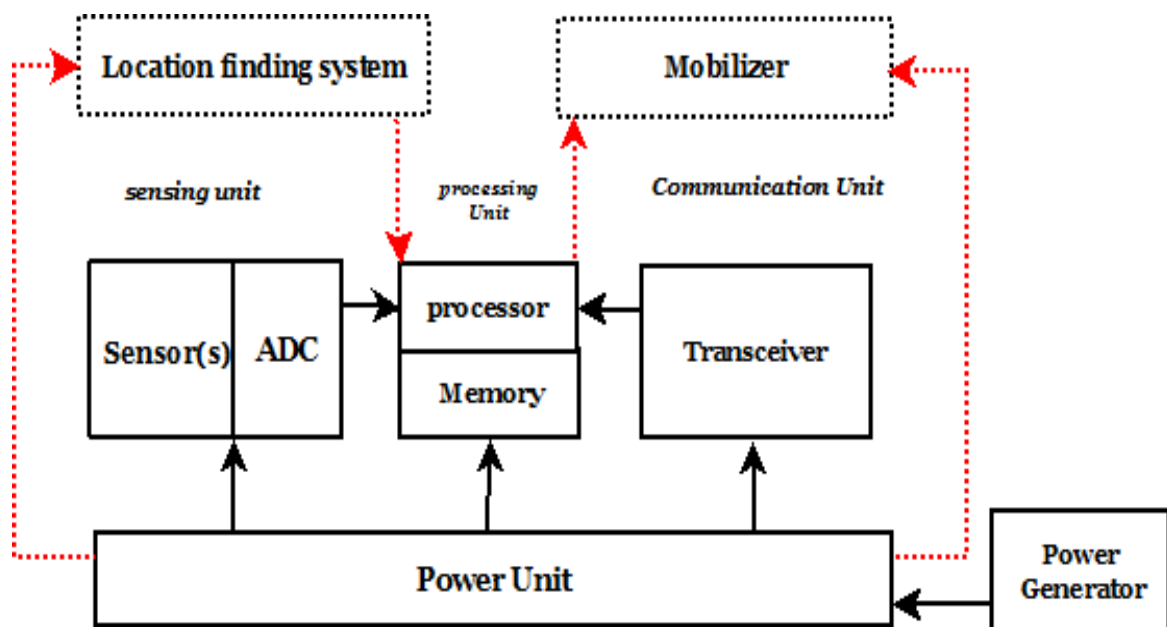


Figure.1.1. Typical Hardware architecture of a sensor node.

Sensing Unit: The sensing unit is usually composed of two subunits: sensors and analog-to-digital converters (ADCs). Each sensor unit is responsible for detecting and measuring physical or environmental data, such as temperature, humidity, light, sound, pressure, or motion. The sensors convert the physical data into electrical signals that are analog in nature. These analog signals are then passed through an analog-to-digital converter (ADC), which converts them into digital signals that can be processed by the processing unit.

Processing Unit: The processing unit typically consists of a microcontroller or microprocessor, which is typically associated with a small storage unit, such as flash memory or RAMS that, is integrated into the embedded board. The processing unit is responsible for performing tasks, sensing operations, and running associated algorithms. It also communicates with other sensor nodes or a central node through wireless communication protocols to exchange information and collaborate on specific tasks.

The transceiver unit: The transceiver unit plays a crucial role in enabling wireless communication between the sensor node and other nodes in the network. It typically comprises a radio transceiver capable of transmitting and receiving data using wireless communication protocols such as Bluetooth, Zigbee, or Wi-Fi. This unit allows the sensor node to establish connections with other nodes in the network and exchange information wirelessly, facilitating collaborative sensing and data sharing among nodes. Ultimately, this enhances network efficiency and performance.

Power supply unit: The power supply unit is regarded as one of the most critical components of a wireless sensor node because it ensures the node's continuous operation by providing a reliable source of energy. Typically, battery power is a common choice for supplying energy to the node, although other energy sources such as solar power are also viable options.

Depending on specific applications, three additional units may be incorporated in the sensor structures: the energy generator, which supplies the sensor with additional energy sources; the mobilizer, which is sometimes used to support the mobility of sensor nodes when it is necessary to carry out assigned tasks; and the position-finding system, which is used because most sensor network routing techniques and sensing tasks require knowledge of sensor node positions with high accuracy.

1.2.2. Sensor Network communication architecture

A Wireless Sensor Network (WSN) is an ad hoc network consisting of multiple tiny sensor nodes distributed in an unknown manner in an unattended and hostile environment [7], this area is commonly referred to as the field or area of interest. The nodes communicate with one another through a wireless connection channel, and each sensor node has the capability to collect, process, and transmit the sensed data to the sink over multiple wireless hops. The sink is a special sensor node that serves as an interface between the network and the end user's network. It obtains information from the source node or intermediate node with the help of a forwarding node and

performs basic processing on the collected data. The sink then transmits only relevant information (or the processed data) via the internet to the users who requested it or use the information by a multi-hop infrastructure-less architecture [8].

To increase the lifetime of the WSN network, sensor nodes should tailor their activities in an energy-efficient way, so scarce energy reserves are used efficiently. Every sensor node utilizes a protocol stack to communicate with one another and with the sink. For effective communication and work across multiple sensor nodes, the protocol stack must work efficiently with regards to energy consumption [9, 10]. Figure.1.2 presents a general architecture of a wireless sensor network (WSN).

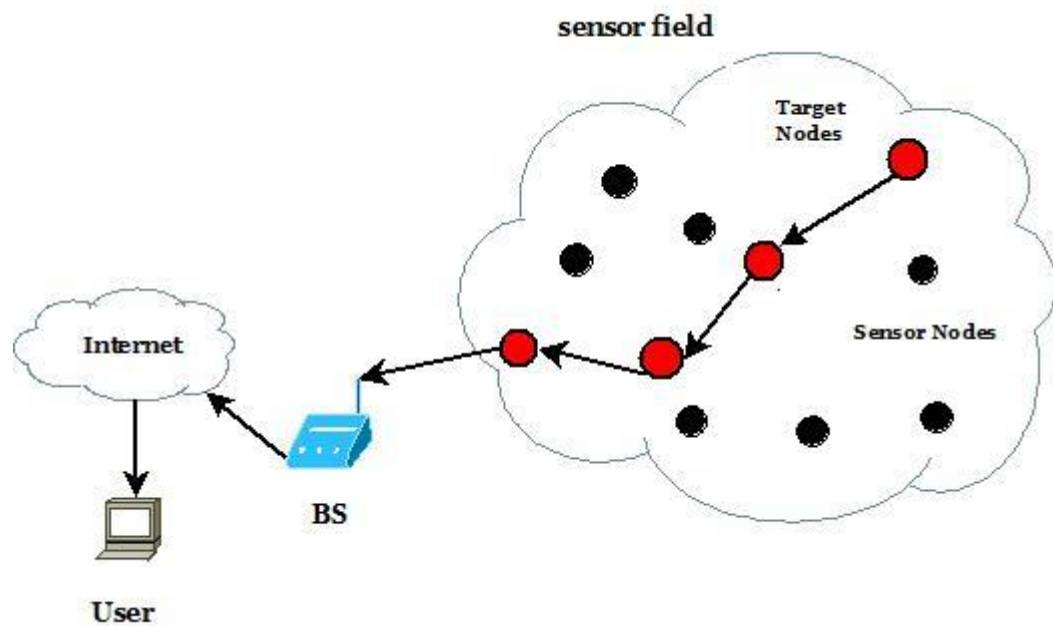


Figure.1.2. General Architecture of a wireless sensor network (WSN).

1.2.3. Types of Network architecture

Sensor nodes collect data from their surrounding environment and relay it to the central sink. Communication between sensor nodes and the sink can occur through two methods: single-hop communication, which involves the direct transmission of information to the sink, or multi-hop

communication, where data is passed to its neighbors. The decision between single-hop and multi-hop networks is contingent upon the specific needs of the application. Typically, single-hop networks are simpler to manage and are well-suited for smaller-scale networks, while multi-hop networks tend to be more advantageous for larger networks comprising hundreds or thousands of nodes [10, 11].

- **Flat architecture :**

In a flat architecture, the network is deployed with homogeneous sensor nodes that have the same capabilities and functionalities in terms of energy and computing. Each node can communicate directly with the sink in single-hop communication or multi-hop communication:

In single-hop communication, each sensor node in the network is responsible for sensing and transmitting the sensed data directly to the base station outside the sensor field. As shown in Figure.1.3(a), the direct communication paradigm can be very expensive because sensor networks often cover large geographic areas. The long distance between a node and the sink requires very high transmission power, while radio transmission power should be kept at a minimum in order to conserve energy.

In multi-hop communication, some sensor nodes use a multi-hop path instead of transmitting the monitored data directly to the sink. This is actually the most popular case used in the network. They use other nodes as relays to deliver their data to the sink. When a sensor node serves as a relay, it has the opportunity to analyze and pre-process sensor data in the network. This leads to the elimination of redundant information and the retention of only relevant information. Figure.1.3(b) represents a flat multi-hop sensor network where nodes collaborate to propagate sensor data towards the base station by multi-hop communications [12].

- **Hierarchical architecture :**

The sensing field is composed into multiple clusters, with each cluster comprising several nodes that act as cluster members and a more powerful node serving as the cluster head. It's important to note that a node with lower energy can still be employed for the sensing task and send its collected data to the cluster head over a short distance. Conversely, a node with higher energy can be designated as the cluster head to process data from its cluster members and then transmit the processed data to the sink. Within a cluster, each member can transmit its collected data to the

cluster head using either single-hop or multi-hop communication methods [8, 12]. This is illustrated in Figure.1.4.

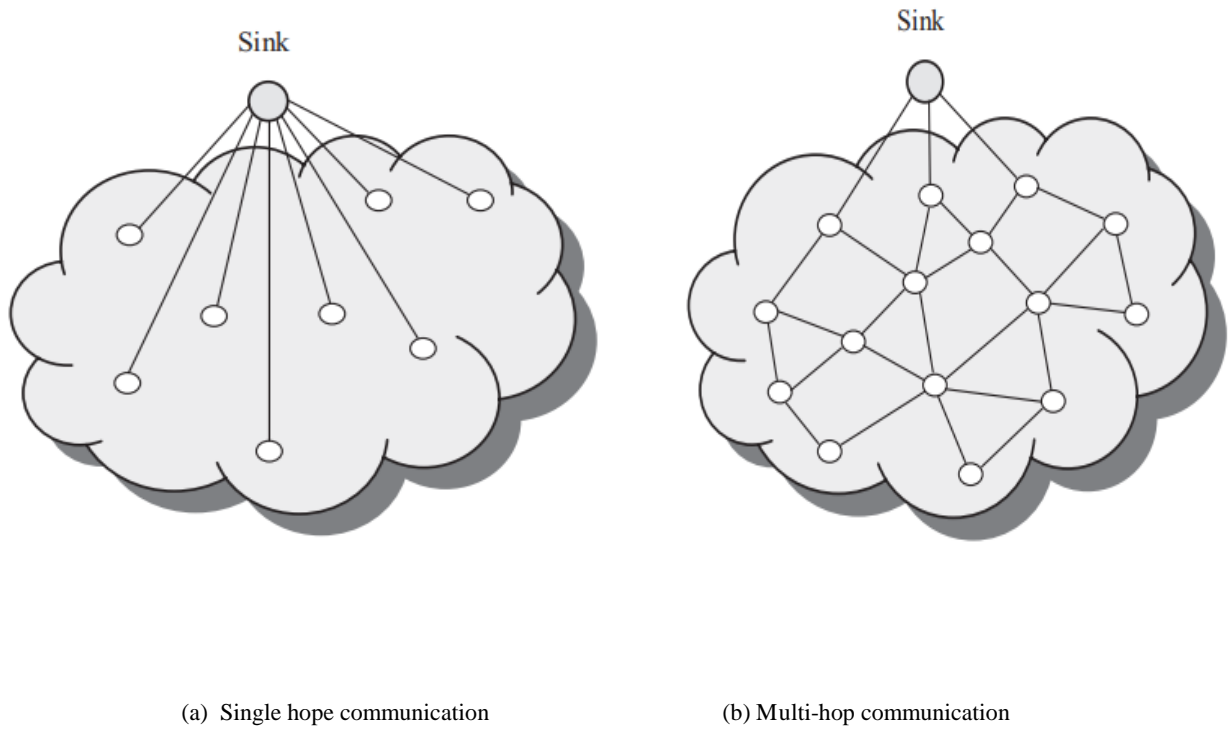


Figure.1.3. WSN flat architecture [12].

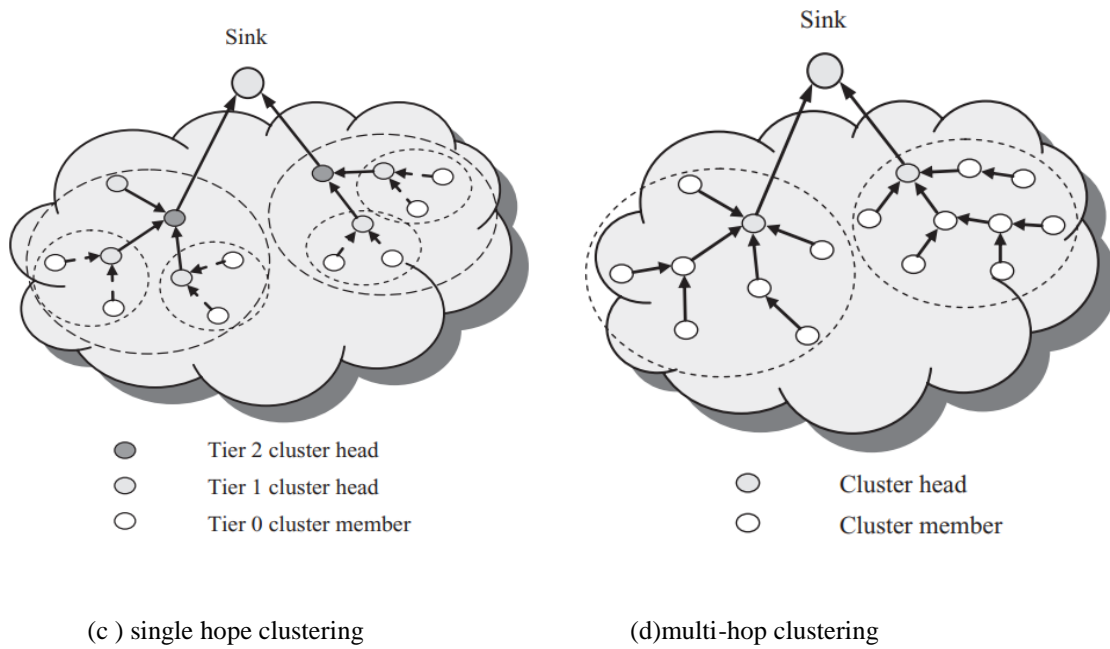


Figure.1.4. WSN hierarchical architecture [12].

1.3. Factors influencing WSN design

The major factors that significantly affect the design of WSNs are scalability, energy consumption, production cost, security, fault tolerance, and sensor network topology. It is important to take these factors into account when designing management architectures for WSNs because they serve as guidelines for designing protocols or algorithms for sensor networks. Additionally, these influencing factors can be used to compare different schemes [1, 13]. In the following section, we will provide an overview of the most important factors that influence the design of sensor networks.

Scalability: Typically, a wireless sensor network contains hundreds or thousands and even millions of sensor nodes. Depending on the application, the number may reach an extreme value of millions, and the schemes must be able to work with this number of nodes. So, in the case of large-scale networks, scalability is a critical factor, guaranteeing that the network performance does not significantly degrade as the network size increases. A good routing protocol is considered scalable and adaptive with modifications in the network topology. Thus, a scalable protocol should perform as well as the network grows or as the workload increases. If additional nodes are added to the network at any time, the routing protocol should not be interrupted.

Energy consumption: energy is one of the major constraints in WSNs. Typically; sensor nodes are equipped with non-rechargeable batteries with limited energy supplies. Moreover, in most applications, these nodes are deployed in hard-to-reach areas, so it is difficult or almost impossible to change or recharge batteries when they are depleted. Thus, the sources that consume energy during the operation of each node should be analyzed and maintained efficiently to operate for a long period of time over months or even years until either its mission time has passed or the battery can be replaced.

Hardware design: when designing hardware for a wireless sensor network, energy efficiency is a crucial consideration. This means that hardware components, including microcontrollers, power control units, and communication modules, must be designed to consume as little energy as possible. By minimizing energy consumption, the sensor nodes can operate for extended periods without the need for frequent battery replacements or recharging, which is especially important in applications where the nodes are deployed in remote or hard-to-reach locations. In addition to energy efficiency, other factors such as the size, weight, and cost of the hardware should also be taken into account when designing sensor nodes for WSNs.

Production cost: is a crucial factor in the design of wireless sensor networks since they often comprise hundreds of tiny sensor nodes. The cost of each individual node is a significant consideration in justifying the overall cost of the network. If the cost of the network is higher than that of traditional sensors, then the deployment of a WSN cannot be justified. Therefore, it is important to keep the price of each node as low as possible. However, the sensor node also incorporates additional units. Consequently, the cost of a sensor node becomes a challenging issue that is directly proportional to the number of functionalities required.

Security: One of the primary challenges in Wireless Sensor Networks (WSNs) is security, as providing high security requirements with limited resources can be difficult. Many wireless sensor networks gather sensitive information, making information security a critical task. It is important to preserve the confidentiality and integrity of data in applications such as monitoring battlefields, structural monitoring, and surveillance. To meet the security requirements, sensor nodes should encrypt data before transmitting it to the neighboring node or base station. Additionally, the accurate and original data should arrive at the base station and then to the end-user. Due to memory constraints, the security code must be small enough to be executed easily by the sensors.

Fault tolerance: Fault tolerance denotes the capacity of a sensor network to keep its functionality without interruption, even in the event of a sensor node failure. Sensor nodes are inexpensive devices that are prone to failure, and each node has a limited battery life. In uncontrolled or harsh environments, the failure rate of a single node can be very high, which is why it is important to ensure that the failure of a single node does not impact the overall functionality of the sensor network. Adaptable protocols can establish new links in case of node failure or link congestion, and the network can adapt by changing its connectivity in the event of a fault. In such cases, a well-designed and efficient routing algorithm is applied to change the overall configuration of the network.

Sensor network topology: is a critical feature for wireless sensor networks (WSNs). The topology in WSNs is dynamic and can change over time due to various reasons, such as node failure due to physical damage, malicious attack, and energy depletion. The positioning of nodes can also change due to their mobility or environmental influences, while new nodes may join the network. Hence, sensor nodes must periodically reconfigure themselves to maintain the desired topology.

1.4. Energy consumption in wireless sensor Network

1.4.1. Power dissipation in a wireless sensor node

A typical sensor node comprises four essential components: a computing subsystem, which consists of a microprocessor or microcontroller; a communication subsystem that utilizes short-range radio technology for wireless communication; a sensing subsystem that connects the node to the physical world, encompassing a group of sensors and actuators; and a power supply subsystem, which often poses challenges when it comes to recharging or replacing it once depleted. During operation, all components, except the power unit, consume energy [14]. Identifying power bottlenecks in the wireless sensor node system and analyzing the sources of energy consumption during the operation of each node is critical. Therefore, this section aims to efficiently analyze the factors that contribute to energy dissipation in a sensor node.

A computing subsystem: The computing subsystem of a sensor node typically consists of a microcontroller unit (MCU) or microprocessor with memory. Its role is to control the sensors and execute communication protocols and signal processing algorithms on the collected sensor data.

Several studies have focused on analyzing the power-performance characteristics of MCUs, and several methods have been suggested to assess the energy consumption of embedded processors. The choice of MCU depends on the required performance levels, and it has a significant and direct impact on the node's power dissipation characteristics. MCUs typically operate in different modes, such as Active, Idle, and Sleep modes, for power management purposes. Each mode is characterized by a specific level of energy consumption. For instance, as per [15], the Strong-ARM consumes 50 mW of power in the idle mode and only 0.16 mW in the Sleep mode. However, transitioning between operating modes incurs a power and latency overhead. Therefore, the energy consumption levels of the different modes, the transition costs, and the amount of time spent by the MCU in each mode all have significant energy consumption implications that affect the battery lifetime of the sensor node.

The sensing subsystem: This subsystem comprises a group of sensors and actuators that establish a connection between the sensor node and the external environment. Each sensor is responsible for measuring specific physical conditions in the environment and converting these measurements into digital signals. However, there are several sources of power consumption within a sensor, including signal sampling, the conversion of physical signals into electrical ones, signal conditioning, and analog-to-digital conversion. Generally, passive sensors like temperature and seismic sensors consume minimal power compared to other components of the sensor node. In contrast, active sensors such as sonar rangefinders, array sensors like imagers, and narrow field-of-view sensors that require repositioning, like cameras with pan-tilt-zoom functionality, can be substantial power consumers [15].

A communication subsystem: the communication subsystem consists of a short-range radio that typically consumes more energy than the other components. Its primary purpose is to enable wireless communication with neighboring nodes and the outside world. However, the power consumption characteristics of a radio are influenced by numerous factors, such as the type of modulation, data rate, transmit power, and operational duty cycle. Generally, radios can work in four distinct modes of operation: transmit, receive, idle, and sleep [16].

1.4.2. Major Reasons of energy waste in WSN

Energy conservation is a critical feature for WSNs, which should be managed wisely to extend the lifespan of the sensor nodes and enable them to function for longer periods. The sensor nodes consume available energy sources during sensing, processing, and transmitting or receiving data to fulfill the requirements of certain applications. Among these functions, the communication subsystem is a greedy source of energy dissipation. Additionally, there is a significant amount of energy wasted in states that are useless from the application point of view [17-19]. Therefore, this section highlights the main causes of energy waste in wireless sensor node communication.

Collision: Typically, sensor nodes use the same radio antenna and share a common transmission channel. This setup increases the possibility of collisions, where a node may receive multiple packets simultaneously, leading to the packets colliding. In the event of a collision, all involved packets need to be discarded, requiring their retransmission, which leads to wasted time and energy.

Overhearing: Overhearing is the phenomenon where a sender transmits a packet, and all nodes within its transmission range receive the packet, even if they are not the intended recipients. This leads to additional energy loss as these nodes consume energy unnecessarily to receive and process packets that are not intended for them.

Control packet overhead: In order to enable data transmissions, many protocols in the MAC layer work by exchanging control messages to ensure various functionalities such as signaling, connectivity, access plan establishment, and collision avoidance. All of these messages require additional energy consumption

Idle Listening: Recognized as a significant source of energy dissipation, idle listening occurs when a sensor node is active and listens for incoming frames, even in the absence of transmitted data. This consumes considerable energy, consequently reducing the lifetime of wireless sensor networks.

Interference: When a packet is transmitted, every node located within the transmission range and interference range receives it, but not all of them can decode it.

1.4.3. Energy conserving techniques

Despite advanced technology in wireless sensor networks, the lifetime of sensor nodes remains a major challenge. Many energy-efficient techniques have been proposed to extend the lifetime of WSNs. In this section, we will describe five main techniques [17].

1. *Data Reduction*: This technique is designed to minimize the volume of generated, processed, and transmitted data. Commonly employed methods include data compression and aggregation.
2. *Protocol Overhead Reduction*: This approach aims to enhance protocol efficiency by minimizing overhead. Techniques involve adjusting transmission periods based on network stability or the distance to the source of transmitted data.
3. *Energy-efficient routing*: A significant task in WSNs is reducing energy consumption in sensor node batteries. Routing protocols can enhance battery lifetime and maximize network lifetime by minimizing end-to-end transmission energy consumption. Routing should be designed to avoid nodes with low residual energy.
4. *Duty cycling*: This technique schedules a sensor node's activity mode and sleep mode. Transmitting, receiving, and idle modes consume a lot of energy, but the sleep mode saves energy. Reducing duty-cycle by shutting down all components except for the part responsible for returning from sleep mode can extend the battery life.
5. *Topology control*: This strategy saves energy by adjusting transmission power while preserving network connectivity and coverage. Topology control is a useful method for reducing energy consumption in wireless sensor networks.

1.5. Wireless Multimedia Sensor Network

1.5.1. WMSN and applications

More recently, the availability of inexpensive hardware such as CMOS (Complementary Metal Oxide Semiconductor) cameras and microphones has encouraged and facilitated the development of so-called Wireless Multimedia Sensor Networks (WMSNs). A WMSN is a new and emerging type of wireless sensor network that is composed of a large number of sensor nodes equipped with multimedia devices such as cameras and microphones. This network allows for the retrieval of multimedia content, such as video and audio streams, still images, as well as scalar

sensor data. In addition to the ability to retrieve multimedia data, WMSNs will also be able to store, process, correlate, and fuse multimedia data originating from heterogeneous sources [20, 21].

Wireless multimedia sensor networks promise a wide range of potential applications in different fields [22, 23] such as battlefield reconnaissance, security monitoring, traffic monitoring and enforcement, industrial process control, automated assistance for the elderly and families, advanced healthcare, and environmental and structural monitoring, among others.

1.5.2. Components of a Wireless Multimedia sensor Network

Typically, a wireless multimedia sensor network is composed of four major components: Wireless Multimedia Node (WMN), Wireless Cluster Head (WCH), Wireless Network Node (WNN), and Base Station (BS). WMN and WCH focus on data processing and WNN on wireless network communications [24, 25].

- **Wireless multimedia node:** Each node is composed of a camera or audio sensor, a processing unit, a communication unit, and a power unit. Each multimedia node captured the desired scene, named image frames, within its Field Of View (FOV). The received data is directly routed to a processing unit for the essential computations aimed at reducing the substantial volume of scene data. In cases where no significant event is detected, images are discarded.
- **Wireless cluster head:** It receives data from several WMNs. Each WCH consists of a processing unit, a communication unit, and a power unit. Sometimes, WMNs' FOV overlaps, so the WCH will perform an aggregation to eliminate overlapping frames.
- **Wireless network node:** The WNN functions similarly to a conventional wireless sensor network, comprising a communication unit and a power unit. The communication unit facilitates the transfer of data between nodes until it reaches the base station.
- **Base Station:** Referred to as the sink, it is equipped with strong processing and energy capabilities. Serving as a type of server, its role involves collecting all network data and transmitting it to the user.

1.5.3. Network Architecture of WMSN

With the emergence of WMSN and its wide variety of multimedia applications, various new types of sensor nodes have been used in addition to scalar sensors (such as multimedia sensors, processing hubs, and storage hubs) with different capabilities and functionalities to gather data of different types and levels of importance. This raises the need to reconfigure the network into different architectures in a way that the network can be more scalable and efficient, depending on its specific application and QoS requirements [26, 27]. In general, the network architectures in WMSNs can be divided into three reference models:

The single-tier flat architecture: it comprises sensor nodes that are homogeneous in terms of energy, computation, and storage capacity. Each node is capable of performing multiple functions, including image capture, multimedia processing, and data delivery to the sink. This architecture is straightforward to manage, and multimedia processing is distributed among the nodes, thereby prolonging the network's lifespan.

The single-tier clustered architecture: deploys a network of heterogeneous sensors, such as multimedia and scalar sensors, within each cluster. In each cluster, all sensor nodes collect scalar and multimedia data from the surrounding environment and transmit it to a cluster head. The cluster head has more resources and computational energy, enabling it to act as a processing hub and perform intensive multimedia processing on the data. The processed information is then wirelessly transmitted to the sink or storage device via the gateway. This architecture provides several advantages, including the ability to address a range of application scenarios, from simple scalar applications to multimedia information processing. Additionally, the use of a cluster head with more resources and computational power allows for more efficient data processing and transmission, leading to reduced energy consumption and extended network lifetime.

The multi-tier architecture: this network is composed of heterogeneous sensors deployed in a hierarchical manner. The first tier consists of scalar WSN nodes that collect basic scalar data from the environment. The second tier comprises camera sensors that gather multimedia data and perform more complicated tasks like object detection and recognition. The final tier contains high-end, powerful camera sensors capable of performing complex tasks like object tracking and feature recognition. Each tier can have a central hub for data processing and communication with higher tiers. This architecture can balance cost, coverage, functionality, and reliability requirements for tasks with varying needs.

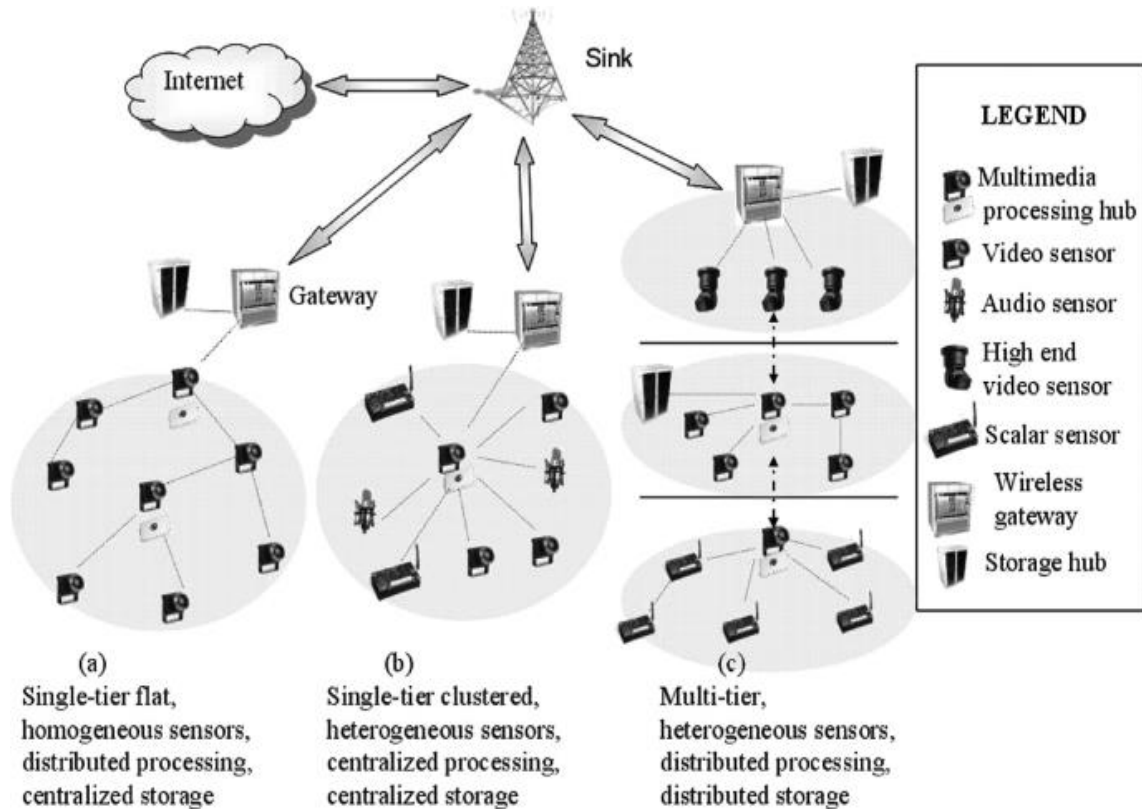


Figure.1.5. Architecture of a wireless multimedia sensor network [28].

1.5.4. Characteristics of wireless multimedia sensor nodes

In general, wireless multimedia sensor networks have similar characteristics to those of a general wireless sensor network. However, they have faced several challenges generated by the multimedia traffic they carry. In this section, we will discuss some of the characteristics that distinguish wireless multimedia sensor networks from general wireless sensor networks and the challenges they face due to multimedia traffic.

1. The information volume and nature of Wireless Multimedia Sensor Networks (WMSNs), which are generally pixel-based, are vastly different from the simple scalar data manipulated by Wireless Sensor Networks (WSNs), such as temperature or humidity. WMSNs, specifically Wireless Multimedia Sensor Networks (WMSNs), are designed to capture visual data such as images or videos, which contain millions of pixels. This makes the data much more complex and voluminous than scalar data. As a result, WMSNs require higher processing power and more energy to handle the large data volumes and complexity of visual data.

2. In Wireless Multimedia Sensor Networks (WMSNs), lost information is frequently acceptable due to the redundant nature of visual flows. Visual data contains a substantial amount of redundant information, and the loss of certain pixels or frames may not significantly impact the overall significance of the captured data. In contrast, within wireless sensor networks, the loss of specific packets can significantly impact the value of gathered data, such as temperature values. As scalar data usually lacks redundancy, the loss of even a minor portion of data can lead to a decrease in accuracy and potentially jeopardize the integrity of the entire dataset.
3. In Wireless Multimedia Sensor Networks (WMSNs), neighboring sensors monitoring the same region of interest may have multiple and dissimilar views of the same scene. This is because visual data, such as images or videos, captures a wide range of information and details that can vary depending on the angle and distance of the sensor from the scene. In contrast, scalar data sensors, such as those measuring temperature or humidity, typically collect a single value for a given region of interest. This value may be the same or similar for neighboring nodes, since scalar data is typically homogeneous and not affected by the angle or distance of the sensor [29].
4. Wireless Multimedia Sensor Networks (WMSNs) typically require higher bandwidth compared to scalar wireless sensor networks (WSNs) due to the larger volume of data that needs to be transmitted. This is particularly challenging for transmitting real-time multimedia applications via wireless communication channels since they demand high bandwidth requirements and strict delay constraints. However, ultra-wideband (UWB) or impulse radio technologies are considered promising communication technologies to provide high bandwidth capacity, especially for multimedia applications in WSNs.
5. Processing scalar data is relatively simple, involving performing mathematical operations on numerical values. However, transmitting multimedia content, such as images and videos, requires a significant amount of bandwidth, and transmitting unprocessed content can be costly. Therefore, the size of the data collected through video sensors in WMSNs must be reduced before transmission by extracting meaningful information from the large and complex visual data captured. Several effective methods can be used to achieve this, such as image coding techniques that remove intraframe and interframe redundancies. However, it's important to note that these techniques must strike a balance between accuracy and computational complexity to ensure that the reduction in data size doesn't sacrifice too much information.
6. a variety of multimedia applications exhibit differing quality-of-service (QoS) requirements such as delay, jitter, phase difference, bandwidth, and path loss. It is crucial to maintain these

QoS requirements to prevent issues with unusable data. Multimedia data in WMSNs can be classified as snapshot-type or streaming. Snapshot-type multimedia data includes event-triggered observations that are obtained within a short time period, such as still images. On the other hand, streaming multimedia content is generated over a longer period of time and requires sustained information delivery. To ensure that these multimedia applications function properly, it is essential to maintain the necessary QoS requirements. This involves providing sufficient bandwidth, reducing delay and jitter, and minimizing the impact of path loss. By meeting these QoS requirements, WMSNs can support various multimedia applications effectively [2, 20].

1.6. Conclusion

In this chapter, we provided an overview of the state of the art of wireless sensor networks (WSNs), which are considered one of the most promising technologies of this century. We described the hardware architecture of a sensor node, network architecture, protocol architecture, and the various factors that affect the design of WSNs. We also highlighted power consumption as an important requirement for wireless sensor networks, as it directly impacts network lifetime. To understand this problem, we identified the different factors that cause energy dissipation in sensor nodes and the major reasons for energy waste in WSNs. We presented various energy conservation techniques that can help extend the lifetime of WSNs.

We have provided a description of a wireless multimedia sensor network (WMSN), which represents a specific instance within the category of wireless sensor networks. Unlike traditional networks that handle only scalar data, WMSNs process large amounts of media, including images and videos, which require higher bandwidth and consume more energy. Therefore, managing the energy consumption in WMSNs is crucial, and an additional effort is necessary to optimize the existing energy conservation methods and minimize power waste in these networks. This will help to extend the network lifetime and ensure the efficient operation of WMSNs.

In the next chapter, we will give an overview of the different image compression techniques proposed in the literature and discuss their applications in wireless multimedia sensor networks.

Chapter 2

Image compression in wireless Multimedia sensor networks

2.1. Introduction

The Wireless Multimedia Sensor Network (WMSN) is an evolution of typical wireless sensor networks. It processes video, audio, and image data in addition to scalar data and sends it to the station base (SB) [30]. However, the multimedia data gathered has a large volume that requires massive storage space and a large bandwidth. This leads to increased energy consumption and causes WMSN to face more issues and limitations due to its limited resources, such as battery power. Consequently, the ideal solution to decrease the data size, decrease power consumption, and increase the sensor's life as much as possible is by using image-compression techniques [31, 32].

Image compression techniques are used to eliminate redundancy in the data that is presented within an image, thereby reducing its size while preserving necessary information [33]. This grants a reduction in storage size, transmission bandwidth, and transmission time [34]. Generally, image compression techniques are classified into two types: lossless and lossy image compression. The advantage of lossy compression over lossless compression techniques is that it gains in decoding time and compression ratio, as well as energy for power-constrained applications [29].

Transform-based compression is a type of lossy compression, as it is used to reduce the size of an image while sacrificing some of its information. The Discrete Cosine Transform (DCT) and the Discrete Wavelet Transform (DWT) are widely used in lossy compression techniques and are integrated into well-known standards such as JPEG and JPEG 2000, respectively. These algorithms are highly encouraged in WMSN as compared with lossless techniques. In this chapter, our focus will be on examining the DCT and DWT transforms. We aim to present a literature review of these transforms, discuss their advantages and shortcomings in the context of Wireless Multimedia Sensor Networks (WMSN), and present various proposed solutions designed to enhance their energy efficiency.

2.2. Image compression in wireless Multimedia sensor network

Digital image compression involves three primary types of redundancies: (1) Spatial redundancy results from the similarity between adjacent pixels in an image. (2) Psychovisual redundancy refers to the unnecessary information that the human visual system overlooks. (3) Coding redundancy occurs when less than optimal code words are employed [32]. Consequently, perfect image compression is attained by eliminating one or more of these redundancies.

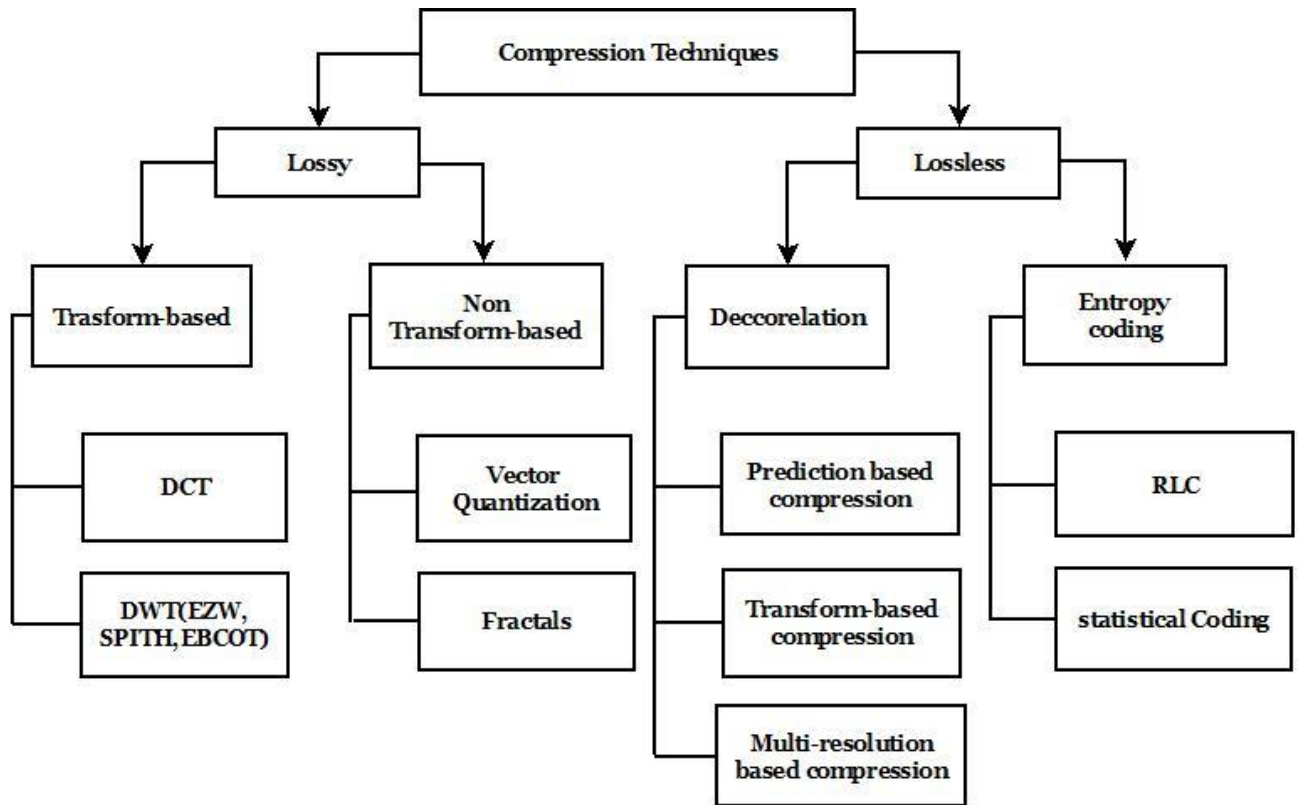


Figure.2.1. Classification of image compression techniques.

Image compression is a process that reduces the size of image data by removing redundant information. In other words, it aims to represent an image in the fewest number of bits possible without losing the essential information content of the original image [35]. This process reduces storage and bandwidth usage while preserving an acceptable visual quality of the reconstructed image.

Generally, image compression techniques are broadly classified into lossy and lossless compression techniques. The classification of image compression techniques is shown in Figure 2.1. Both of these compression techniques have their own advantages and drawbacks. The lossy compression technique achieves a high compression ratio with low image quality, while the lossless technique achieves a lower compression ratio, but the image quality is much closer to the original [32].

2.2.1. Lossless image compression techniques

Lossless Compression is a reversible process that allows the original image to be perfectly reconstructed from the compressed image without any loss of information [36]. The lossless image compression techniques consist of two-stage algorithms:

1. **Decorrelation:** The first step is decorrelation, which aims to remove spatial redundancy between neighboring pixel values using one of the lossless image compression techniques. We can classify these techniques into three types: prediction-based techniques [37], transform-based techniques [38], and multi-resolution-based techniques [39].
2. **Entropy encoding:** The second step after decorrelation is entropy encoding. This process is used to remove the coding redundancy of the image. The most widely used encoding schemes are Run Length Coding (RLC) and Statistical Coding (SC) [40, 41].

2.2.2. Lossy image compression techniques

Lossy compression is a technique that sacrifices some of the original data to produce a reconstructed image that is a close approximation to the original but not identical to it [32, 42]. Lossy techniques are generally classified into two categories:

1. **Non-transform-based image compression:** Techniques that do not use any transforms have the advantage of reducing the computational load caused by the use of transforms to obtain the frequency domain coefficients. Vector Quantization [43, 44] and Fractal compression [45] are the two algorithms used.
2. **Transform-based image compression:** Transform-based techniques are based on converting an input image through a transform into another domain that is less correlated than the original one. The two most commonly used image compression transforms are Discrete Cosine Transform (DCT) and Discrete Wavelet Transform (DWT) [46, 47]. In general, a transform-based algorithm is based on three main stages: spatial decorrelation (also called a source encoder), followed by a quantizer, and finally an entropy encoder.

In the following subsection, our attention will be specifically directed to transform-based image compression, such as JPEG, JPEG2000, and SPITH due to their efficiency in WMSN.

2.3. Principle of image compression algorithm

The main advantage of lossy compression techniques over lossless compression techniques is that they provide gains in encoding and decoding time, compression ratio, and energy consumption in the case of power-constrained applications. As a result, lossy schemes are well-suited for resource-constrained WMSNs [29]. Figure.2.2 shows the whole compression and decompression model. Transform-based image compression mainly consists of three major steps which are [48]:

Transformation: converts images from the spatial domain into the frequency domain in order to remove redundant information from the original data and compact a large fraction of the signal energy into a relatively small set of transform coefficients [49]. Note that this operation is reversible and does not achieve any compression. A significant number of linear transformations have been used for compression, for example [50]: the Karhunen–Loeve transform (KLT), the Walsh–Hadamard transform (WHT), the discrete cosine transform (DCT), the discrete wavelet transform (DWT), and the integer wavelet transform (IWT). Note that the DCT and DWT are widely supported transformations for image and video analysis.

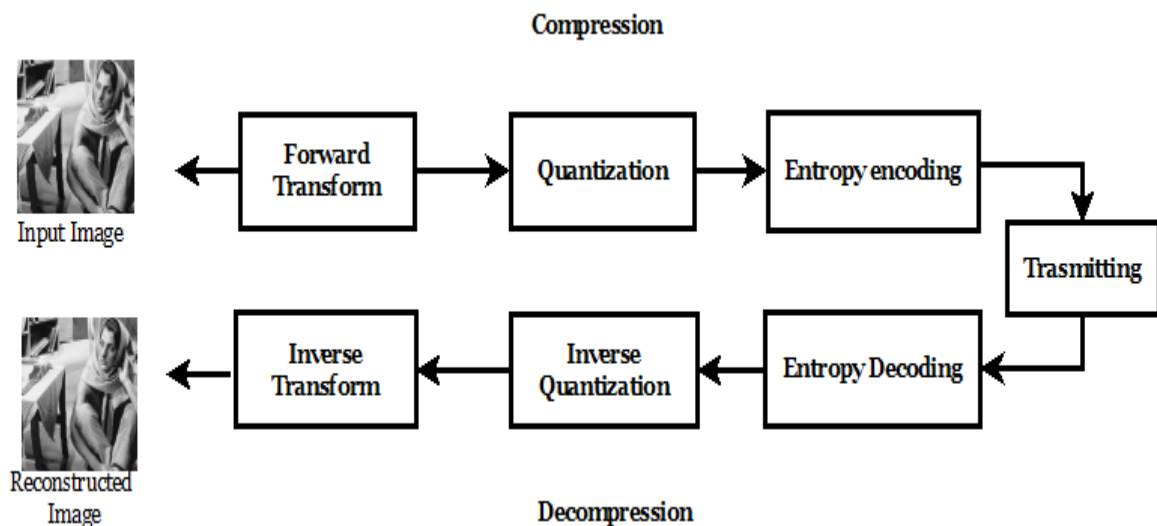


Figure.2.2. The basic Image compression/ decompression model.

Quantization: Quantization, frequently regarded as the primary source of data loss in compression techniques, maps the transformed digital image to a discrete set of levels or a discrete number. In other words, it approximates the coefficients after the transformation with predefined values [49]. This stage is irreversible and introduces a loss in image information, which leads to a degradation in

image quality. The two fundamental types of quantization are scalar and vector quantization, where scalar quantization (SQ) is performed on each individual coefficient and vector quantization (VQ) is performed on a group of coefficients together [35].

Entropy encoding: After quantization, entropy encoding is the final stage in transform-based image compression. It is a popular technique for lossy image compression because it reduces the bit rate without loss of precision. The quantized values are transformed into a binary code word stream to achieve good compression results. The length of each code word in the output bit stream represents the probability of occurrence of each symbol, with symbols of high probability taking short lengths and symbols of low probability taking long lengths. The most commonly used entropy coding methods are Huffman coding, arithmetic coding, and Golomb coding [51, 52].

2.4. Transform-Based DCT Methods

The Discrete Cosine Transform (DCT) is widely used in the field of image and video processing due to its strong energy compaction and decorrelation properties. The DCT is an orthogonal transform that aims to decorrelate image data and minimize spatial redundancy [53]. However, one of the drawbacks of the DCT is the presence of blocking artifacts and contour effects in the reconstructed image at higher compression ratios [54].

JPEG is an acronym for Joint Photographic Experts Group. It is the most popular lossy image compression method that employs the Discrete Cosine Transform (DCT) as a transform coding method. The JPEG standard includes four modes of operation: sequential encoding, progressive encoding, hierarchical encoding, and lossless encoding. The sequential encoding, also known as baseline JPEG coding, is the simplest form and is widely used for lossy methods [55]. The commonly used operation modes for JPEG are:

- ✓ *Sequential encoding:* It is the default JPEG mode each image component is encoded in a single left-to-right, top-to-bottom scan;
- ✓ *Progressive encoding:* the image is encoded in multiple scans rather than in a single scan., in order to produce a quick rough decode image when the transmission time is long;

- ✓ *Hierarchical encoding:* in this mode the image is compressed at multiple resolutions. The lower resolution is accessed without first decompressing the image at its full resolutions, while the image at successively higher resolutions furnishes additional details.
- ✓ *Lossless encoding:* It is a very special case of JPEG because the image is encoded into a single scan while preserves exact, original image reproduction, no loss in its image quality.

In the following section, we will describe sequential encoding, which forms the foundation for other modes. We will use the widely adopted JPEG baseline with an 8 x 8 partitioning.

Sequential JPEG Encoder: In JPEG compression, the input image is first divided into blocks of size 8x8. Then, a 2-dimensional DCT transformation is applied to each block, working from left to right and top to bottom, in order to separate the high and low frequency information. After that, each of the 64 DCT coefficients is uniformly quantized. Following quantization, all of the quantized DCT coefficients are ordered into a zigzag sequence. In the final stage, an entropy encoder such as Huffman coding or Arithmetic Coding is used to efficiently compress the data. For image reconstruction, the inverse operations are performed for each step [55]. Figure 2.3 illustrates the principal steps involved in JPEG baseline image compression and decompression.

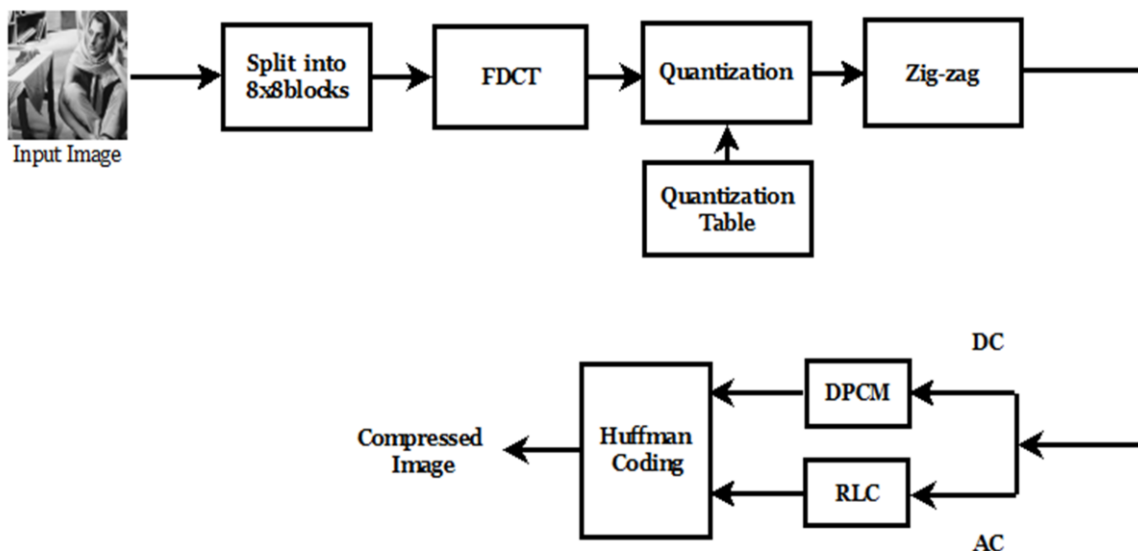


Figure.2.3.Baseline JPEG Compression scheme.

2.4.1. The Discrete Cosine Transform (DCT)

The discrete cosine transform (DCT) is a commonly used technique for signal processing and data compression. This technique permits the conversion of a signal into elementary frequency components [56]. Given that an image is represented as a two-dimensional matrix, the two-dimensional discrete cosine transform (2-D DCT) is employed to calculate the DCT coefficients of an image. The 2-D DCT [57] for an $N \times N$ input sequence $x(i,j)$ can be described as follows:

$$Y(u, v) = \frac{C(v)}{2} \frac{C(u)}{2} \sum_{j=0}^{N-1} \left[\sum_{i=0}^{N-1} x(i, j) \cos \frac{(2i+1)u\pi}{2N} \right] \cos \frac{(2j+1)v\pi}{2N} \quad (2.1)$$

Where: u and $v = 0 \dots N$ and

$$C(u) = \begin{cases} \frac{1}{\sqrt{N}} & \text{If } u = 0 \\ \frac{2}{\sqrt{N}} & \text{else} \end{cases} \quad (2.2)$$

The whole image is first partitioned into small 8×8 rectangular blocks of data in the raster scan order left-to-right and top-to-bottom. By subtracting 128 from each pixel, each pixel is level shifted to convert to a signed integer because the DCT is created to work on pixel values ranging from -128 to 127 [58]. In the next step, the DCT is applied in each bloc using the following function:

$$Y = C * X * C^t \quad (2.3)$$

Where:

X is the leveled input matrix;

Y is the orthogonal matrix and is the transpose;

C is the transformed matrix.

Matrix X is first multiplied by C to create CX . So we will have the row transformation, the obtained result will be multiplied with C' to have the column transformation.

2.4.2. Quantization

Quantization is a lossy compression technique that involves converting a large set of possible infinite values into a much smaller set. In other words, many of the higher frequency components are rounded to zero, and many of the remaining components become small numbers. This process is the primary source of information loss, resulting in degradation in the reconstructed image. After DCT transformation, the element located in the upper-left corner of the block is known as Direct Components (DC) and the other 63 values are Alternative Components (AC). So, all 64 DCT coefficients are quantized using a 64-element quantization table specified by the application or user. Usually, the quantization matrix can be multiplied by a scalar, known as the quality factor, which allows the user to vary the levels of image compression and quality. A very low-quality factor produces the poorest image quality and the highest compression ratio, and vice versa [59]. Therefore, quantization is achieved by dividing each of the 64 DCT coefficients by its corresponding quantizer step size, followed by rounding to the nearest integer value using the formula described below [60]:

$$Y_Q(u, v) = \text{Round} \left(\frac{Y(u, v)}{Q(u, v)} \right) \quad (2.4)$$

Where $Y(u, v)$ are the DCT coefficients and $Q(u, v)$ is the quantization table and it given by:

$$Q = \begin{bmatrix} 16 & 11 & 10 & 16 & 24 & 40 & 51 & 61 \\ 12 & 12 & 14 & 19 & 26 & 58 & 60 & 55 \\ 14 & 13 & 16 & 24 & 40 & 57 & 69 & 56 \\ 14 & 17 & 22 & 29 & 51 & 87 & 80 & 62 \\ 18 & 22 & 37 & 56 & 68 & 109 & 103 & 77 \\ 24 & 35 & 55 & 64 & 81 & 104 & 113 & 92 \\ 49 & 64 & 78 & 87 & 103 & 121 & 120 & 101 \\ 72 & 92 & 95 & 98 & 112 & 100 & 103 & 99 \end{bmatrix}$$

Table.1: JPEG Quantization Table.

For color image, JPEG standard used two quantization matrices for luminance and chrominance planes. These achieved from psychophysical studies with the goal of increasing the compression ratio while decreasing perceptual losses in JPEG images [61-62].

2.4.3. Zigzag Scanning

After the quantization process, a Zig-Zag scan is performed on the resulting quantized coefficients. The main principle of this process is to generate a 1-D vector of coefficients from an 8x8 matrix. It is important to note that low-frequency coefficients are grouped at the top level of the vector, as they are less likely to be zero, while high coefficients are placed at the bottom.

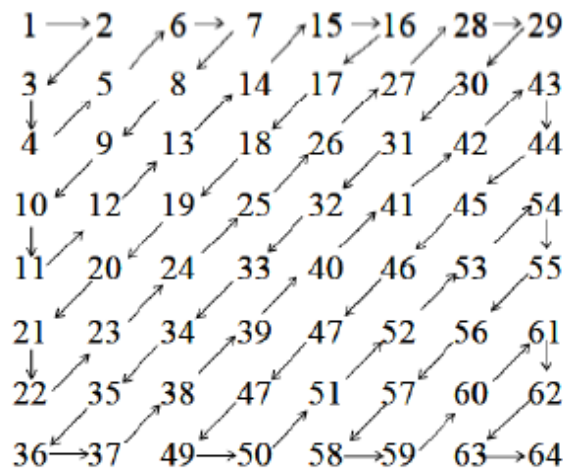


Figure.2.4. Zigzag scanning [2].

After quantization, the DC coefficient is separated from the remaining string of 63 AC coefficients. Both the DC and AC coefficients are encoded separately using two methods: Differential Pulse Code Modulation (DPCM) is used to encode the DC coefficients, while the Run Length Coding (RLC) method is used for encoding the AC coefficients in each block.

DPCM on DC coefficients: The strong correlation between the quantized DC coefficients of neighboring 8x8 blocks is exploited in the DPCM method used for encoding DC coefficients. The DC coefficients are encoded by taking the mean of the differences between each DC value of the current block and the previous block.

RLC on AC coefficients: The 63 coefficients are AC coefficients, and they are scanned from left to right and top to bottom in a zigzag pattern for each block. The AC coefficients are then ordered into the "zigzag" sequence. Finally, a lossless encoding method called RLC is applied to the result of the zigzag scan [55, 63].

2.4.4. Entropy encoder

The final step in the encoding process involves Huffman coding, which is used in the baseline JPEG standard. Huffman coding is a lossless data compression algorithm designed to minimize the size of transmitted data without sacrificing any details. It works by assigning shorter code words to more frequently occurring symbols and longer code words to less frequently occurring symbols. In the JPEG standard, the Huffman tables are defined and used to encode the output of the differential and run-length processes. Each differential coded DC coefficient is encoded by a pair of symbols as (size, amplitude), while each AC coefficient can be represented by the pair (run/size, amplitude) [64-65].

2.4.5. JPEG - Based Schemes for WMSN

The Joint Photographic Expert Group (JPEG) is JPEG is a popular technique for lossy compression that is widely employed. This compression standard uses the DCT transform technique, which is known for its good decorrelation properties. The DCT gives good compression results and uses less memory compared to the DWT. However, one of the prominent drawbacks of this method is that it can produce blocking artifacts in the image, which can lead to a degradation in performance, especially at very low bit rates.

While the DCT has many advantages, using the JPEG compression standard in a wireless multimedia sensor network can be inefficient in terms of power consumption because the DCT stage alone consumes at least 60% of the encoder's power. To address this issue, several approaches have been proposed in the literature to speed up the DCT by reducing its computational complexity and make JPEG a more viable compression scheme for WMSNs [2, 29]. Some of these approaches are discussed below:

Parallel and pipelined implementation of multidimensional DCT consists of using the row/column decomposition based on two 1D processors and an intermediate buffer memory. This approach utilizes the concept of parallelism, which enables the main processing elements and arithmetic units

to operate in parallel, leading to a reduction in both computational complexity and internal storage requirements. Additionally, it allows for high throughput.

Working with fixed-point DCT instead of the more complicated floating-point DCT: In fact, working with floating-point DCT is both energy-intensive and expensive, which is why most hardware platforms choose fixed-point DCT due to its simplicity and low cost [66]. According to [67], for example, encoding a grayscale QCIF image at 1 bit-per-pixel using the StrongARM SA1110 processor with JPEG-integer-point DCT requires 2.87mJ, while using floating-point DCT requires more than 22mJ. Therefore, using fixed-point DCT can help reduce energy consumption and cost while still achieving acceptable levels of performance for multimedia applications.[67, 29].

Converting the greedy operations such as multiplications into light operations: Several fast schemes have been suggested to decrease the computational complexity of the DCT by transforming operations that consume a lot of energy, such as multiplications, into simpler ones like additions and shifts. These multiplierless versions of DCT are low-cost and their implementation in resource-constrained Wireless Multimedia Sensor Networks can be very beneficial in terms of computational complexity and energy consumption [68].

2.5. Transform-Based DWT Methods

The wavelet transform has become one of the most important and powerful tools for signal processing in general, particularly in the field of image compression research. This is due to its ability to work with multiple levels of resolution [69]. This property allows the representation of an image with different locations and scales. The wavelet transform solves the problem of blocking artifacts introduced during DCT compression and provides significant improvements in picture quality [70-71]. The 2D-DWT is depicted by the block diagram in Figure.2.5.

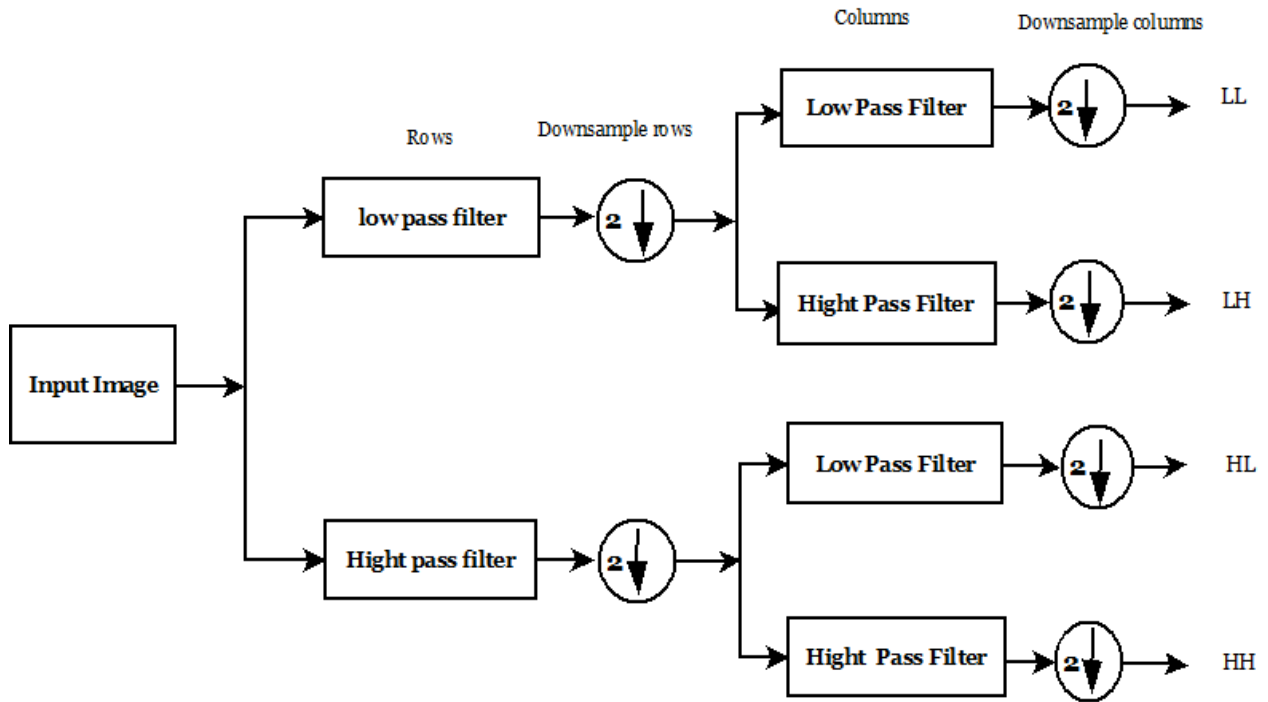


Figure.2.5. Block diagram of DWT.

The DWT transform decomposes and de-correlates the data into multi-resolution sub-bands using a set of basic functions called wavelets, which allows an image analyst to extract the significant components of the sample. In image compression, the 2D wavelet transform is a 2D separable filtering operation across rows and columns of the input image [72]. Its implementation can be achieved by first applying the low-pass filter L and high-pass filter H to the lines of samples, row-by-row, and then re-filtering the output to the columns by the same filters. As a result, four sub-images are obtained: the approximation, the vertical detail, the horizontal detail, and the diagonal detail. They can also be represented as low-low (LL1), high-low (HL1), low-high (LH1), and high-high (HH1). We refer to this process of decomposing the image samples into the four sub-bands as one level of the 2-D DWT [73].

Multiple levels of the transform may be performed by iteratively applying this process to the resulting sub-band. For example, the LL1 sub-band from the previous level can be transformed again to form LL2, LH2, HL2, and HH2 sub-bands, producing the two-level wavelet transform. This process can be repeated to decompose the image into 3, 4, and so on levels. An example of a two-level decomposition into sub-bands is depicted in Figure.2.6. Note that the most important

information is concentrated in the sub-band LL2 of the highest level, also known as DWT approximation, while the high frequencies are not as important to the human eye and are therefore isolated [74-75].

Numerous image compression schemes based on wavelets have been developed due to their effectiveness in compressing images. This paper introduces two well-established compression algorithms utilizing the Discrete Wavelet Transform (DWT): JPEG 2000 and "Set Partitioning in Hierarchical Trees" (SPIHT).

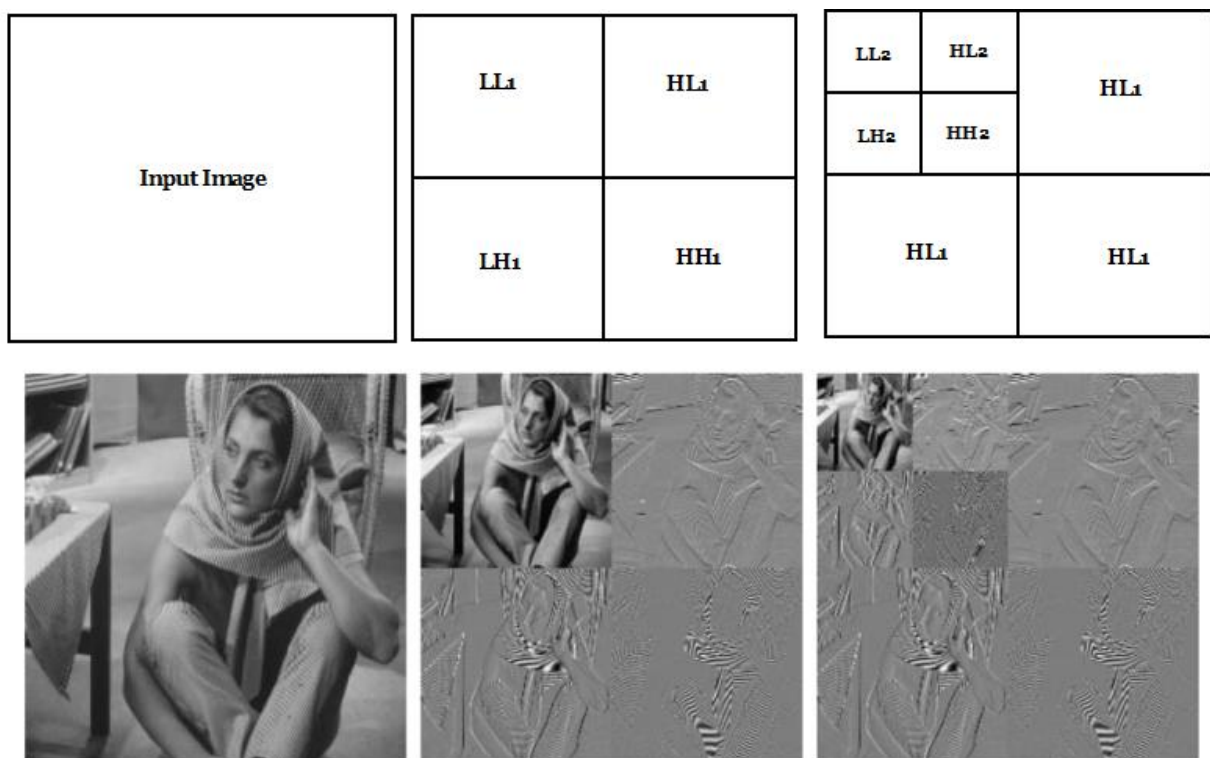


Figure.2.6. Example of two levels DWT decomposition.

2.5.1. Joint Photographic Expert Group 2000 (JPEG2000)

JPEG 2000 is a widely employed compression scheme that utilizes DWT. This standard is an improved version of JPEG that provides many additional functions such as high-resolution image compression, progressive transmission, and scalable image coding. The JPEG 2000 approach is based on the discrete wavelet transform (DWT) and embedded block coding with optimized

truncation (EBCOT) [76-77]. Figure.2.7. shows the coding procedure of the JPEG 2000 encoder and decoder.

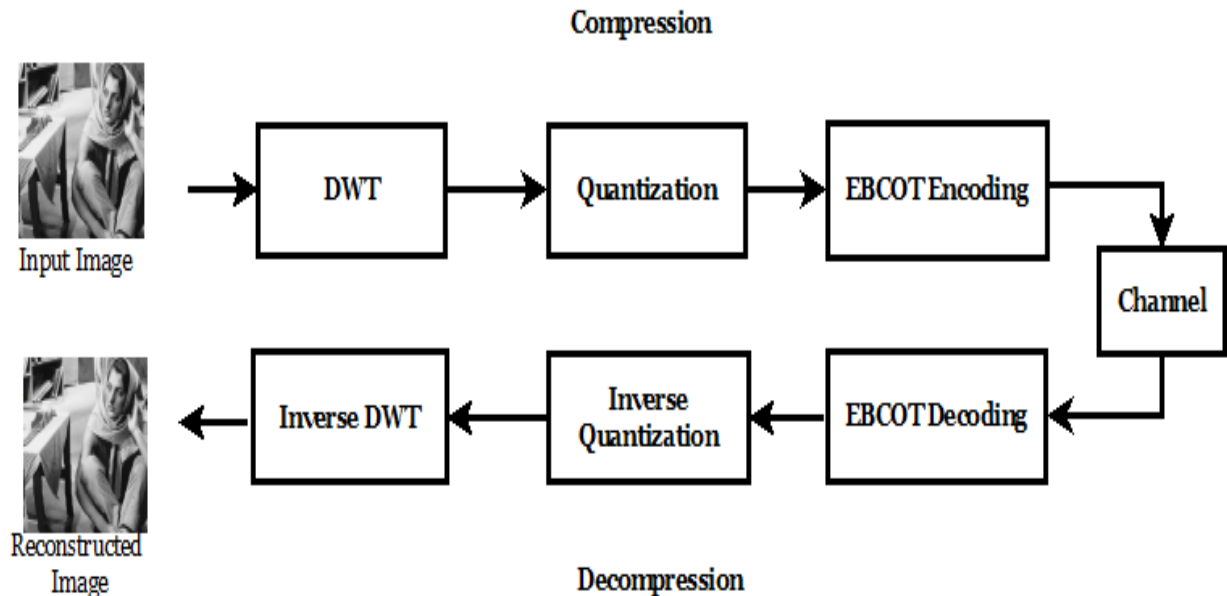


Figure.2.7. The JPEG2000 encoder/decoder.

In JPEG2000, the input image is divided into rectangular regions called tiles, which offers benefits such as reduced memory requirements for the decoder and the ability to decode specific parts of the image while disregarding others. Each tile is then subjected to 2D DWT to decompose it into sub-bands with certain decomposition levels, as described earlier. . After the wavelet transform, all the sub-bands are then quantized using scalar quantization, the simplest quantization method in JPEG 2000. Each sub-band is further divided into small blocks of samples, known as code blocks, which are encoded individually. The EBCOT scheme is used to decompose each code-block into bit-planes, starting from the most significant bit-plane to the least significant bit-plane. The EBCOT process is divided into two tiers - tier-1 and tier-2. Tier-1 is a block coder responsible for forming contexts and arithmetic encoding of the bit-plane data, generating embedded block bit-streams. Tier-2 organizes the bit-streams generated from Tier-1 for transmission purposes [29, 78-79].

2.5.1.1. JPEG 2000 -Based Schemes for WMSN

In JPEG 2000, the most computationally intensive part is the entropy coding, which uses the EBCOT encoder and is divided into two tiers: Tier-1 and Tier-2. Tier-1 is responsible for context formation and arithmetic encoding of the bit-plane data and generates embedded block bit-streams. It is reported that Tier-1 consumes more than 70% of the encoding time, followed by the DWT stage [80]. This high computational intensity increases power consumption, computational complexity, memory requirements, and processing time, making the implementation of JPEG 2000 in power-constrained WMSNs less than an excellent choice. [29, 32].

Several efforts have been made to ameliorate the coding speed and minimize the memory usage of EBCOT by proposing efficient techniques; almost all of them focus on enhancing the context formation phase in different ways. For instance, two speed-up methods known as "sample skipping" and "group-of-column skipping" were suggested to accelerate the encoding process of EBCOT [81]. Another architecture is proposed in [80], where the principle idea is to merge the three coding passes into one pass to improve the overall system performance, reduce system complexity, and minimize memory requirements [29].

2.5.2. Set Partitioning in Hierarchical Tree (SPIHT)

Set Partitioning in Hierarchical Trees (SPIHT) is an improved version of the EZW algorithm and is a powerful wavelet-based image compression algorithm. This algorithm can achieve a much more compact output bitstream than the Embedded Zero Tree of wavelet coefficients (EZW) without the need to add an entropy encoder [82].

In SPIHT, an image is initially transformed into the wavelet domain. The sub bands which are obtained by wavelet transform are then grouped into sets known as spatial orientation trees. After that, the coefficients in each spatial orientation tree are encoded progressively from the most significant bit planes to the least significant bit planes, starting with the coefficients with the highest magnitude. There are two coding passes in SPIHT algorithm, the sorting pass and the refinement pass. The sorting pass looks for zerotrees and sorts significant and insignificant coefficients with respect to a given threshold. And the refinement pass sends the precision bits of the significant coefficients. After one sorting pass and one refinement pass, which can be considered as one scan pass, the threshold T is halved, and the coding process is repeated until the expected bit rate is achieved [29].

2.5.2.1. SPIHT-Based Schemes for WMSN

SPIHT is a powerful image compression technique with several advantages. One of its main benefits is the ability to achieve a very compact output bit stream and a low bit rate, resulting in a high compression ratio without adding an entropy encoder, which makes it efficient in terms of computational complexity. Additionally, it uses a subset partitioning scheme in the sorting pass to reduce the number of magnitude comparisons and decrease the algorithm's computational complexity. Lastly, the progressive mode of SPIHT enables the coding/decoding process to be interrupted at any compression stage [83]. Therefore, implementing SPIHT on WMSN is the best choice [29, 32]. Several efforts have been made to further decrease the computational complexity of SPIHT. For example, in [84], lists were replaced by flags to reduce memory usage. Another approach is the use of a wavelet lifting scheme instead of the convolutional-based wavelet used in the original algorithm.

2.6. Conclusion

In this chapter, we provided an overview of image compression techniques for WMSN, including lossy and lossless compression. Lossy compression techniques are generally classified into two types: transform-based and non-transform-based algorithms. Through our literature review, we found that transform-based algorithms are typically preferred over non-transform-based ones due to their lower computational complexity. We discussed the well-known standards prevalent in WMSN, including JPEG, JPEG2000, and SPIHT, along with their advantages and shortcomings. We also presented some research directions for implementing these techniques in WMSN. Among the discussed schemes, we found that SPIHT is the most powerful technique suitable for WMSN, although DCT can also be useful if its computational complexity is reduced more.

In the following chapter, our focus will be on the low complexity DCT approximation algorithm regarded as an excellent alternative to the exact DCT. We will explain several DCT approximations and evaluate their performance.

Chapter 3

*Energy efficient image compression techniques
in WMSN*

3.1. Introduction

The 8-point discrete cosine transform (DCT) is an essential mathematical tool in image and video coding. This popular transform is well known for its high energy compaction capability and is considered a close approximation to the Karhunen-Loève transform (KLT), which has optimal properties [85]. As a result, the DCT has been adopted as part of many image and video coding standards [86].

In recent years, researchers have proposed several fast transforms that can be used as exact alternatives to the discrete cosine transform (DCT). These transforms have been designed to be fast and efficient, with some being multiplierless approximations of the 8-point DCT that require only additions and bit-shift operations. This feature makes them particularly attractive for multimedia applications in resource-constrained systems such as wireless multimedia sensor networks (WMSNs). In addition to their computational efficiency, these multiplication-free transforms also allow for low-power, high-speed implementations while ensuring adequate numerical accuracy. This balance between computational efficiency and accuracy is crucial in WMSNs and other resource-constrained systems where power consumption and processing speed are critical factors. The efficacy and usefulness of these multiplication-free transforms in such applications have been demonstrated by various studies [87-94].

In the context of low-powered wireless multimedia sensor networks, it is crucial to develop energy-efficient image compression algorithms with low complexity to ensure the efficient use of limited resources. Many researchers have focused on reducing the arithmetic operations of fast transforms by combining approximate DCT with the pruning approach. The pruning technique selectively removes less significant coefficients, which reduces the memory resources and computation required for image compression. Therefore, the combination of approximate DCT with the pruning approach has been shown to maintain a good trade-off between energy consumption, processing time, and image quality as reported in [95-98].

3.2. The properties of DCT

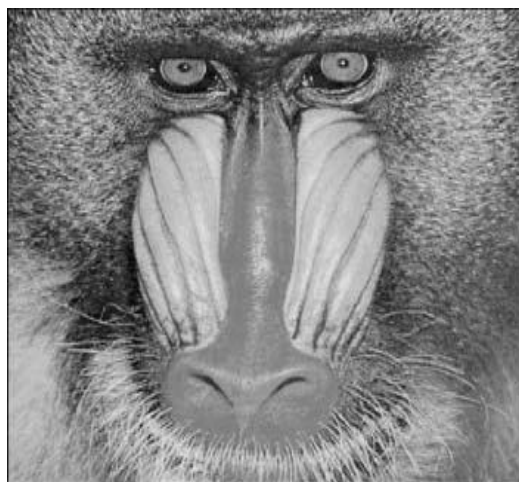
The DCT is a well-known transform that is commonly used in image and video compression standards. It allows for transforming a signal from the spatial domain to the frequency domain, which provides a more compact representation of the signal. There are different variations of the DCT, such as DCT types I-VIII, each with slightly modified definitions and properties. Among the different versions of DCT, Types II and III of the DCT have received significant attention in digital signal processing due to their usefulness. The DCT has several important properties, in this section, we will describe the most important properties of the DCT [57, 99], including:

3.2.1. Decorrelation

Decorrelation is a key advantage of image transformation because it enables the removal of redundancy between neighboring pixels. By reducing correlation between adjacent pixels, transform coefficients become uncorrelated, which allows them to be encoded independently. This process increases the efficiency of image compression, as it reduces the amount of information that needs to be stored or transmitted without loss of quality. Therefore, decorrelation is an important technique in image and video compression applications, enabling high compression ratios while maintaining a visually acceptable level of quality.

3.2.2. Energy compaction

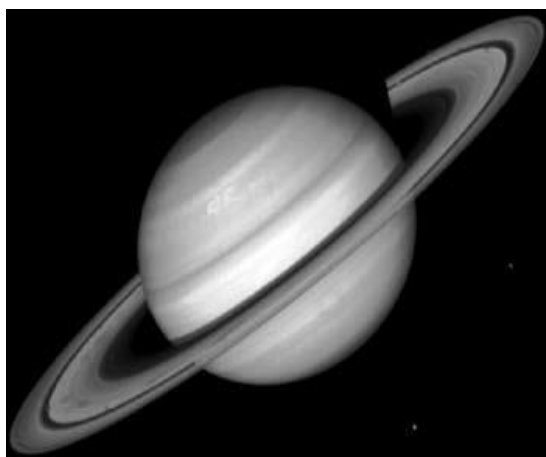
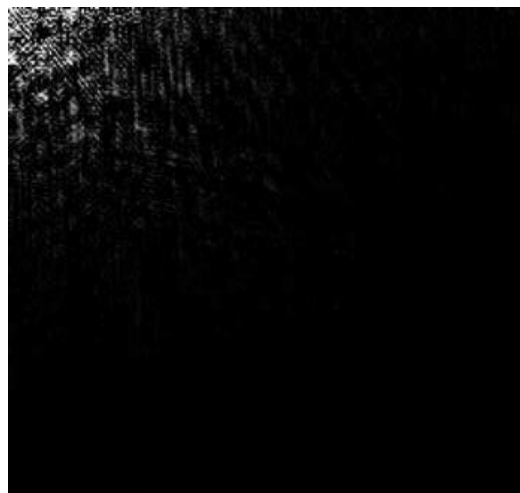
Energy compaction is an important property of the Discrete Cosine Transform (DCT), allowing the concentration of a significant portion of the input signal's energy into a small number of transform coefficients. Specifically, the majority of the signal's energy is concentrated in a few low-frequency coefficients, while the high-frequency coefficients contain less energy. This property is highly beneficial in image and video compression as it permits compression algorithms to discard high-frequency coefficients with relatively little energy while still retaining the most important information present in the low-frequency coefficients.



(a)



(b)



(c)

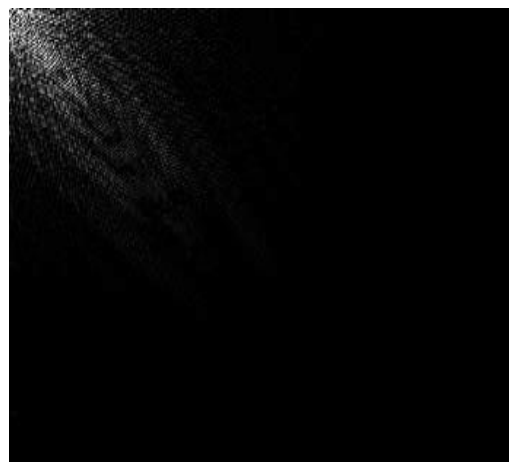


Figure.3.1. (a) Baboon and its DCT. (b) Child and its DCT. (c) Saturn and its [57].

3.2.3. Separability

The separability property of the DCT enables the computation of a 2-D DCT in two steps by applying successive 1-D operations along the rows and columns of the input image data. This row-column decomposition is a valuable property in image and video compression because it reduces the computational complexity of the 2-D DCT and makes it faster to compute, while also requiring less memory and processing resources. This simplifies the hardware requirements for compression and decompression systems and makes it more feasible to use the DCT in real-world applications.

The calculation for the 2-D Discrete Cosine Transform (DCT) equation (2.1) can be expressed as:

$$y(v, j) = \frac{C(v)}{2} \sum_{j=0}^{N-1} y(v, j) \cos \frac{(2j+1)v\pi}{2N} \quad (3.1)$$

Where $y(u, v)$ denotes the row transformation. The representation of this transformation is as follows:

$$y(u, i) = \frac{C(v)}{2} \sum_{i=0}^{N-1} x(u, i) \cos \frac{(2i+1)u\pi}{2N} \quad (3.2)$$

Therefore, the 2-D transform is separable, and consequently, equations (3.1) and (3.2) can be calculated through two successive 1-D transforms applied row-wise and column-wise on the 2-D input data array. This operation can be succinctly described in matrix notation as [2]:

$$Y = (C \cdot (C \cdot X)^t)^t \quad (3.3)$$

Where, C is the $M \times N$ transformation matrix.

3.2.4. Orthogonality

The DCT transformation matrix C is reversible, and its inverse, denoted as C^{-1} , is related by $C^{-1} = C^t$. Hence, the existence of the inverse transform is confirmed, and its computation is expressed as [2]:

$$Y = ((C^t Y).C)^t \quad (3.4)$$

3.3. Review of approximate DCT methods

The discrete cosine transform (DCT) is widely used in various applications, such as image and video compression, due to its ability to reduce redundant information in the original signal, enabling more efficient storage and transmission of data. Despite the development of fast algorithms that significantly decrease the computational complexity of computing the DCT, these algorithms still require the use of floating-point operations, which can be costly in terms of circuit complexity and power consumption. Thus, minimizing the number of floating-point operations is desirable. To tackle this issue, researchers have investigated the use of approximate transforms as a potential solution [94].

In existing research, several approximate methods have been developed for calculating the discrete cosine transform (DCT). Some researchers have developed prominent 8-point approximation-based techniques that take a different approach to further reduce computational complexity. These techniques use a fixed-point arithmetic framework for all calculations instead of floating-point operations, resulting in zero multiplicative complexity and requiring only addition and shift operations. The hardware implementations of these techniques are economical as they do not require multipliers. Consequently, DCT approximations have potential applications in real-time video transmission and processing[88-94].

In this context, Haweel, in [104], suggested a signed DCT (SDCT) which was obtained by applying a signum function to the DCT. It preserves good de-correlation and power compactions properties of the DCT. The SDCT necessitates 24 additions but it lacks the orthogonality. The

transform presented in [87], which is called biorthogonal transform (BinDCT) needs 13 additions and 14 shift operations. This transform presents a good approximation to the exact DCT. In [88] Cintra *et al.*, proposed a rounded DCT approximation (RDCT) with 22 additions. This approximation has shown a better performance in image and video compression especially in HEVC implementation. In [89], Bayer *et al.*, introduced a very low-complexity approximation called modified rounded DCT (MRDCT). This approximation is derived from the RDCT by introducing some zeros to its matrix and needs only 14 additions. Despite its huge reduction of the computational complexity, it gives an acceptable image quality, Bouguezél–Ahmad–Swamy in [90-93] proposed several DCT approximations such as, BAS-2008, BAS-2009, BAS-2011 and BAS-2013. The series of BAS have shown a good efficiency in image and video compression due to their good tradeoff between complexity and performance. In [94] Potluri *et al.*, created a new approximation which has 14 additions, just like the MRDCT, but highly better in terms of peak signal to noise ratio (PSNR).

3.4. Mathematical Background

3.4.1. 8-point DCT approximations

This section presents a discussion on the popular 8-point DCT approximations that have been documented in the literature. These approximations only require addition and/or shift operations, which are faster than multiplication operations. The transformation matrix of these approximations can be represented as a product of two matrices: a low-complexity matrix \mathbf{T} and a scaling diagonal matrix \mathbf{S} . The entries of the low-complexity matrix \mathbf{T} are restricted to powers of two in the set $\{0, \pm 1/2, \pm 1, \pm 2\}$, which eliminates the need for multiplication operations. The scaling diagonal matrix \mathbf{S} ensures orthogonality in the approximation and does not add any extra computation overhead to image and video compression applications. It can be easily integrated into the quantization step of certain compression algorithms [94].

The following format of the approximation is furnished by:

$$\mathbf{C} = \mathbf{S} \cdot \mathbf{T} \quad (3.5)$$

Where \mathbf{S} is the scaling diagonal matrix given by:

$$\mathbf{S} = \sqrt{\text{diag}(\mathbf{T} \cdot \mathbf{T}^T)^{-1}} \quad (3.6)$$

Where, $\text{diag}(\cdot)$ returns a diagonal matrix with the diagonal elements of its argument.

A. Bouguezel-Ahmad-Swamy (BAS-2008)

In [90], Bouguezel et al. introduced a low-complexity approximation referred to as the BAS-2008 approximation. This approximation has null multiplicative complexity and requires only 14 additions and 1 shift. It was obtained from the SDCT matrix described in [104] by appropriately introducing some 0s and $\frac{1}{2}$ s in its entries. The mathematical structure of the BAS-2008 approximation can be described as follows:

$$\mathbf{C}_1 = \mathbf{S}_1 \cdot \mathbf{T}_1 \quad (3.7)$$

$$= \mathbf{S}_1 \cdot \begin{bmatrix} 1 & 1 & 1 & 1 & 1 & 1 & 1 & 1 \\ 1 & 1 & 0 & 0 & 0 & 0 & -1 & -1 \\ 1 & \frac{1}{2} & -\frac{1}{2} & -1 & -1 & -\frac{1}{2} & \frac{1}{2} & 1 \\ 0 & 0 & -1 & 0 & 0 & 1 & 0 & 0 \\ 1 & -1 & -1 & 1 & 1 & -1 & -1 & 1 \\ 1 & -1 & 0 & 0 & 0 & 0 & 1 & -1 \\ \frac{1}{2} & -1 & 1 & -\frac{1}{2} & -\frac{1}{2} & 1 & -1 & \frac{1}{2} \\ 0 & 0 & 0 & -1 & 1 & 0 & 0 & 0 \end{bmatrix} \quad (3.8)$$

Where

$$\mathbf{S}_1 = \text{diag} \left(\frac{1}{\sqrt{8}}, \frac{1}{\sqrt{4}}, \frac{1}{\sqrt{5}}, \frac{1}{\sqrt{2}}, \frac{1}{\sqrt{8}}, \frac{1}{\sqrt{4}}, \frac{1}{\sqrt{5}}, \frac{1}{\sqrt{2}} \right) \quad (3.9)$$

B. Bouguezel –Ahmed-Swamy (BAS-2009)

In [91], Bouguezel *et al*, presented a new low-complexity approximate that required 18 additions and it named as BAS-2009 approximation. The latter is derived from the 8x8 SDCT matrix by setting some of its entries to zero. The following mathematical structure of BAS-2009 approximation is given by:

$$C_2 = S_2 \cdot T_2 \quad (3.10)$$

$$= S_2 \cdot \begin{bmatrix} 1 & 1 & 1 & 1 & 1 & 1 & 1 & 1 \\ 1 & 1 & 0 & 0 & 0 & 0 & -1 & -1 \\ 1 & 1 & -1 & -1 & -1 & -1 & 1 & 1 \\ 0 & 0 & -1 & 0 & 0 & 1 & 0 & 0 \\ 1 & -1 & -1 & 1 & 1 & -1 & -1 & 1 \\ 1 & -1 & 0 & 0 & 0 & 0 & 1 & -1 \\ 1 & -1 & 1 & -1 & -1 & 1 & -1 & 1 \\ 0 & 0 & 0 & -1 & 1 & 0 & 0 & 0 \end{bmatrix} \quad (3.11)$$

Where

$$S_2 = \text{diag} \left(\frac{1}{2\sqrt{2}}, \frac{1}{2}, \frac{1}{2\sqrt{2}}, \frac{1}{\sqrt{2}}, \frac{1}{2\sqrt{2}}, \frac{1}{2}, \frac{1}{2\sqrt{2}}, \frac{1}{\sqrt{2}} \right) \quad (3.12)$$

C. Parametric Transform

A one-parameter eight-point orthogonal approximation is suggested by Bouguezel-Ahmad-Swamy [92]. This approximation is known as the BAS-2011 transform, and it is achieved by introducing an arbitrary parameter into the transform matrix, as reported in [90], and by making certain row permutations.

The transform matrix is given by:

$$C^{(a)} = S^{(a)} \cdot T^{(a)} \quad (3.13)$$

$$= S^{(a)} \cdot \begin{bmatrix} 1 & 1 & 1 & 1 & 1 & 1 & 1 & 1 \\ 1 & 1 & 0 & 0 & 0 & 0 & -1 & -1 \\ 1 & a & -a & -1 & -1 & -a & a & 1 \\ 0 & 0 & -1 & 0 & 0 & 1 & 0 & 0 \\ 1 & -1 & -1 & 1 & 1 & -1 & -1 & 1 \\ 1 & -1 & 0 & 0 & 0 & 0 & 1 & -1 \\ a & -1 & 1 & -a & -a & 1 & -1 & a \\ 0 & 0 & 0 & -1 & 1 & 0 & 0 & 0 \end{bmatrix} \quad (3.14)$$

Where

$$S^{(a)} = \text{diag}\left(\frac{1}{\sqrt{8}}, \frac{1}{\sqrt{2}}, \frac{1}{\sqrt{4+4a^2}}, \frac{1}{\sqrt{2}}, \frac{1}{\sqrt{8}}, \frac{1}{\sqrt{2}}, \frac{1}{2}, \frac{1}{\sqrt{4+4a^2}}\right). \quad (3.15)$$

Typically, the parameter a is chosen as a small integer to reduce the complexity of $T^{(a)}$ and to maintain the orthogonality property of the resulting parametric. It's worth noting that suggested values for a include $a \in \{0, 1, \frac{1}{2}\}$. Additionally, certain row permutations are applied to the transform matrix, as mentioned in [bas2008], to enhance the energy compaction capability of the transform.

D. Binary DCT (BAS-2013)

Bouguezel et al. introduced an effective approximation of the DCT [93]. This transformation has been proposed by exploiting the Walsh-Hadamard transform (WHT) and has been successfully used to develop the binary discrete cosine transform (BDCT).

The Binary DCT (BDCT) matrix is defined as:

$$C_3 = S_3 \cdot T_3 \quad (3.16)$$

$$=S_3 \cdot \begin{bmatrix} 1 & 1 & 1 & 1 & 1 & 1 & 1 & 1 \\ 1 & 1 & 1 & 1 & -1 & -1 & -1 & -1 \\ 1 & 1 & -1 & -1 & -1 & -1 & 1 & 1 \\ 1 & 1 & -1 & -1 & 1 & 1 & -1 & -1 \\ 1 & -1 & -1 & 1 & 1 & -1 & -1 & 1 \\ 1 & -1 & -1 & 1 & -1 & 1 & 1 & -1 \\ 1 & -1 & 1 & -1 & -1 & 1 & -1 & 1 \\ 1 & -1 & 1 & -1 & 1 & -1 & 1 & -1 \end{bmatrix} \quad (3.17)$$

Where

$$S_3 = \text{diag} \left(\frac{1}{\sqrt{8}}, \frac{1}{\sqrt{8}}, \frac{1}{\sqrt{8}}, \frac{1}{\sqrt{8}}, \frac{1}{\sqrt{8}}, \frac{1}{\sqrt{8}}, \frac{1}{\sqrt{8}}, \frac{1}{\sqrt{8}} \right) \quad (3.18)$$

E. CB-2011 Approximation

In [88], Cintra et al. introduced the Rounded Discrete Cosine Transform (RDCT). This method involves applying rounding operations to the standard DCT matrix, resulting in a matrix with entries exclusively $\{0, 1, -1\}$. As a result, multiplication operations are eliminated. The RDCT achieves competitive performance compared to the current state-of-the-art DCT approximations, requiring only 22 additions. The transformation matrix produced by this approach can be expressed as follows:

$$C_4 = S_4 \cdot T_4 \quad (3.19)$$

$$=S_4 \cdot \begin{bmatrix} 1 & 1 & 1 & 1 & 1 & 1 & 1 & 1 \\ 1 & 1 & 1 & 0 & 0 & -1 & -1 & -1 \\ 1 & 0 & 0 & -1 & -1 & 0 & 0 & 1 \\ 1 & 0 & -1 & -1 & 1 & 1 & 0 & -1 \\ 1 & -1 & -1 & 1 & 1 & -1 & -1 & 1 \\ 1 & -1 & 0 & 1 & -1 & 0 & 1 & -1 \\ 0 & -1 & 1 & 0 & 0 & 1 & -1 & 0 \\ 0 & -1 & 1 & -1 & 1 & -1 & 1 & 0 \end{bmatrix} \quad (3.20)$$

Where

$$S_4 = \text{diag}\left(\frac{1}{\sqrt{8}}, \frac{1}{\sqrt{6}}, \frac{1}{2}, \frac{1}{\sqrt{6}}, \frac{1}{\sqrt{8}}, \frac{1}{\sqrt{6}}, \frac{1}{2}, \frac{1}{\sqrt{6}}\right). \quad (3.21)$$

F. Modified CB-2011 Approximation

In [89], Bayer et al. introduced a modified version of the Rounded DCT called the MRDCT. This approximation is derived from the RDCT matrix by replacing some of its elements with zeros. The resulting approximation has the lowest computational complexity among all DCT approximations found in the literature, requiring only 14 additions and its matrix is given by:

$$C_5 = S_5 \cdot T_5 \quad (3.22)$$

$$= S_5 \cdot \begin{bmatrix} 1 & 1 & 1 & 1 & 1 & 1 & 1 & 1 \\ 1 & 0 & 0 & 0 & 0 & 0 & 0 & -1 \\ 1 & 0 & 0 & -1 & -1 & 0 & 0 & 1 \\ 0 & 0 & -1 & 0 & 0 & 1 & 0 & 0 \\ 1 & -1 & -1 & 1 & 1 & -1 & -1 & 1 \\ 0 & -1 & 0 & 1 & -1 & 0 & 1 & 0 \\ 0 & -1 & 1 & 0 & 0 & 1 & -1 & 0 \\ 0 & 0 & 0 & -1 & 1 & 0 & 0 & 0 \end{bmatrix} \quad (3.23)$$

Where

$$S_5 = \text{diag}\left(\frac{1}{\sqrt{8}}, \frac{1}{\sqrt{2}}, \frac{1}{2}, \frac{1}{\sqrt{2}}, \frac{1}{\sqrt{8}}, \frac{1}{\sqrt{2}}, \frac{1}{2}, \frac{1}{\sqrt{2}}\right). \quad (3.24)$$

3.4.2. Pruned approximate DCT

After the successful uses of all the above approximations in image and video compression, many efforts paid more attention to the pruning approach for reducing more the computational complexity of these approximations. This pruned approach consists on computing only the significant subset of 2D DCT of size $L \times L$ (where $L < 8$) where most of the energy is concentrated in

that region while, the high-frequency DCT coefficients are often zeroed by the quantization process. In [95] Lecuire *et al.*, suggested the two-dimensional version (2D) of the pruned DCT. This method called Zonal DCT where Zonal is an alternative terminology. On the other hand, several 2D DCT approximations have also been combined with the pruned approach. For instance, Coutinho *et al.*, in [96] introduced a very low complexity DCT approximation that necessitates only 10 additions. It was obtained by mixing the MRDCT approximation with the pruned version (P.MRDCT). However, its performance in image compression is not sufficient due to the significant reduction in computational complexity. Kouadria *et al.*, in [97] introduced an excellent pruned approximation based on the binary DCT. This method achieved a competitive performance which makes it very suitable in Wireless visual sensor Networks (WVSNs). In [98] Mechouek *et al.*, suggested a new pruned approximation which is named pruned rounded DCT approximation (P.RDCT). This latter keeps a good trade-off between energy consumption, processing time and image quality. Therefore, the pruned approach has shown a very good ability to minimize considerably the number of arithmetic operations and memory resources and hence ensuring low energy consumption in resource constrained systems.

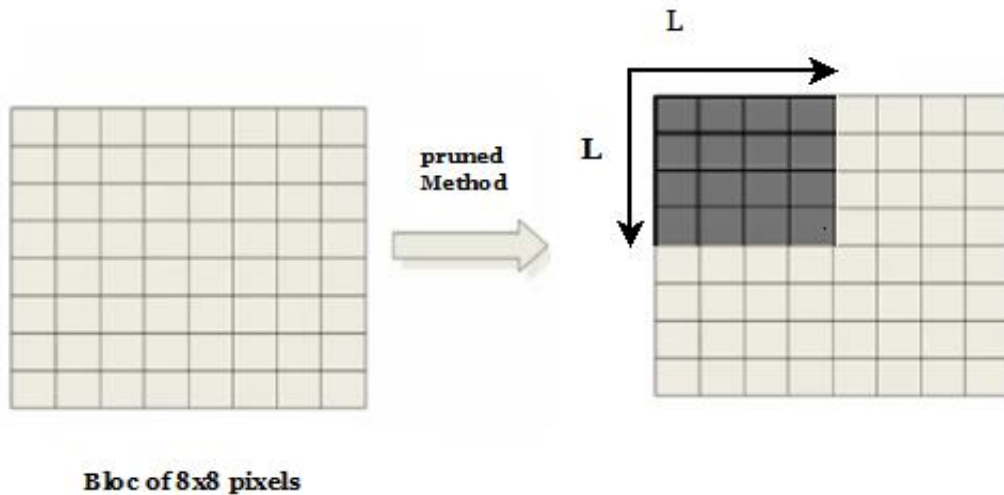


Figure.3.2. Pruned method adopted in several approximations.

It is indeed a well-known fact that the useful signal information in some applications, such as data compression, is often concentrated in the lower DCT coefficients due to the strong energy compaction property of the DCT. The 2-D 8x8 DCT transform allows for almost all of this block energy to be concentrated in the 4x4 first DCT coefficients, which correspond to the low-frequency components of the signal. This methodology is known as the zonal DCT, and it involves selecting a square zone of size LxL, where L<8, within the 8x8 block of DCT coefficients and keeping these coefficients close to the DC component. This allows for the useful signal information to be preserved while reducing the number of DCT operations required for compression [95,101].

In a JPEG chain, we can compute these 4x4 DCT coefficients for each 8x8 block of the image, instead of computing the full 8x8 DCT. This leads to a significant reduction in the number of operations required for compression [102].

$$Y_{LXL} = C_{LX8} \cdot X_{8X8} \cdot C_{8XL}^t \tag{3.25}$$

Where C_{LX8} is the -pruned transformation matrix and its expression is as follows:

$$C_{LX8} = S_{LXL} \cdot T_{LX8} \tag{3.26}$$

Where

$$T_{LX8} = \begin{bmatrix} T_{0,0} & T_{0,1} & \dots & T_{0,7} \\ T_{1,0} & T_{1,1} & \dots & T_{1,7} \\ \vdots & \vdots & \ddots & \vdots \\ T_{L-1,0} & T_{L,1} & \dots & T_{L-1,7} \end{bmatrix} \tag{3.27}$$

$$S_{LXL} = \text{diag}(S_{0X0}, S_{1X1}, \dots, S_{L-1,L-1}) \tag{3.28}$$

Note that C_{LX8} is a semi-orthogonal matrix.

Table.3.1. shows the various pruned approximations obtained by applying the pruning approach to DCT approximations. This is done by discarding the lower rows of the low-complexity matrix. Each of these pruned approximations is semi-orthogonal and requires fewer operations than the 8-

point DCT approximations. In the next section, we will provide more details about their efficiency in terms of computational complexity, image quality, and energy consumption.

Method	T	S
P.BAS-2008	$\begin{bmatrix} 1 & 1 & 1 & 1 & 1 & 1 & 1 & 1 \\ 1 & 1 & 0 & 0 & 0 & 0 & -1 & -1 \\ 1 & \frac{1}{2} & -\frac{1}{2} & -1 & -1 & -\frac{1}{2} & \frac{1}{2} & 1 \\ 0 & 0 & -1 & 0 & 0 & 1 & 0 & 0 \end{bmatrix}$	$diag\left(\frac{1}{\sqrt{8}}, \frac{1}{\sqrt{4}}, \frac{1}{\sqrt{5}}, \frac{1}{\sqrt{2}}\right)$
P.BAS-2009	$\begin{bmatrix} 1 & 1 & 1 & 1 & 1 & 1 & 1 & 1 \\ 1 & 1 & 0 & 0 & 0 & 0 & -1 & -1 \\ 1 & 1 & -1 & -1 & -1 & -1 & 1 & 1 \\ 0 & 0 & -1 & 0 & 0 & 1 & 0 & 0 \end{bmatrix}$	$diag\left(\frac{1}{2\sqrt{2}}, \frac{1}{2}, \frac{1}{2\sqrt{2}}, \frac{1}{\sqrt{2}}\right)$
P.BAS-2013	$\begin{bmatrix} 1 & 1 & 1 & 1 & 1 & 1 & 1 & 1 \\ 1 & 1 & 1 & 1 & -1 & -1 & -1 & -1 \\ 1 & 1 & -1 & -1 & -1 & -1 & 1 & 1 \\ 1 & 1 & -1 & -1 & 1 & 1 & -1 & -1 \end{bmatrix}$	$diag\left(\frac{1}{\sqrt{8}}, \frac{1}{\sqrt{8}}, \frac{1}{\sqrt{8}}, \frac{1}{\sqrt{8}}\right)$
P.RDCT	$\begin{bmatrix} 1 & 1 & 1 & 1 & 1 & 1 & 1 & 1 \\ 1 & 1 & 1 & 0 & 0 & -1 & -1 & -1 \\ 1 & 0 & 0 & -1 & -1 & 0 & 0 & 1 \\ 1 & 0 & -1 & -1 & 1 & 1 & 0 & -1 \end{bmatrix}$	$diag\left(\frac{1}{\sqrt{8}}, \frac{1}{\sqrt{6}}, \frac{1}{2}, \frac{1}{\sqrt{6}}\right)$
P.MRDCT	$\begin{bmatrix} 1 & 1 & 1 & 1 & 1 & 1 & 1 & 1 \\ 1 & 0 & 0 & 0 & 0 & 0 & 0 & -1 \\ 1 & 0 & 0 & -1 & -1 & 0 & 0 & 1 \\ 0 & 0 & -1 & 0 & 0 & 1 & 0 & 0 \end{bmatrix}$	$diag\left(\frac{1}{\sqrt{8}}, \frac{1}{\sqrt{2}}, \frac{1}{2}, \frac{1}{\sqrt{2}}\right)$

Table.3.1: Pruned DCT approximations.

3.5. Conclusion

The DCT is employed in numerous images and video coding standards because of its effective energy compaction properties, which are closely related to the Karhunen-Loeve transform. In this chapter, we have discussed some important properties of the DCT that are of particular value to image processing applications. Several low computational complexity approximations of the DCT have been presented in this chapter. These techniques possess extremely low arithmetic complexities, requiring only addition and/or bit-shift operations. Indeed, their performance characteristics seem similar to those of the exact DCT, such as orthogonality, separability, energy compaction, making them a viable alternative to the DCT. Additionally, their hardware implementations are very economical due to the absence of multipliers.

We have also introduced another approach for reducing the computation cost of the DCT transform, which is called pruning. This method reduces the number of DCT coefficients that need to be computed by encoding and transmitting only the coefficients within a specified region. To address the problem of energy consumption in WMSNs (Wireless Multimedia Sensor Networks), numerous approximations have been combined with this technique, allowing for a good trade-off between energy consumption and computation cost.

In the next chapter, we will introduce our new pruned approach, designed to ensure a good tradeoff between image quality, computational complexity, and energy consumption. These characteristics make it highly suitable for resource constrained Wireless Multimedia Sensor Networks (WMSNs) that demand low bitrates.

Chapter 4

Proposed low complexity pruned DCT approximation for image compression

4.1. Introduction

Actually, wireless multimedia sensor networks (WMSNs) face significant challenges in transmitting multimedia content due to the limited bandwidth, energy, and processing capabilities of the sensor nodes. Image compression is a widely used technique to address these challenges by removing redundant information from raw data, which enables more efficient transmission of multimedia content. Images captured by sensor nodes must be processed and compressed before transmission to achieve this efficiency. Removing redundant information from raw data via compression helps to conserve limited bandwidth and energy resources in WMSNs [32].

While conventional algorithms such as JPEG, JPEG2000, and SPIHT have demonstrated commendable performance in image compression concerning the compromise between distortion and bitrate, they may not always be suitable for software implementation, especially in embedded systems designed for low power consumption. These algorithms often require substantial computational costs and memory access, posing challenges for the limited energy resources of Wireless Multimedia Sensor Networks (WMSNs) [103].

The discrete cosine transform (DCT), which is widely used in image and video compression standards due to its good energy compaction properties, has been identified as one of the most energy-intensive parts of the JPEG standard. In fact, it alone consumes more than 60% of the whole encoder energy[86]. As a result, researchers have focused on proposing fast algorithms for the exact DCT that reduce its algorithmic complexity to benefit from time, speed, and energy [87-98].

As we mentioned in the previous chapter, several approximate DCT methods have been proposed to reduce the computational complexity of exact DCT method. While these methods may sacrifice some level of precision for faster computation, they can still provide significant benefits for WMSN in terms of reducing energy consumption[104-105].

To further decrease the algorithmic complexity of DCT, this chapter proposes to combine an approximate DCT method with a pruning approach. The new pruned approximation has an extremely low computational cost, requiring only 10 additions for its calculation. The objective of this chapter is twofold: firstly, to reduce the computational cost of DCT by using only addition

operations instead of expensive multiplication operations, and secondly, to calculate only the most important low-frequency coefficients using the pruning approach. This results in a reduction in energy consumption and, therefore, a longer lifespan of the network, which is a common problem in wireless sensor networks.

4.2. Proposed Transform

4.2.1. Pruned RDCT approximation

The pruned version of the RDCT approximation (discussed in the previous chapter) which is referred to as pruned rounded DCT (P.RDCT) [97] has shown a good performance especially in WMSN due to the reduction in energy consumption and processing time. Moreover, it maintains an excellent image quality in terms of PSNR.

Let $X_{8 \times 8}$ be an 8×8 block of an image. Thus, the pruned DCT approximation coefficients $Y_{4 \times 4}$ are given by:

$$Y_{4 \times 4} = C_{4 \times 8} \times X_{8 \times 8} \times C_{8 \times 4}^t \quad (4.1)$$

The exponent t defines the transposed matrix. $C_{4 \times 8}$ is the 4-pruned transform matrix that can be written as:

$$C_{4 \times 8} = D_{4 \times 4} \times T_{4 \times 8} \quad (4.2)$$

And D is a scaling diagonal matrix, given by:

$$D = \text{diag}\left(\frac{1}{2\sqrt{2}}; \frac{1}{\sqrt{6}}; \frac{1}{2}; \frac{1}{\sqrt{6}}\right) \quad (4.3)$$

Where T matrix is given by:

$$T = \begin{bmatrix} 1 & 1 & 1 & 1 & 1 & 1 & 1 & 1 \\ 1 & 1 & 1 & 0 & 0 & -1 & -1 & -1 \\ 1 & 0 & 0 & -1 & -1 & 0 & 0 & 1 \\ 1 & 0 & -1 & -1 & 1 & 1 & 0 & -1 \end{bmatrix} \quad (4.4)$$

The forward and inverse pruned DCT approximations proposed are as follows:

$$Y_{4 \times 4} = D \times (T_{4 \times 8} \times X_{8 \times 8} \times T_{8 \times 4}^t) \times D \quad (4.5)$$

$$X_{8 \times 8} = T_{8 \times 4}^t \times (D \times Y_{4 \times 4} \times D) \times T_{4 \times 8} \quad (4.6)$$

The Pruned DCT approximation is computed based on the separability property of DCT 2D and using 1D transform along the lines then along the columns of an image block. The P.DCT 1D approximation of each row will give 4 coefficients. Then, on this intermediate result, a P.DCT 1D approximation is performed on each column. The end result is a P.DCT 2D approximation with 4×4 size. Thus, the 1D transformation of a single row of the 8×8 image block using the transformation T can be represented by the signal flow graph (SFG) presented in Figure.4.1. Dashed rows represent multiplications by -1.

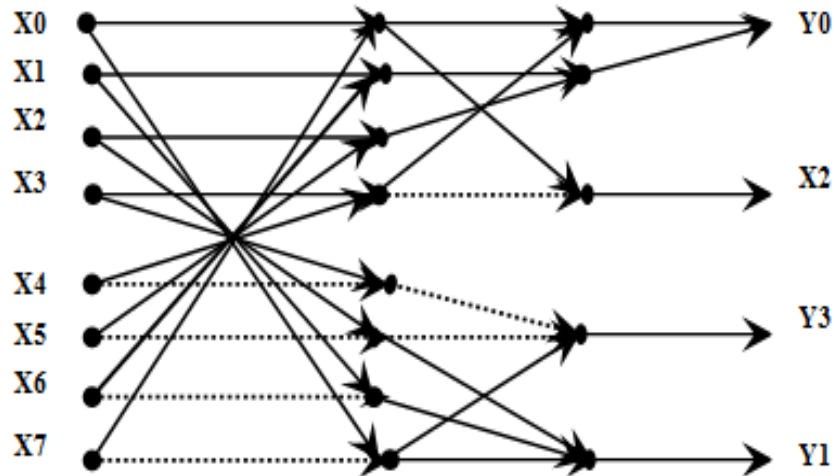


Figure.4.1. The signal flow graph (SFG) of the Pruned RDCT.

4.2.2. New pruned DCT approximation

Depending on what was mentioned above, the proposed Transform T^* is derived from the P.RDCT by modifying certain elements of the transformation matrix T . This is in order to reduce the number of operations, as taken up in many works, see Refs. 89-93. However, we impose for this modification, the preservation of all the basic mathematical properties. First, the semi orthogonality of the transformation matrix is preserved. A semi-orthogonal matrix is a non-square matrix with real entries where, the rows are orthonormal vectors (if the number of columns is greater than the number of rows). Indeed, our transformation has more columns than rows. Second, to be compatible with the DCT, the modification must also ensure a low MSE compared to the exact DCT. Third, an acceptable energy compaction must be provided to be efficient in image compression. Finally, the proposed transformation must be sparse (i.e high number of zeroes in its entries) to ensure a fewer number of arithmetic operations. So, the expression of the obtained semi-orthogonal matrix transformation T^* is the following:

$$T^* = \begin{bmatrix} 1 & 1 & 1 & 1 & 1 & 1 & 1 & 1 \\ 1 & 1 & 0 & 0 & 0 & 0 & -1 & -1 \\ 1 & 0 & 0 & -1 & -1 & 0 & 0 & 1 \\ 0 & 0 & -1 & 0 & 0 & 1 & 0 & 0 \end{bmatrix} \quad (4.7)$$

The proposed forward and inverse pruned DCT approximations are expressed respectively according to:

$$Y_{4 \times 4} = D^* \times (T_{4 \times 8}^* \times X_{8 \times 8} \times T_{8 \times 4}^{*f}) \times D^* \quad (4.8)$$

$$X_{8 \times 8} = T_{8 \times 4}^{*f} \times (D^* \times Y_{4 \times 4} \times D^*) \times T_{4 \times 8}^* \quad (4.9)$$

Where T^* is the 4-pruned proposed transform matrix and D^* is a scaling diagonal matrix, given by:

$$D^* = \text{diag}\left(\frac{1}{2\sqrt{2}}; \frac{1}{2}; \frac{1}{2}; \frac{1}{\sqrt{2}}\right) \quad (4.10)$$

The suggested 2D Discrete Cosine Transform (DCT) approximation, utilizes the separability property which described before. The implementation of this architecture is illustrated in Figure.4.2.

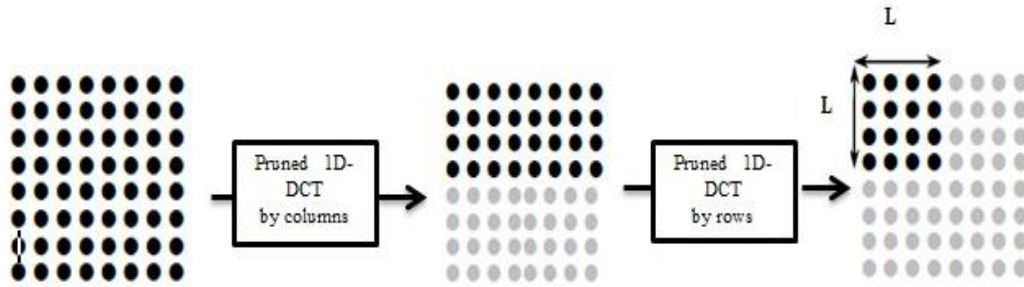


Figure.4.2. The proposed pruned 2-D DCT approximation for $L=4$.

The obtained approximate ensures a good compromise quality / bitrate but also a very low cost of calculation and a very significant compatibility with the exact DCT. It is clear from (4.10) that the obtained approximate is semi-orthogonal, it can be verified that the relation $T^* \cdot T^{*t}$ gives a diagonal matrix [96, 97]. Matrix T^{*t} denotes the matrix transpose. Moreover, the presence of only 0, 1, -1 proves that the proposed transform requires only additions. While the scaling diagonal matrix D^* does not introduce any computational overhead, it can be merged into the quantization/dequantization step (see Esq. (4.11) – (4.13)) as adopted in several works, see Refs. 89-94. Therefore, the unique source of computational complexity is bounded into the matrix T^*

$$Y_{4 \times 4} = (T_{4 \times 8}^* \times X_{8 \times 8} \times T_{8 \times 4}^{*t}) \otimes (d^* \times d^{*t}) \quad (4.11)$$

Where \otimes denotes the element by element multiplication and d is a column vector correspond to the main diagonal of D^* . Hence the combined transform and the quantization pairs are given by :

$$Y_{4 \times 4}^{Quant} = Round(T_{4 \times 8}^* \times X_{8 \times 8} \times T_{8 \times 4}^{*t}) \phi Q_m \quad (4.12)$$

Where ϕ denotes the element by element division and Q_m is the modified quantization table given by (4.13):

$$Q_m = Q \phi (d^* \times d^{*t}) \quad (4.13)$$

We note that the equations of the inverse process can be derived using the same methodology. The matrix T^* can be decomposed to a product of sparse matrix $T^* = P \cdot A_3 \cdot A_2 \cdot A_1$. This decomposition allows a derivation of a fast algorithm illustrated in Figure.4.3. The number of additions can be clearly determined from the flow graph. The proposed transformation requires only 12 additions.

$$P = \begin{bmatrix} 1 & 0 & 0 & 0 \\ 0 & 0 & 1 & 1 \\ 0 & 1 & 0 & 0 \\ 0 & 0 & 0 & 0 \end{bmatrix} \quad (4.14)$$

$$A_3 = \begin{bmatrix} 1 & 1 & 0 & 0 & 0 \\ 0 & 0 & 1 & 0 & 0 \\ 0 & 0 & 0 & 1 & 0 \\ 0 & 0 & 0 & 0 & 1 \end{bmatrix} \quad (4.15)$$

$$A_2 = \begin{bmatrix} 1 & 0 & 0 & 1 & 0 & 0 & 0 \\ 0 & 1 & 1 & 0 & 0 & 0 & 0 \\ 1 & 0 & 0 & -1 & 0 & 0 & 0 \\ 0 & 0 & 0 & 0 & -1 & 0 & 0 \\ 0 & 0 & 0 & 0 & 0 & 1 & 1 \end{bmatrix} \quad (4.16)$$

$$A_1 = \begin{bmatrix} 1 & 0 & 0 & 0 & 0 & 0 & 0 & 1 \\ 0 & 1 & 0 & 0 & 0 & 0 & 1 & 0 \\ 0 & 0 & 1 & 0 & 0 & 1 & 0 & 0 \\ 0 & 0 & 0 & 1 & 1 & 0 & 0 & 0 \\ 0 & 0 & 1 & 0 & 0 & -1 & 0 & 0 \\ 0 & 1 & 0 & 0 & 0 & 0 & -1 & 0 \\ 1 & 0 & 0 & 0 & 0 & 0 & 0 & -1 \end{bmatrix} \quad (4.17)$$

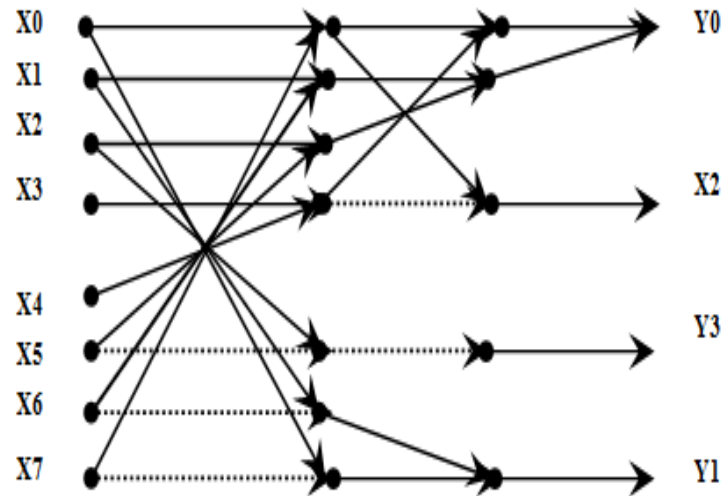


Figure.4.3. The signal flow graph (SFG) of the proposed method.

4.3. Performance evaluations

4.3.1. Evaluation in terms of complexity assessment

In this section, we will assess the performance of several pruned DCT approximations in terms of the complexity cost. The latter is habitually measured by counting the number of additions, bitshifting and multiplications operations required by the fast approximations. For a good comparison, we have selected the well-known approximations found in the literature in their pruned version, namely: Transform in Ref. 95, P.SDCT [99, 100], P.BAS-2008[90,96] , P.BAS-2009[91,96], P.BAS-2013[97], P.RDCT[98] and the P.MRDCT[96].

As mentioned above, the computation complexity of the proposed pruned approximation is related to the Matrix T^* , consequently, the 2D pruned approximate DCT is counted after eight column-wise calls of the 1D pruned approximate DCT and L row-wise call of 1D pruned approximate DCT[55]. The expression that estimates the additive complexity $A_{2D}(L)$ of the 2D pruned approximate DCT is demonstrated in (4.18):

$$A_{2D}(L) = (L + 8) \times A_{1D}(L) \quad (4.18)$$

Where

$A_{1D}(L)$ is the number of arithmetic complexity required to compute the 1-D transform for a bloc of $N=8$.

For our particular case the pruning parameter $L=4$. Then, we can obtain the formula below:

$$A_{2D}(4) = (12) \times A_{1D}(4) \quad (4.19)$$

4.3.2. Evaluation in terms of image quality

The purpose of this section is to further investigate the efficiency of the proposed pruned approximation in image compression. To do so, we have selected the best effective pruned methods, which have proven their efficiency in image and video compression. Then, we have performed an experiment on the image compression simulation similar to that detailed in Refs. 88-98, each pruned approximation is used instead of the 2-D DCT basis transformation stage in JPEG-Like compression chain. Note that the other stages contain the standard quantization table and Huffman encoder. A set of standard gray scale images of size=512x512 pixels (each 8- bits/pixel or 8 bpp) have been chosen for the tests and were taken from [10]

In resource constrained WMSNs, multimedia data like an image needs to be highly compressed before transmission to reduce the power consumed per each node during transmission. Taking into account these requirements, we preferred to compress test images at low bit rate at a range of [0-0.5] bpp. To evaluate the image quality after reconstruction we have obviously used peak signal to noise ratio (PSNR) [55] but also the structural similarity index (SSIM) [107]. Indeed, unlike the PSNR based on the MSE (Mean Square Error) that estimate absolute errors between original and reconstructed images, the SSIM is a perception-based model. The SSIM allows us to have more significant evaluation results.

The MSE and PSNR are calculated using equation (4.20) and equation (4.21) respectively:

$$\text{MSE} = \frac{1}{M \cdot N} \sum_{m=1}^M \sum_{n=1}^N (f(m, n) - \hat{f}(m; n))^2 \quad (4.20)$$

Where, MSE denotes the mean squared error between the original $f(m, n)$ and the reconstructed images $\hat{f}(m; n)$. $M \times N$ is the image size.

$$\text{PSNR} = 10 \log_{10} \frac{(d)^2}{\text{MSE}} \text{ dB} \quad (4.21)$$

Where d is the maximum signal amplitude. In general, in the case of an 8 bit per pixel (bpp) image, $d = 255$.

The Structural Similarity Index (SSIM) is indeed a full reference metric used to measure the quality of an image. It compares an original or reference image to a distorted or compressed image to determine the degree of similarity between them.

The SSIM index between two windows of size $N \times N$ is given by the following formula:

$$SSIM(A, B) = \frac{(2\mu_A \mu_B + C_1)(2\sigma_{AB} + C_2)}{(\mu_A^2 + \mu_B^2 + C_1)(\sigma_A^2 + \sigma_B^2 + C_2)} \quad (4.22)$$

Where;

A and B are the reference and distorted images;

μ_A, μ_B = mean intensities of original data A and reconstructed data B;

σ_A^2, σ_B^2 = standard deviation of original data A and reconstructed data B;

C_1, C_2 = constant. The standard value of and are 0.01 and 0.03 respectively [110].

The mean intensity can be calculated as below.

$$\mu = \frac{1}{N} \sum_{i=1}^N x_i \quad (4.23)$$

The standard deviation is mathematically represented as:

$$\sigma = \sqrt{\frac{1}{N} \sum_{i=1}^N (x_i - \mu)^2} \quad (4.24)$$

$$\sigma_{AB} = \frac{1}{N-1} \sum_{i=1}^N (A_i - \mu_A)(B_i - \mu_B) \quad (4.25)$$

If A and B are identical then SSIM=1. For highly uncorrelated case SSIM = -1.

- **A subjective fidelity criterion** is a method that uses human perception to assess the quality of a reconstructed image by visually comparing it to the original. It's used when objective quality criteria are not enough and provides useful information on image quality.

4.3.3.Evaluation in terms energy consumption

- **mathematical model**

A significant reduction of the arithmetic operations minimizes directly the power consumption of sensor nodes and thus leading to prolong the network lifetime of WVSNS [97,98]. So, to evaluate the energy consumption of the proposed transform we use the model that was adopted in several works see Refs. 108-110, it is specifically designed to evaluate the energy consumption of WSN nodes. For an input image of size M×N, the energy consumed by the proposed transformation can be given by:

$$E_{M \times N}(L) = \frac{M \times N}{8 \times 8} \times E_{8 \times 8} \quad (4.26)$$

The energy spent by the transforms for an 8x8 bloc, is given by:

$$E_{8 \times 8} = A. \epsilon_{ADD} + B. \epsilon_{shift} + C. \epsilon_{Mult} \quad (4.27)$$

Where

- ✓ A, B and C are the number of additions, shift and multiplication operations respectively.

- ✓ ϵ_{ADD} , ϵ_{shift} and ϵ_{Mult} Represent the energy consumption respectively for Add, Shift and Mul operations over one-pixel.

Where, $N_{Add}=144$ is the number of additions needed for an 8×8 block in the case of proposed transform and $\epsilon_{Add}=3.3$ nJ is the energy consumption for one Add operation[110] .

4.4. Results and discussion

4.4.1. Results in term of Arithmetic complexity

Table 4.1 compares the number of arithmetic operations required by numerous pruned DCT approximations. It is obvious from this table that the proposed transform requires 12 additions operations which correspond to 70%, 40%, 20%, 14.3%, 40% and 25% less arithmetic operations than the transform in Ref. 95, P.SDCT, BAS-2008, P.BAS-2009, P.BAS-2013 and P.RDCT respectively. While The P.MRDCT with 10 addition operations is the only one that has the lowest arithmetic complexity among all transforms. P.SDCT [104, 96], P.BAS-2008 [90,96], P.BAS-2009[91,96], P.BAS-2013[105], P.RDCT[97] and the P.MRDCT[96] .

Pruned Method	Add	Shift	Total
Transform in Ref. 95,	29	11	40
P.SDCT [96,100]	20	0	20
P.BAS-2008 [90,96]	14	1	15
P.BAS-2009 [91,96]	14	0	14
P.BAS-2013[97]	20	0	20
P.RDCT[98]	16	0	16
P.MRDCT[96]	10	0	10
Proposed	12	0	12

Tbale.4.1: Computational complexity comparison of different 1D pruned approximation.

4.4.2. Results in terms of image quality

Figure.4.4. illustrates the obtained PSNR, using different approximations P.BAS-2013, P.RDCT and P.MRDCT. The comparison of the curves clearly shows that the suggested method outperforms the Pruned MRDCT in terms of PSNR; on the other hand it gives the same PSNR as pruned BAS-2013. We should note that this latter method needs more operations (20 additions) than the proposed. For the P.RDCT, which gives a slightly higher PSNR compared to the proposed one, the number of operations needed is higher than the proposed transform.

Figure.4.5. shows a visual comparison of reconstructed Barbara, Lena and boat images at 0.35 bpp using different transformations. It is inferred from these figures that the suggested approach reproduces the image with better quality, in addition to the significant reduction it offers in terms of computational complexity.

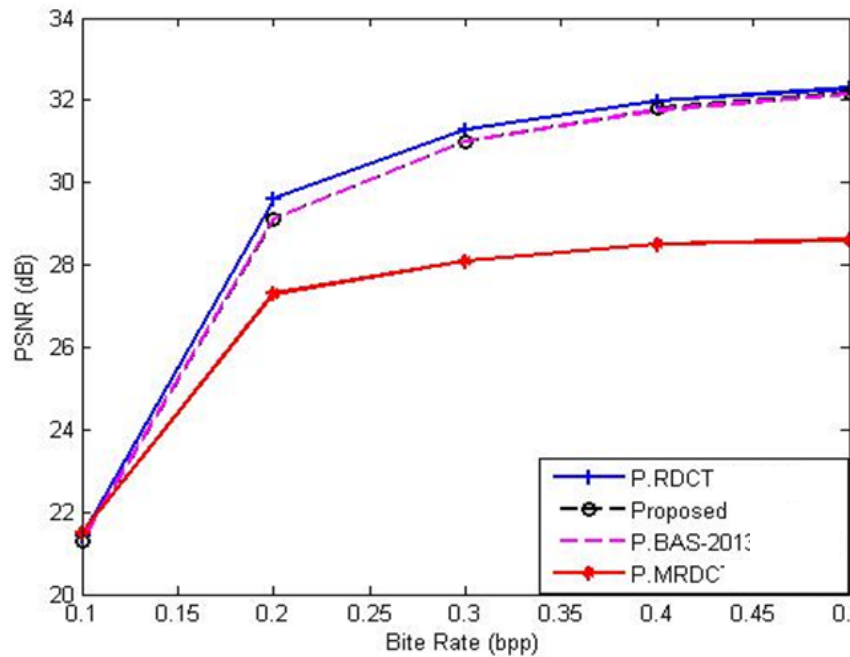


Figure.4.4. PSNR acquired by different transforms for Lena image.

It can be easily observed from these figures that the proposed method, P.RDCT and P.BAS-2013 have a closer SSIM and thus explains that the proposed transform gives a comparable image quality as P.RDCT and P.BAS-2013. Note that these latter demand 16 and 20 additions respectively. On the other hand the P.MRDCT has a bad visual quality of the reconstructed image compared with all transforms and it can be observed from SSIM results.



Figure.4.5. Reconstructed images at 0.35 bpp using different approximations.

4.4.3. Results in terms of mean square error

In addition to its computational complexity reduction, the proposed DCT also checks the constraint of a minimum Mean Squared Error (MSE) with the exact DCT. Figure.4.6. shows that the proposed DCT provides the second-best compatibility with exact DCT for standard ρ values compared to other transforms. Indeed, we often determine the MSE for $\rho = 0.9$ and 0.95 considered as standard values for real natural images.

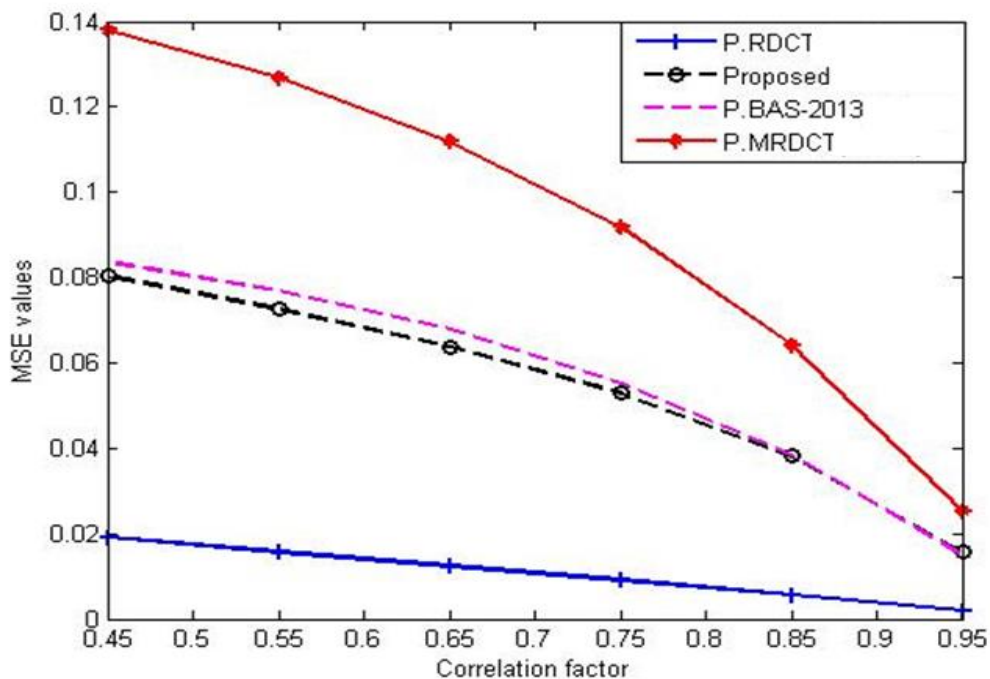


Figure.4.6. MSE of several pruned DCT approximations.

4.4.4. Results in terms of energy consumption

Table 4.2 summarizes the energy consumption of different approximations. It should be noted that Mica2 platform is a sensor node that includes a low-power microcontroller namely Atmel Atmeg128. The parameters that refer to the characteristics of Mica2 platform was adopted [108,111].

As it can be seen from the above results the suggested scheme not only decreases the computational complexity but also decreases the energy consumption. This approximation is more energy-efficient and it guarantees an excellent performance in terms of energy efficiency compared

to the P.BAS-2013 and P.RDCT. While, P.MRDCT transform saves more the energy spent than all transforms, but its huge reduction of arithmetic operations affects too much the image quality as seen earlier in image quality.

Method	Energy for 8×8 blocs $E_{8 \times 8}$ (μJ)	Energy for 512 ×512 images $E_{512 \times 512}$ (mJ)
P.BAS-2013[97]	0.79	3.24
P.RDCT [98]	0.63	2.58
P.MRDCT [96]	0.40	1.64
Proposed	0.48	1.97

Table.4.2: Energy consumption obtained by several transforms.

4.5. Testbed for real measurements

To better understand the energy autonomy of a wireless sensor node in operation, it is necessary to clearly define its different operating modes. Thus, each operating mode of this sensor node will have its own energy consumption. A possible working sequence of a sensor node usually presents the following operating modes, according to its internal components in particular the processing unit, the sensor module and the transmission / reception module.

- The ‘‘measure’’ operating mode,
- The ‘‘processing’’ operating mode,
- The ‘‘emission’’ operating mode,
- The ‘‘reception’’ operating mode.

Each operating mode has its own energy consumption. Generally, the operating modes of transmission and reception are the most power intensive followed by measurement mode, then processing and finally the sleep mode where the power consumption is the lowest. Remember that a greater consumed current does not necessarily mean a greater energy consumed. Indeed, it will also

depend on the temporal duration of each mode. The energy consumed can be estimated in general according to the currents consumed during the different operating modes by [111-112]:

$$E \approx V \times (I_{sleep} T_{sleep} + I_{Tx} T_{Tx} + I_{Rx} T_{Rx} + I_{mes} T_{mes} + I_{proc} T_{proc}) \quad (4.28)$$

Where I_{mode} is the current consumed by sensor node in the mode for time period T_{mode} . The mode can be: Sleep, transmission (T_x), reception (R_x), measure (mes) or processing (proc). V is the time invariant voltage based on power supply.

Thus, for real measurements of the energy consumption of a sensor node during any operating mode, like the processing mode, it is necessary to measure the current consumed during this operating mode as well as its temporal duration. In our case we will limit ourselves only to the processing mode and in particular to the DCT approximation. We therefore propose to implement an experiment based on a sensor node capable of measuring the current consumed by the calculation of different DCT approximations implanted in a sensor node. There are many small onboard modules, like the MICAz (Manufacturer is Memsic USA, Controller is ATmega128L – 16bit 8MHz and Operating system is TinyOS), Telos (Manufacturer is University of California, Berkeley/Sentilla, Controller is TI MSP430 – 16bit 8MHz and Operating system is TinyOS), Waspmote (Manufacturer is Libenium, Controller is AT Atmega 1281 and Operating system is Libelium OTAP or “ Over the Air Programming”), cyclops, imote2, Arduino due, raspberry PI3/PI4... etc, equipped with image sensors (such as uCamIII, Camera IMB400, Camera Module V2- 8, CMUcam, ARducam... etc) allowing us to build a testbed of sensor node[113]. One of the simplest solution from a design and programming point of view while ensuring great flexibility is to use an Arduino Due, based on an Atmel ARM Cortex SAM3X8E clocked at 84 MHz under 32 bits, especially if we limit ourselves to an application based on image acquisition and compression. Indeed, this type of module has a largely sufficient technology, in particular the size of its SRAM (Static Random Access Memory) of 96kbytes to handle images in raw format (RAW) of a certain resolution, for example of 128×128 pixels coded on 8 bits each.

4.5.4. Experiment

To this end, we have implemented a fairly simple and sufficient testbed (Figure.4.7 and 4.8), based on an Arduino due module and using a Fluke 192B Scopemeter and a Fluke 287 multimeter working as a DC milliammeter. Fluke 192B allows to display and to measure the execution time of DCTs and the current consumed during the processing mode. While the Milliammeter will measure these consumed currents with precision.

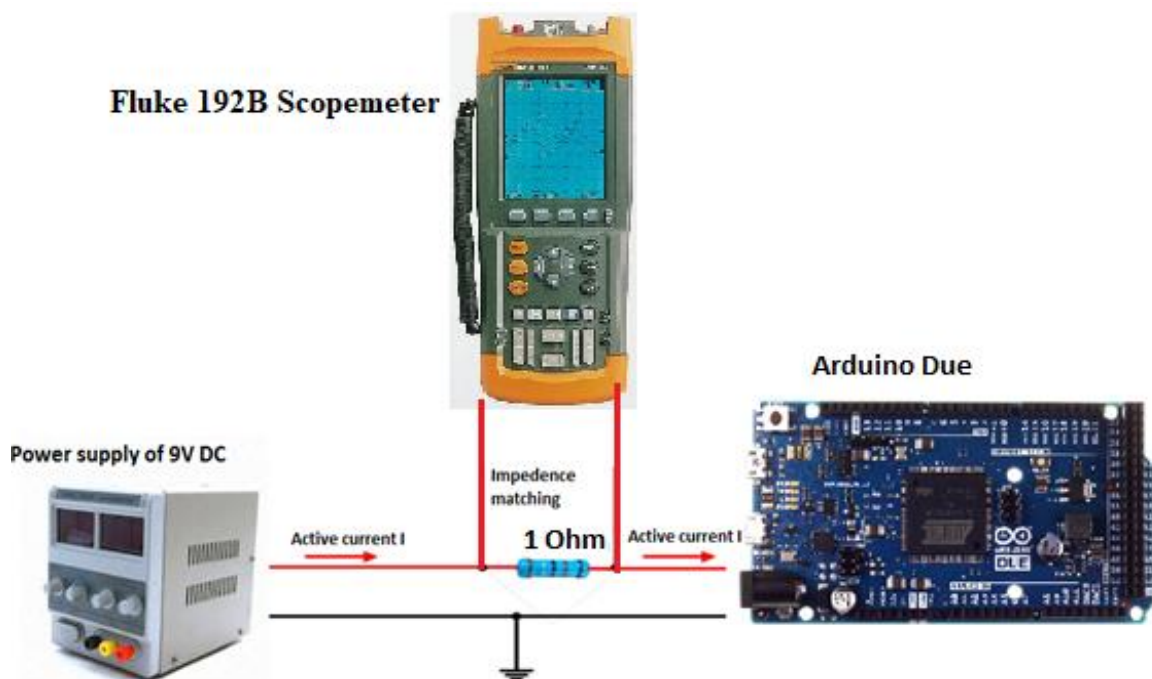


Figure.4.7. Testbed used to real measurement of execution time and the current consumed during the calculation of DCT approximations.



Figure.4.8. Testbed photograph.

Thus, different Pruned 2D DCT approximations as well as the proposed one have been programmed and implemented in the Arduino Due. The currents consumed for the different 2D DCTs of an 8×8 image block, based on 1D DCT approximations, were measured and displayed using the Fluke 192B Scopemeter.

A. Real execution time for different DCTs on 8×8 image block

First of all, we measured the execution time of the four Pruned DCTs for an 8×8 frame block, using specific instructions that we integrated into the program code of these transformations, using a powerful Arduino Due. The processing time, in microseconds, is critical in determining the energy consumed. In fact, the current is practically the same for the four transformations given that it results from the same simple arithmetic operations (addition or subtraction) for the four transforms. But the duration changes because it depends on the number of operations.

B. Real energy consumption for Pruned DCTs on 8×8 image block

From Fig.4.9 representing current measurements by the Fluke 287 precision milliammeter, it can be noticed that the current actually consumed by the Arduino Due module is almost the same for the four transformations for an 8×8 frame block. Indeed, the four pruned transformations are based on the same simple arithmetic operations, namely additions which lead to the same current consumption instantly. But as the number of these operations is different from one transformation to

another is reflected on the duration of the execution that is quite different. Thus, by referring to equation (4.30), the energy consumed is much lower in the case of the proposed transformation



Consumed current by proposed Pruned Transform.

Consumed current by Pruned RDCT.



Consumed current by proposed Pruned MRDCT.

Consumed current by Pruned P.BAS-2013.

Figure.4.9. Measured currents for the different DCT approximations.

To better check the execution time of each of these four Pruned DCT transformations, we have visualized their consumed currents over a processing cycle. We have taken the same Scopemeter configuration parameters for the four signals namely a caliber of 100mV / div and a time base of 50 μ s / div. We used a resistance of around 10 Ω . What interests us most here is the duration of the impulse which corresponds to the processing time. Indeed,

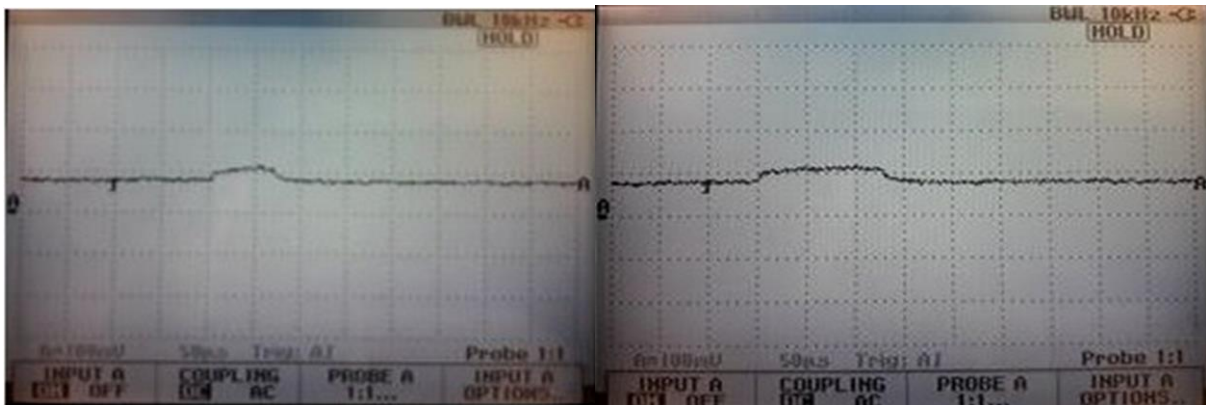
We have introduced in the Arduino program code a sleep mode time of 10ms for each measurement cycle. This allows us to clearly see a single pulse on the Scopemeter screen

corresponding to the processing time in relation to the rest which represents the standby mode of the microcontroller and where consumption is relatively low. Thus, we clearly notice in figure 4.10, the difference between the four curves in relation to this impulse duration. This fits perfectly with the study we conducted.



Consumed current by proposed Pruned Transform.

Consumed current by Pruned RDCT.



Consumed current by Pruned MRDCT.

Consumed current by Pruned P.BAS-2013.

Figure.4.10. Visualized currents for the different DCT approximations.

The following table shows real execution times, measured from the currents shown in figure. 4.10. From this table we see that these measurements are consistent with the theoretical models used in the article to estimate the energy consumed.

As shown in figures.4.9 and 4.10. The experimental results obtained prove clearly the energy gain, as a function of the measured current and the time period necessary for the execution of 8×8

image block transform, provided by the proposed method compared to all the other transformations. This is shown for an 8×8 image block and it is valid for a whole image.

DCTs	Execution time (μ s)
	Arduino DUE
P.BAS-2013[97]	140
P.RDCT [98]	110
P.MRDCT[96]	70
Proposed	80

Table.4.3: Execution time of the four pruned DCT.

4.6. Conclusion

In this chapter, a novel pruned DCT approximation has been proposed, which is particularly suitable for embedded systems requiring low power consumption and real-time applications. This semi-orthogonal transform is obtained by setting some entries of the P-RDCT matrix to zero. The resulting scheme is a multiplication-free transform that requires only 12 additions. Experimental comparisons with recent works, using a testbed for real measurements, demonstrate that the proposed low complexity pruned approximation is extremely simple, fast, and consumes less energy. It has a good trade-off between computational complexity and performance compared to the most recent approximations reported in the literature. The reconstructed image is obtained without any noticeable degradation, despite the significant reduction in computational complexity. Furthermore, the significant reduction in algorithmic complexity inevitably leads to a decrease in energy consumption. Thus, the proposed approach presents a potential solution for WMSNs by increasing their lifetime.

Chapter 5

*Stereo image compression using proposed
pruned transform*

5.1. Introduction

In recent years, the widespread adoption of 3D imaging systems has become widely popular due to their ability to provide a more realistic and immersive visual experience. This technology has found extensive use in various application domains, including entertainment (such as 3D TV and digital cinema), virtual reality, and gaming, videoconferencing, robot vision, and medical surgery. The use of 3D imaging systems can improve depth perception, enhance the viewing experience, and provide more accurate spatial information for a variety of applications [114, 115].

A stereo image pair is comprised of two images depicting the same scene, captured from two slightly different angles, usually representing the perspectives of the left and right eyes. These images are referred to as the left and right images, respectively. When viewed with the appropriate viewing equipment (such as 3D glasses), the left and right images are combined to create a three-dimensional (3D) image that appears to have depth and dimensionality. This enhances the viewer's depth perception and provides a more immersive and vivid 3D experience [116].

Transmitting or storing stereo images over wireless multimedia sensor networks (WMSNs) presents challenges. Stereo images require twice the bandwidth and energy compared to single images, which can deplete the battery resources of the sensors and reduce the network lifetime. Standard image compression algorithms like JPEG, JPEG2000, and SPIHT require high computational complexity, which is impractical for WMSNs, as discussed in previous chapters. Therefore, low-complexity and energy-efficient image compression algorithms are needed to minimize power consumption and prolong the network lifetime. In this chapter, we suggest a stereo image coder based on the suggested approximation, which we have previously shown to be the best method for still image compression, offering a combination of high quality, low computational complexity, and minimized energy consumption [117].

5.2. Principles of stereoscopic vision

5.2.1. Principles of function in the Human Visual System

Stereopsis is the mechanism through which depth perception is achieved when observing a scene with both eyes simultaneously. When an individual looks at an object or scene with both eyes, the difference in the relative position and angle between the target and each eye creates two

slightly different images, known as parallax. These two images are transmitted to the visual cortex via the optic nerves and fused together to form stereopsis. The left hemisphere of the visual cortex receives signals from the right eye, while the right hemisphere receives signals from the left eye. The visual cortex then matches corresponding parts of the two input images and calculates the binocular disparities in the matched areas to achieve stereoscopic depth perception [118].

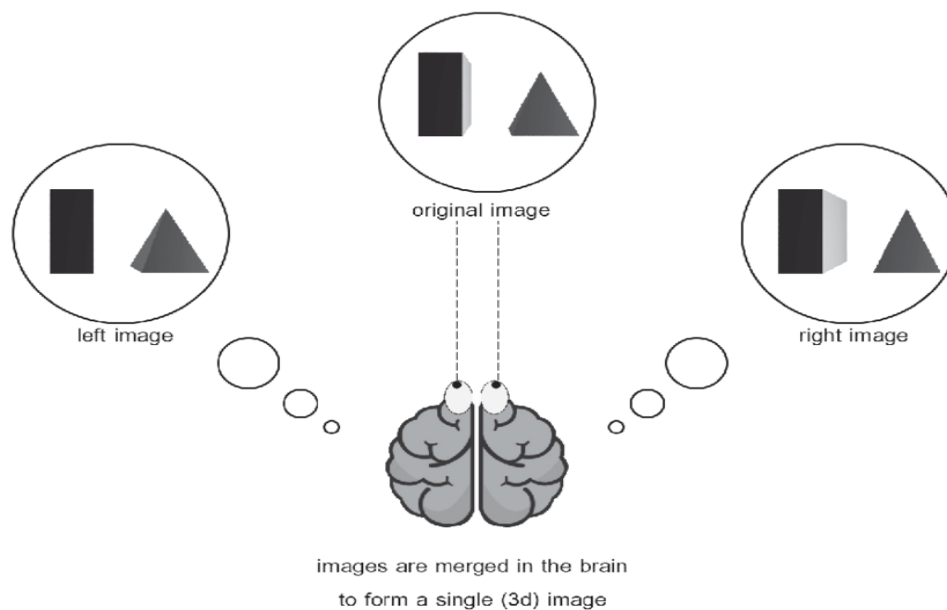


Figure.5.1. Demonstration of how a pair of stereo images creates an illusion of 3D scene/objects [119].

5.2.2. Stereoscopic imaging systems

Stereoscopic vision using a pair of cameras is based on the principle of stereopsis, which is the perception of depth that occurs when a scene is viewed with both eyes. When a scene is captured using a pair of cameras positioned a short distance apart that are placed in parallel, two slightly different images are obtained, which correspond to the images received by each eye in a natural setting. The points of the scene are recorded to different positions in the two images. This position difference is called disparity. To achieve an optimal stereoscopic effect, the cameras must be properly aligned and calibrated to ensure that the distance between the cameras matches the average inter-ocular distance of the intended audience. The cameras should also be synchronized to ensure that both images are captured at the same time and that the images are properly aligned. Overall, the

principles of stereoscopic vision using a pair of cameras involve capturing two slightly different images, presenting them separately to each eye, and allowing the brain to fuse the images together to create a 3 D effect [120].

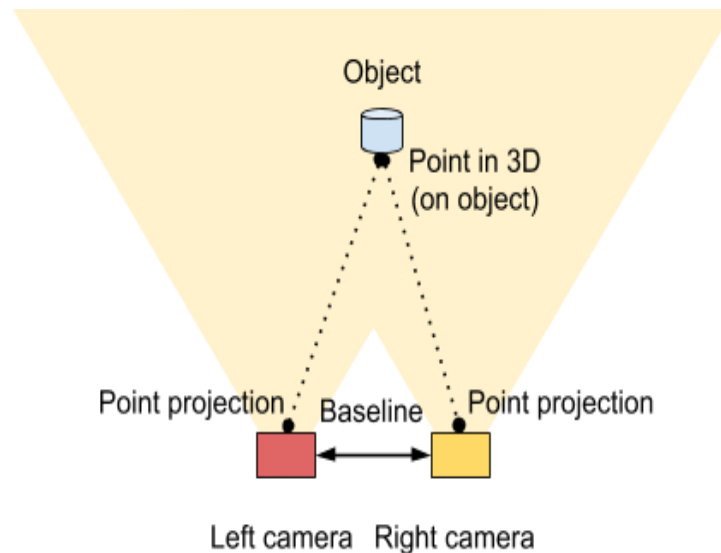


Figure.5.2. A stereo vision system using a couple of cameras [120].

5.3. Experimental results and discussion

In reality, the task of encoding stereo images with low computational complexity over wireless multimedia sensor networks (WMSNs) has not received significant attention from researchers. Many of the previously mentioned studies have utilized methods such as DCT, DWT, and SPITH to compress stereo images. However, these compression techniques are not well-suited for WMSNs due to their computationally intensive nature, which in turn increases energy consumption.

The binocular redundancy that exists between the two images within a stereo pair effectively doubles the data size when compared to encoding a single image. Consequently, this results in a significant amount of stereo data. As a solution, numerous existing stereo coding methods have incorporated disparity-compensated prediction to leverage the inherent cross-image redundancy present within the stereo pair. This approach aims to reduce computational complexity and energy consumption while still effectively encoding stereo imagery.

The primary focus of our work is to encode stereo images with low computational complexity, using our novel pruned DCT approximation. This approach not only reduces energy consumption but also extends the overall network lifetime. The foundational steps for encoding stereo images align with the well-established concept found in many existing methods [120], as detailed in these steps:

1. First, the right image is chosen as the reference image, and is encoded independently.
2. Then, the disparity map, representing the displacement field between the pixels of the right and left images, is computed using a block matching approach. The reference image is divided into $k \times k$ blocks, and each block of the reference image is matched with an approximating block in the target image by minimizing a data cost function such as the sum of absolute difference (SAD).
3. After that, the left image, referred to as the target image, is predicted from the reference one using the estimated disparity map, and the difference between the original target image and the predicted one, named the residual image, is obtained.
4. Finally, the reference, residual image and the disparity map are encoded.

We use the JPEG chain, which uses the proposed pruned DCT approximation to encode the reference image and the residual image. While, the disparity map is often lossless encoded using a DPCM technique. At the decoder, we first decode the first image and then decompress the left image using the reference image, error image, and the disparity. A block diagram of the stereo coder is shown in Figure.5.3.

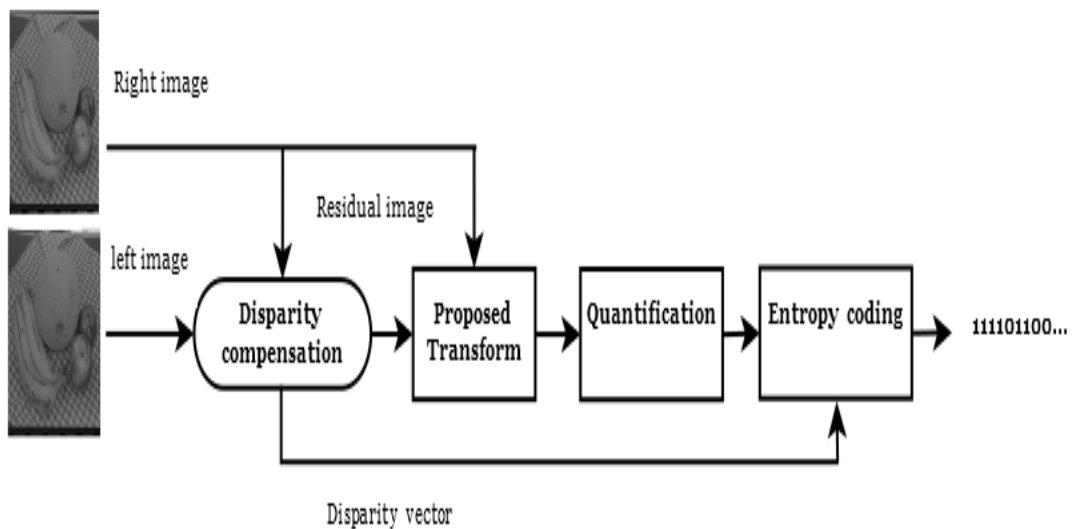


Figure.5.3. The proposed Stereo coder.

5.3.1. Stereo image compression

In our simulation, our objective is to assess the effectiveness of the proposed pruned approximation on stereo images. To achieve this goal, we have integrated it into a stereo coder/decoder setup, as illustrated in Figure.5.3. The experimental evaluation of the proposed coders was performed on the well-known standard stereo images, namely "Pentagon" (512x512), "Fruit" (512x512), downloaded from some public stereovision datasets[121]. For comparison, we have selected the Loeffler-DCT[122], which computes the exact float DCT. The results are presented both visually and in terms of peak signal-to-noise ratio (PSNR).



Figure.5.4. Typical standard test stereo images used in the simulation.

Figure.5.5. and 5.6. Present a visual comparison of the reconstructed stereo image using the proposed method and Loeffler-DCT at 0.45 bpp. From these figures, it is evident that the new approximation generates a stereo image with good quality, even though JPEG-Loeffler has the best quality in terms of PSNR. When using our naked eyes as a metric for comparison, we can observe that there is no visual difference between the new scheme and JPEG-Loeffler. Therefore, the proposed scheme can provide good visual quality at low computational complexity, which is the main requirement for WMSNs.



PSNR=37.64 dB



PSNR=36.66 dB

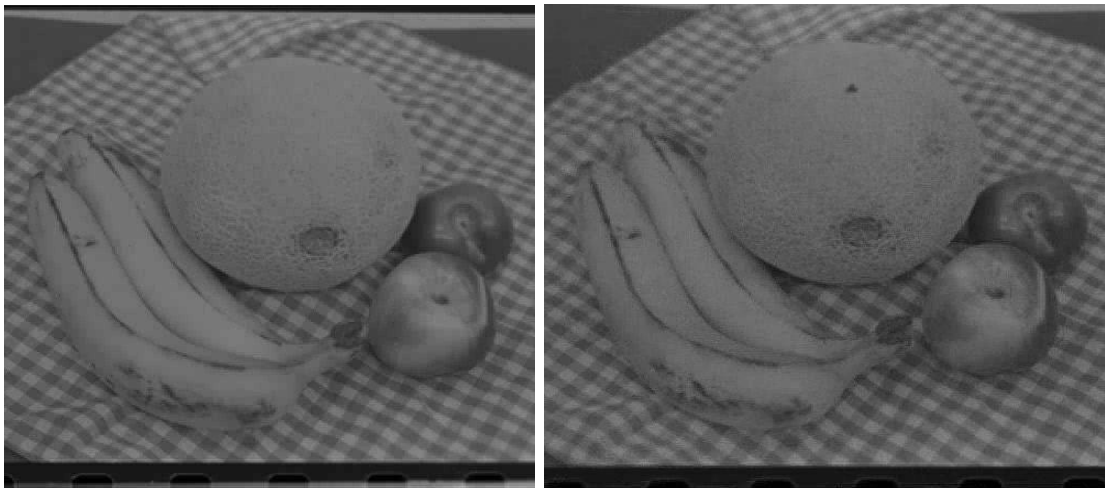


PSNR=28.18dB



PSNR=28.52dB

Figure.5.5. Reconstructed stereo image: ‘fruit’ and ‘pentagon’ using DCT Loffler at 0.45 bpp.



PSNR=35.07dB

PSNR=31.57dB



PSNR=27 dB

PSNR=27.32dB

Figure5.6. Reconstructed stereo image: “fruit” and “pentagon” using proposed transform at 0.45 bpp.

5.3.2. Computational complexity

In this part, we analyze the arithmetic complexity of the proposed transform and the exact DCT for stereo images. It should be noted that the complexity of block matching and the entropy encoder are neglected; we only take the computational complexity of the transformation step for each method.

Table.5.1 shows the arithmetic complexity assessment and comparisons of the suggested transform and the exact DCT in terms of addition, multiplication, and bit-shift counts. From the

table below, it is evident that the proposed transform is considerably less complex than the exact DCT. It requires few additional operations compared to the exact DCT, whereas the latter demands more additions and multiplications, making it very expensive in terms of hardware implementation and energy consumption. This significant reduction in computational complexity is only for the left image, and when we consider stereo images (the left and residual images), which involve large amounts of data, the reduction will be more considerable by this fast proposed transform. Therefore, the proposed fast transform is suitable because it leads to smaller, faster, and more energy-efficient circuitry designs.

Stereo image	Right image		Residual image	
	Add 1D/2D	Mul 1D/2D	Add 1D/2D	Mul 1D/2D
Loeffler DCT	28/464	11/176	28/464	11/176
Proposed Method	12/144	0	12/144	0

Tbale.5.1: Computational complexity comparison of 1D/2D by exact DCT and the proposed transform for stereo image.

5.3.3. Energy consumption

In a typical Wireless Multimedia Sensor Network (WMSN) node, energy consumption is directly correlated to the number of operations required by the compression techniques utilized within that node [1–4]. Consequently, to evaluate the energy consumption of the suggested approximation applied to stereo images, we applied the same methodology as used for single images, as detailed in Chapter 4.

Table.5.2 presents a comparison between the energy consumption of the DCT and the proposed transform. We excluded the energy values for the DCT due to our limited knowledge of the energy associated with multiplication. However, it should be noted that multiplication consumes much more energy compared to addition and shift operations, making the DCT very energy-intensive. Based on the below results, we can confirm that our proposed DCT approximation significantly reduces energy consumption while preserving acceptable image quality compared to the exact DCT.

Consequently, this approach provides a more energy-efficient method for stereo image compression, contributing to extended network lifetimes and enhanced operational efficiency.

Method	Energy for 8×8 blocs $E_{8 \times 8}$ (μJ)	Energy for 512 ×512 images $E_{512 \times 512}$ (mJ)
DCT	High	High
proposed	0.48	1.97

Table.5.2: Energy consumption obtained by exact DCT and the proposed transform.

5.4. Conclusion

A stereoscopic pair is a pair of images of the same scene, called the left and right images, recorded from two slightly different perspectives. The presence of binocular redundancy between these images leads to a doubling of the image data size compared to a single image and, consequently, involves a large amount of stereo data. Therefore, a stereo image pair needs to be compressed before being transmitted over a wireless multimedia sensor network to minimize transmission bandwidth usage and energy consumption.

This chapter is dedicated to the compression of stereo images with low computational complexity, designed specifically for Wireless Multimedia Sensor Networks (WMSNs). We have developed an efficient stereo image coder/decoder that takes into account a key feature of WMSNs: energy consumption. Our proposed approach employs a pruned DCT approximation, delivering competitive performance in terms of complexity, image quality, and energy consumption when compared to the exact DCT. This positions our approach as a promising solution for resource-limited WMSNs.

Conclusion and perspectives

6. Conclusion

The popularity of wireless visual sensor networks (WVSNs) has grown significantly over the past decade due to their potential applications in a wide range of fields. Unlike traditional sensor networks, WMSN utilizes cameras or other visual sensors to gather and transmit data, providing rich visual information that can be used for various applications. However, WVSNs face significant challenges related to energy consumption, as visual sensors typically require more power than traditional sensors, and image processing can be computationally intensive. To address this challenge, researchers in this field are exploring innovative techniques to optimize energy consumption and improve WSN performance. These efforts aim to reduce energy consumption while maintaining data quality and network reliability, making WMSNs a more feasible technology for deployment.

In this thesis, we have focused on still and stereo image compression over wireless multimedia sensor networks. To achieve this, we have proposed an energy-efficient algorithm based on the JPEG standard. The main objective of our proposed algorithm was to reduce the algorithmic complexity of the JPEG image compression standard, thereby reducing energy consumption and prolonging the network's lifetime. By reducing the computational complexity of image compression, we can minimize the energy requirements of wireless sensor nodes and extend their operational lifetime.

The image compression technique JPEG is based on the linear orthogonal transformation DCT. For several decades, the JPEG standard has proven its efficiency in terms of bitrate and distortion compromise. Nevertheless, the computational complexity of the DCT is relatively high, which leads to consequential energy consumption during its execution and therefore limits its use in wireless sensor networks. For this purpose, maintaining acceptable image quality and reducing energy consumption are significant goals in WMSNs. So, in this thesis, we have proposed a viable transformation approximation that can replace the exact DCT in a JPEG chain. This is a 48 semi-orthogonal transform matrix that needs only 12 additions. This approximate method is very appropriate for image and video coding.

The proposed low-complexity pruned approximation, according to the simulations and comparisons performed, has shown its performance in terms of computational complexity, image distortion, and energy consumption. Indeed, this new approach makes it possible to obtain a

reconstructed image with good quality and low computational complexity compared to the most recent methods reported in the literature. Furthermore, the significant reduction in computation costs inevitably leads to a decrease in energy consumption. Thus, the proposed approach would make WMSN networks with limited resources even more attractive by increasing their lifetime.

7. Perspective

In this thesis, our focus has been on the development of an energy-efficient image compression method that is well-suited for wireless multimedia sensor networks. The results presented in this thesis are significant and compelling. However, there are still many perspectives that deserve to be explored to complement this work. We organize them as follows:

- 1.** Establishment of a WMSN network for realistic applications like environmental monitoring (for forest and wetland fauna and flora) and also for monitoring agricultural fields (early detection of plant diseases, parasitic weeds, pollution from the ground....etc)
- 2.** Developing new types of algorithms with low computational complexity suitable for resource-constrained.
- 3.** Interested in studying Regions of Interest (ROI) in still and stereo image. First, we need to detect and extract the ROI from the source image. Then, we will compress and transmit only this ROI through the network to conserve energy.
- 4.** Multiview and stereovision in WMSN: Exploit inter-view redundancy to predict one view from another to reduce the amount of data that needs to be encoded independently.
- 5.** Energy Harvesting: Using a hybrid energy harvesting source from the surroundings to power the sensor node without relying on traditional power sources like batteries.

References

References

- [1] Akyildiz, Ian F., et al. "Wireless sensor networks: a survey." *Computer networks* 38.4 (2002): 393-422.
- [2] Mechouek K., "Low complexity image compression and region of interest coding in WSN. " *Phd these* (2016).
- [3] HAMAMI, Loubna, and Bouchaib NASSEREDDINE. "Factors influencing the use of wireless sensor networks in the irrigation field." *International Journal of Advanced Computer Science and Applications* 12.3 (2021).
- [4] Patil, Ramesh, and Vinayadatt V. Kohir. "Energy efficient flat and hierarchical routing protocols in wireless sensor networks: A survey." *IOSR Journal of Electronics and Communication Engineering (IOSR-JECE)* 11.6 (2016): 24-32.
- [5] Engmann, Felicia, et al. "Prolonging the lifetime of wireless sensor networks: a review of current techniques." *Wireless Communications and Mobile Computing* 2018 (2018).
- [6] Dargie, Walteneus, and Christian Poellabauer. *Fundamentals of wireless sensor networks: theory and practice*. John Wiley & Sons, 2010.
- [7] Tang, Xiaofeng. "Data collection strategy in low duty cycle wireless sensor networks with mobile sink." *International Journal of Communications, Network and System Sciences* 10.05 (2017): 227.
- [8] Djedouboum, Asside Christian, et al. "Big data collection in large-scale wireless sensor networks." *Sensors* 18.12 (2018): 4474.
- [9] Matin, Mohammad Abdul, and M. M. Islam. "Overview of wireless sensor network." *Wireless sensor networks-technology and protocols* 1.3 (2012).
- [10] Sharma, Gaurav, Suman Bala, and Anil K. Verma. "Extending certificateless authentication for wireless sensor networks: A novel insight." *International Journal of Computer Science Issues (IJCSI)* 10.6 (2013): 167.
- [11] Mohammad Hossein Homaei, Behnam Farhadi, Vahid Moghiss. "Introduction, evaluation and analysis covering different models in WSN." *Conference: CEIT2011*, March 2011.
- [12] Zheng, Jun, and Abbas Jamalipour. *Wireless sensor networks: a networking perspective*. John Wiley & Sons, 2009.
- [13] Gajjar, Sachin. "Factors influencing the wireless sensor network design." *Proceedings of the 2009 International Conference on Signals, Systems and Automation (ICSSA 2009)*. Universal-Publishers, 2010.
- [14] Maraiya, Kiran, Kamal Kant, and Nitin Gupta. "Application based study on wireless sensor network." *International Journal of Computer Applications* 21.8 (2011): 9-15.
- [15] Raghunathan, Vijay, et al. "Energy-aware wireless microsensor networks." *IEEE Signal processing magazine* 19.2 (2002): 40-50.
- [16] Maraiya, Kiran, Kamal Kant, and Nitin Gupta. "Application based study on wireless sensor network." *International Journal of Computer Applications* 21.8 (2011): 9-15.

- [17] Soua, Ridha, and Pascale Minet. "A survey on energy efficient techniques in wireless sensor networks." *2011 4th joint IFIP wireless and mobile networking conference (WMNC 2011)*. IEEE, 2011.
- [18] Anastasi, Giuseppe, et al. "Energy conservation in wireless sensor networks: A survey." *Ad hoc networks* 7.3 (2009): 537-568.
- [19] Khriji, Sabine, et al. "Energy-efficient techniques in wireless sensor networks." *Energy Harvesting for Wireless Sensor Networks: Technologies, Components and System Design; De Gruyter Oldenbourg: Berlin, Germany* (2018).
- [20] Akyildiz, Ian F., Tommaso Melodia, and Kaushik R. Chowdhury. "A survey on wireless multimedia sensor networks." *Computer networks* 51.4 (2007): 921-960.
- [21] Okwor, Candidus, et al. "A Review of the state-of-the-art Ubiquitous Multimedia Sensor Networks." *FUOYE Journal of Engineering and Technology* 2.1 (2017).
- [22] Akyildiz, Ian F., Tommaso Melodia, and Kaushik R. Chowdhury. "Wireless multimedia sensor networks: Applications and testbeds." *Proceedings of the IEEE* 96.10 (2008): 1588-1605.
- [23] Baith, Shashi, et al. "Wireless multimedia sensor network." *International Journal for Advance Research and Development* 3.4 (2018): 150-155.
- [24] ANTHONY TANNOURI. "Using wireless multimedia sensor networks for 3D scene acquisition and reconstruction." *Phd thesis*, University of Burgundy 2018.
- [25] Ang, Li-minn, et al. *Wireless multimedia sensor networks on reconfigurable hardware*. Heidelberg: Springer, 2013.
- [26] Almalkawi, Islam T., et al. "Wireless multimedia sensor networks: current trends and future directions." *Sensors* 10.7 (2010): 6662-6717.
- [27] Arjav Bavarva, Preetida Vinayakray-Jani. "An introduction to Wireless Multimedia Sensor Networks." *Sensors*, 2015.
- [28] Sharif, Atif, Vidyasagar Potdar, and Elizabeth Chang. "Wireless multimedia sensor network technology: A survey." *2009 7th IEEE International Conference on Industrial Informatics*. IEEE, 2009.
- [29] Mammeri, Abdelhamid, Brahim Hadjou, and Ahmed Khoumsi. "A survey of image compression algorithms for visual sensor networks." *International Scholarly Research Notices* 2012 (2012).
- [30] Bouakkaz, Fatima, Wided Ali, and Makhlof Derdour. "Forest fire detection using wireless multimedia sensor networks and image compression." *Instrum. Mes. Métrologie* 20 (2021): 57-63.
- [31] Şenturk, Arafat, and Zehra karapinar . "A Study on Energy Efficiency in Wireless Multimedia Sensor Networks." *Düzce Üniversitesi Bilim ve Teknoloji Dergisi* 3.1 (2015): 145-151.
- [32] ZainEldin, Hanaa, Mostafa A. Elhosseini, and Hesham A. Ali. "Image compression algorithms in wireless multimedia sensor networks: A survey." *Ain Shams engineering journal* 6.2 (2015): 481-490.

- [33] Alarabeyyat, A., et al. "Lossless image compression technique using combination methods." *Journal of Software Engineering and Applications* 5.10 (2012): 752.
- [34] Gaganjot Singh Jasneet Singh Sandh. "Comparative Analysis of Various Image Compression Techniques." *international journal of engineering research and technology (IJERT) ESDST* 5.5 (2017).
- [35] Vijayvargiya, Gaurav, Sanjay Silakari, and Rajeev Pandey. "A survey: various techniques of image compression." *arXiv preprint arXiv:1311.6877* (2013).
- [36] Preethika, S., and A. Umamakeswari. "Image Compression and Wireless Multimedia Sensor Networks–A Survey." *Indian Journal of Science and Technology* 9 (2016): 48.
- [37] Babu, P. Suresh, and S. Sathappan. "Efficient lossless image compression using modified hierarchical prediction and context adaptive coding." *Indian Journal of Science and Technology* 8.34 (2015): 1-6.
- [38] Dhawan, Sachin. "A review of image compression and comparison of its algorithms." *International Journal of electronics & Communication technology* 2.1 (2011): 22-26.
- [39] Carreto-Castro, M. F., et al. "Comparison of lossless compression techniques." *Proceedings of 36th Midwest Symposium on Circuits and Systems*. IEEE, 1993.
- [40] Li, Ze-Nian, Mark S. Drew, and Jiangchuan Liu. *Fundamentals of multimedia*. Upper Saddle River (NJ):: Pearson Prentice Hall, 2004.
- [41] Samra, H. S. "Image compression techniques." *International Journal of Computers & Technology* 2.2 (2012).
- [42] Dhawan, Sachin. "A review of image compression and comparison of its algorithms." *International Journal of electronics & Communication technology* 2.1 (2011): 22-26.
- [43] Gersho, Allen, and Robert M. Gray. *Vector quantization and signal compression*. Vol. 159. Springer Science & Business Media, 2012.
- [44] Linde, Yoseph, Andres Buzo, and Robert Gray. "An algorithm for vector quantizer design." *IEEE Transactions on communications* 28.1 (1980): 84-95.
- [45] Xu, Chang-man, and Zhao-yang Zhang. "A fast fractal image compression coding method." *Journal of Shanghai University (English Edition)* 5 (2001): 57-59.
- [46] Ram, Bhupendra. "Digital image watermarking technique using discrete wavelet transform and discrete cosine transform." *Available at SSRN 4173742* (2013).
- [47] Vetterli, Martin, and Jelena Kovacevic. *Wavelets and subband coding*. No. BOOK.
- [48] Kurniawan, Andri, Tito Waluyo Purboyo, and Anggunmeka Luhur Prasasti. "Implementation of image compression using discrete cosine transform (DCT) and discrete wavelet transform (DWT)." *International Journal of Applied Engineering Research* 12.23 (2017):13951-13958.
- [49] Deshlahra, Archana. *Analysis of Image Compression Methods Based On Transform and FractalCoding*.Diss.2013.
- [50] Thyagarajan, Kadayam S. *Still image and video compression with MATLAB*. John Wiley & Sons, 2011.

- [51] N.S. Singh, H.J. Singh. "Data Compression Techniques in Wireless Sensor Network A Survey." *International journal of computer sciences and engineering* 7. 1 (2019):697-706.
- [52] Carreto-Castro, M. F., et al. "Comparison of lossless compression techniques." *Proceedings of 36th Midwest Symposium on Circuits and Systems*. IEEE, 1993.
- [53] Ahmed, Nasir, T_ Natarajan, and Kamisetty R. Rao. "Discrete cosine transform." *IEEE transactions on Computers* 100.1 (1974): 90-93.
- [54] Luo, Ying, and Rabab Kreidieh Ward. "Removing the blocking artifacts of block-based DCT compressed images." *IEEE transactions on Image Processing* 12.7 (2003): 838-842.
- [55] Wallace, Gregory K. "The JPEG still picture compression standard." *IEEE transactions on consumer electronics* 38.1 (1992): xviii-xxxiv.
- [56] Agarwal, Nitesh, and A. M. Khan. "Application of DCT in image processing." *Conference Etrasct 14 Proceedings at International Journal of Engineering Research & Technology*. 2014.
- [57] Khayam, Syed Ali. "The discrete cosine transform (DCT): theory and application." *Michigan State University* 114.1 (2003): 31.
- [58] Abdl-majjed, Ielaf O. "Image compression using Modified Fuzzy Adaptive Resonance Theory." *AL-Rafidain Journal of Computer Sciences and Mathematics* 6.3 (2009): 151-160.
- [59] Minguillo´ n, Julia, and Jaume Pujol. "JPEG standard uniform quantization error modeling with applications to sequential and progressive operation modes." *Journal of electronic imaging* 10.2 (2001): 475-485.
- [60] Raid, A. M., et al. "Jpeg image compression using discrete cosine transform-A survey." *arXiv preprint arXiv:1405.6147* (2014).
- [61] Shams, Ahmed M., et al. "NEDA: A low-power high-performance DCT architecture." *IEEE transactions on signal processing* 54.3 (2006): 955-964.
- [62] Sharma, Vijay K., Kamala Kanta Mahapatra, and Umesh C. Pati. "Non-recursive computation of 8×8 2D DCT for high accuracy and low area." *Journal of Circuits, Systems, and Computers* 23.10 (2014): 1450143.
- [63] Ansari, Rashid, Christine Guillemot, and Nasir Memon. "Jpeg and jpeg2000." *The Essential Guide to Image Processing*. Academic Press, 2009. 421-461.
- [64] Ghadi, Musab, Lamri Laouamer, and Tarek Moulahi. "Enhancing digital image integrity by exploiting JPEG bitstream attributes." *Journal of Innovation in Digital Ecosystems* 2.1-2 (2015): 20-31.
- [65] Viraktamath, S. V., and Girish V. Attimarad. "Impact of Quantization Matrix on the Performance of JPEG." *International Journal of Future Generation Communication and Networking* 4.3 (2011): 107-118.
- [66] Ma, Tao, et al. "A survey of energy-efficient compression and communication techniques for multimedia in resource constrained systems." *IEEE Communications Surveys & Tutorials* 15.3 (2012): 963-972.
- [67] Chiasserini, C-F., and Enrico Magli. "Energy consumption and image quality in wireless video-surveillance networks." *The 13th IEEE international symposium on personal, indoor and mobile radio communications*. Vol. 5. IEEE, 2002.

- [68] Liang, Jie, and Trac D. Tran. "Fast multiplierless approximations of the DCT with the lifting scheme." *IEEE transactions on signal processing* 49.12 (2001): 3032-3044.
- [69] Nasri, Mohsen, et al. "Images compression techniques for wireless sensor network applications." *International Journal of Speech Technology* 18.2 (2015): 205-216.
- [70] Rehna, V. J., and M. K. Kumar. "Wavelet based image coding schemes: A recent survey." *arXiv preprint arXiv:1209.2515* (2012).
- [71] Mallat, Stephane G. "A theory for multiresolution signal decomposition: the wavelet representation." *IEEE transactions on pattern analysis and machine intelligence* 11.7 (1989): 674-693.
- [72] Suseela, G., and Y. Asnath Vicky Phamila. "Energy efficient image coding techniques for low power sensor nodes: A review." *Ain Shams Engineering Journal* 9.4 (2018): 2961-2972.
- [73] Nasri, Mohsen, et al. "Adaptive image compression technique for wireless sensor networks." *Computers & Electrical Engineering* 37.5 (2011): 798-810.
- [74] Khemiri, Randa, et al. "Implementation and Comparison of the Lifting 5/3 and 9/7 Algorithms in MatLab on GPU." *Journal of Electrical Systems* 12.3 (2016): 490-499.
- [75] Kour, Prabhjot. "Image processing using discrete wavelet transform." *International journal of electronics and communication* 3.1 (2015).
- [76] Xing, Yafei, Béatrice Pesquet-Popescu, and Frederic Dufaux. "Compression of computer generated phase-shifting hologram sequence using AVC and HEVC." *Applications of Digital Image Processing XXXVI*. Vol. 8856. SPIE, 2013.
- [77] Babu, D. Vijendra, et al. "EBCOT using energy efficient wavelet transform." *2008 International Conference on Computing, Communication and Networking*. IEEE, 2008.
- [78] Taubman, David S., Michael W. Marcellin, and Majid Rabbani. "JPEG2000: Image compression fundamentals, standards and practice." *Journal of Electronic Imaging* 11.2 (2002): 286-287.
- [79] Lian, Chung-Jr, et al. "Analysis and architecture design of block-coding engine for EBCOT in JPEG 2000." *IEEE Transactions on circuits and systems for video technology* 13.3 (2003): 219-230.
- [80] Chiang, Jen-Shiun, et al. "High-speed EBCOT with dual context-modeling coding architecture for JPEG2000." *2004 IEEE International Symposium on Circuits and Systems (ISCAS)*. Vol. 3. IEEE, 2004.
- [81] Senturk, Arafat, and Resul Kara. "An analysis of image compression technique in wireless multimedia sensor networks." *Tehnicki vjesnik/Technical Gazette* 23.6 (2016).
- [82] Kaur, Chandandeep, and Sumit Budhiraja. "Improvements of spiht in image compression-survey." *International Journal of Emerging Technology and Advanced Engineering* 3.1 (2013): 652-656.
- [83] Akter, M., et al. "A modified-set partitioning in hierarchical trees algorithm for real-time image compression." *Journal of Communications Technology and Electronics* 53 (2008): 642-650.
- [84] Sun, Yong, Hui Zhang, and Guangshu Hu. "Real-time implementation of a new low-memory SPIHT image coding algorithm using DSP chip." *IEEE Transactions on Image Processing* 11.9 (2002): 1112-1116.

- [85]. Ding, Huijun, Yann Soon, and Chai Kiat Yeo. "A DCT-based speech enhancement system with pitch synchronous analysis." *IEEE Transactions on audio, speech, and language processing* 19.8 (2011): 2614-2623.
- [86] Bhaskaran, Vasudev, and Konstantinos Konstantinides. "Image and video compression standards: algorithms and architectures." (1997).
- [87] Tran, Trac D. "The BinDCT: Fast multiplierless approximation of the DCT." *IEEE Signal processing letters* 7.6 (2000): 141-144.
- [88] Cintra, Renato J., and Fábio M. Bayer. "A DCT approximation for image compression." *IEEE Signal Processing Letters* 18.10 (2011): 579-582.
- [89] Bayer, Fábio M., and Renato J. Cintra. "DCT-like transform for image compression requires 14 additions only." *arXiv preprint arXiv:1702.00817* (2017).
- [90] Bouguezel, Saad, M. Omair Ahmad, and M. N. S. Swamy. "Low-complexity 8×8 transform for image compression." *Electronics Letters* 44.21 (2008): 1249-1250.
- [91] Bouguezel, Saad, M. Omair Ahmad, and M. N. S. Swamy. "A fast 8×8 transform for image compression." *2009 International Conference on Microelectronics-ICM*. IEEE, 2009.
- [92] Bouguezel, Saad, M. Omair Ahmad, and M. N. S. Swamy. "A low-complexity parametric transform for image compression." *2011 IEEE International Symposium of Circuits and Systems (ISCAS)*. IEEE, 2011.
- [93] Bouguezel, Saad, M. Omair Ahmad, and M. N. S. Swamy. "Binary discrete cosine and Hartley transforms." *IEEE Transactions on Circuits and Systems I: Regular Papers* 60.4 (2012): 989-1002.
- [94] Potluri, Uma Sadhvi, et al. "Improved 8-point approximate DCT for image and video compression requiring only 14 additions." *IEEE Transactions on Circuits and Systems I: Regular Papers* 61.6 (2014): 1727-1740.
- [95] Lecuire, Vincent, Leila Makkaoui, and J-M. Moureaux. "Fast zonal DCT for energy conservation in wireless image sensor networks." *Electronics Letters* 48.2 (2012): 125-127.
- [96] Coutinho, Vitor A., et al. "A multiplierless pruned DCT-like transformation for image and video compression that requires ten additions only." *Journal of Real-Time Image Processing* 12 (2016): 247-255.
- [97] Kouadria, N., et al. "Low complexity DCT for image compression in wireless visual sensor networks." *Electronics Letters* 49.24 (2013): 1531-1532.
- [98] Mechouek, Khaoula, et al. "Low complexity DCT approximation for image compression in wireless image sensor networks." *Journal of Circuits, Systems and Computers* 25.08 (2016): 1650088.
- [99] Roma, Nuno, and Leonel Sousa. "A tutorial overview on the properties of the discrete cosine transform for encoded image and video processing." *Signal Processing* 91.11 (2011): 2443-2464.
- [100] Haweel, Tarek I. "A new square wave transform based on the DCT." *Signal processing* 81.11 (2001): 2309-2319.
- [101] Makkaoui, Leila, Vincent Lecuire, and Jean-Marie Moureaux. "Fast zonal DCT-based image compression for wireless camera sensor networks." *2010 2nd International Conference on Image Processing Theory, Tools and Applications*. IEEE, 2010.

- [102] Cintra, Renato J., et al. "Energy-efficient 8-point DCT approximations: Theory and hardware architectures." *Circuits, Systems, and Signal Processing* 35 (2016): 4009-4029.
- [103] Ferrigno, Luigi, et al. "Balancing computational and transmission power consumption in wireless image sensor networks." *IEEE Symposium on Virtual Environments, Human-Computer Interfaces and Measurement Systems, 2005..* IEEE, 2005.
- [104] Phamila, Yesudhas Asnath Vicky, and Ramachandran Amutha. "Low-complex energy-aware image communication in visual sensor networks." *Journal of Electronic Imaging* 22.4 (2013): 041107-041107.
- [105] Chafi, Ahmed, Adel Soudani, and Gilles Sicard. "Hardware compression scheme based on low complexity arithmetic encoding for low power image transmission over WSNs." *AEU-International Journal of Electronics and Communications* 68.3 (2014): 193-200.
- [106] J. Kominek, Waterloo BragZone, University of Waterloo. Available at <http://links.uwaterloo.ca/Repository.html>. (Accessed on February 2019).
- [107] Wang, Zhou, et al. "Image quality assessment: from error visibility to structural similarity." *IEEE transactions on image processing* 13.4 (2004): 600-612.
- [108] Kouadria, Nasreddine, et al. "Region-of-interest based image compression using the discrete Tchebichef transform in wireless visual sensor networks." *Computers & Electrical Engineering* 73 (2019): 194-208.
- [109]. Kouadria, Nasreddine, et al. "Pruned discrete Tchebichef transform for image coding in wireless multimedia sensor networks." *AEU-International Journal of Electronics and Communications* 74 (2017): 123-127.
- [110] Lecuire, Vincent, Cristian Duran-Faundez, and Nicolas Krommenacker. "Energy-efficient image transmission in sensor networks." *International Journal of Sensor Networks* 4.1-2 (2008): 37-47.
- [111] Bouguera, Taoufik, et al. "Energy consumption model for sensor nodes based on LoRa and LoRaWAN." *Sensors* 18.7 (2018): 2104.
- [112] Khriji, Sabrine, et al. "Dynamic autonomous energy consumption measurement for a wireless sensor node." *2019 IEEE International Symposium on Measurements & Networking (M&N)*. IEEE, 2019.
- [113] Abuarqoub, Abdelrahman, et al. "A survey on wireless sensor networks simulation tools and testbeds." *Sensors, transducers, signal conditioning and wireless sensors networks advances in sensors: reviews* 3.14 (2016): 283-302.
- [114] Kaaniche, Mounir, et al. "Vector lifting schemes for stereo image coding." *IEEE Transactions on Image Processing* 18.11 (2009): 2463-2475.
- [115] Hachicha, Walid, et al. "Optimized residual image for stereo image coding." *2014 5th European Workshop on Visual Information Processing (EUVIP)*. IEEE, 2014.
- [116] Ellinas, J. N., and Manolis S. Sangriotis. "Stereo image compression using wavelet coefficients morphology." *Image and Vision Computing* 22.4 (2004): 281-290.
- [117] Ellinas, J. N., and Manolis S. Sangriotis. "Morphological wavelet-based stereo image coders." *Journal of Visual Communication and Image Representation* 17.4 (2006): 686-700.

- [118] Sperling, George. "Stereoscopic visual displays: Principles, viewing devices, alignment procedures." *Behavior Research Methods & Instrumentation* 3.3 (1971): 154-158.
- [119] Vasiljevic, Ivana Stojan, et al. " Analysis of compression techniques for stereoscopic images." *Информатика и автоматизация* 6.61 (2018): 197-220.
- [120] Frajka, Tama´ S., and Kenneth Zeger. "Residual image coding for stereo image compression." *Optical Engineering* 42.1 (2003): 182-189.
- [121] <https://vision.middlebury.edu/stereo/data/>(Accessed on February 2023).
- [122] Loffler, Christoph, Adriaan Ligtenberg, and George S. Moschytz. "Practical fast 1-D DCT algorithms with 11 multiplications." *International Conference IEEE*, (1989).